UNIVERSIDADE D
COIMBRA

Joana Alexandra Lima Gonçalves

THE IMPACT OF PROTEIN TYROSINE PHOSPHATASES ON THE ACTIVATION OF INTRAEPITHELIAL LYMPHOCYTES

Dissertação no âmbito do Mestrado em Investigação Biomédica, no ramo de Infeção e Imunidade, orientada pela Doutora Birte Blankenhaus e pela Doutora Cláudia Pereira e apresentada à Faculdade de Medicina da Universidade de Coimbra.

Dezembro de 2020

UNIVERSIDADE D
COIMBRA

Joana Alexandra Lima Gonçalves

THE IMPACT OF PROTEIN TYROSINE PHOSPHATASES ON THE ACTIVATION OF INTRAEPITHELIAL LYMPHOCYTES

Thesis submitted to the Faculty of Medicine of the University of Coimbra in fulfilment of the requirements for the degree of Master of Science in Biomedical Research.
The research work presented in this dissertation was performed at the Instituto de Medicina Molecular – João Lobo Antunes, under the supervision of Doctor Birte Blankenhaus and Professor Doctor Cláudia Pereira.

Dissertação apresentada à Faculdade de Medicina da Universidade de Coimbra, para cumprimento dos requisitos necessários à obtenção do grau de Mestre em Investigação Biomédica. O trabalho conducente à dissertação foi realizado no Instituto de Medicina Molecular – João Lobo Antunes, sob a orientação da Doutora Birte Blankenhaus e da Doutora Cláudia Pereira.

December 2020

Acknowledgements

Throughout the writing of this dissertation, I have received invaluable support and encouragement from extraordinary people.

I would like to express my deepest appreciation to Dr Marc Veldhoen for kindly welcoming me into his laboratory and allowing me to take on such a stimulating and interesting project. I am truly grateful for all the conversations and scientific discussions, the precious feedback and word of advice when the path ahead was not so clear.

I am deeply indebted to Dr Birte Blankenhaus, my supervisor, for all the kindness, patience and unparalleled support throughout the thesis work and writing process. I am beyond grateful for all you have taught me during this year, for all the valuable advice and unwavering guidance, for your profound belief in my abilities and insightful suggestions. Thank you for considering me as a peer, for debating ideas with me and allowing me to bring my work to a higher level, sharpening my thinking and improving my skills. My deepest thanks, for the numerous conversations, constant availability and understanding. Lastly, I truly am grateful for the great company and neighborship that turned every day into so much more than just work.

I would also like to express my sincere gratitude to Prof. Dr. Rose Zamoyska for kindly providing key mice for my experiments.

I gratefully acknowledge Prof. Dr. Cláudia Pereira for kindly accepting to supervise this work.

I would also like to extend my deepest gratitude to the coordinator of the Master programme, Prof. Dr. Henrique Girão, for being so enthusiastic and devoted to this Masters as he is to its students. Thank you for always going the extra mile, for treating us as peers and rooting for us every step of the way.

I'm extremely grateful to the Veldhoen Lab, "The Veldhoens", for all the buzz in busy days, for the immense support and willingness to help and of course for the great company. A special word of gratitude to my amiguinha, for always presenting me with words of encouragement, acts of kindness and most of all for completely trusting my skills and competence. Your support cannot be overestimated Patricinha, thank you for all the help and generosity. To my Martasinha, Silviacita, Leandrinho and Roosinha, the long names we gave you are not nearly as vast as your kindness, cheerful attitude, witty jokes, and overall great energy! I really could not have better colleagues, that so soon became friends. I could not have done this without you. Thank you for turning every day in "Bring your friends to work" Day! I cannot wait for a reunion!

I cannot begin to express my thanks to Marta, my incredibly encouraging and patient sidekick during this master, and an instrumental source of inspiration. Your unrelenting support and trust have steered me into a clearer and more fruitful path. Thank you for inspiring me to follow it and constantly pushing me towards my goals. Whether in the happiest or the most challenging times, you were always the wise voice I sought and needed to hear. I am genuinely grateful to have been able to share these years with you by my side every step of the way, every day, always present. Like two peas in a pod. And now, I cannot wait for the future.

To Sofia, without whom I would not have found the path leading to Coimbra, undoubtfully you brought me closer to the future I now claim for myself. There have been many highlights to our friendship, and I am so grateful to have shared this chapter with you, turning it into one more memorable milestone moment in our lives. For the long friendship and love, in all its forms, even in the face of pain. To you Sofs, for all the laughter and the tears, and for the countless times they come hand in hand.

To Ponce, for the words of advice that brought me clarity numerous times, for reassuring me and defying me to do better every time. For the friendship and affection. It takes one to know one.

To Nana, I lack the words to describe the continued support and life-support you have given me over the years, and how it has helped me to pull through in the darkest most stressful times and burst with laughter and joy in countless others. These years were no different. Thank you for being a constant in my life.

To Tati, for her profound admiration and belief in me. Thank you for your words in the most difficult times, for your advice whenever I felt lost and for always listening. Thank you for being the one to bring out the best in me.

To Afonso, Diogo, Marta and Sofia for being such powerful sources of love and friendship in my life. Thank you for being so positive and always cheering me on. To Maria and Pedro, for always rooting for me and celebrating my successes, and despite knowing me all too well, still believing I could pull this off. I know you will join me in celebrating one more achievement, like you always do.

Em bom português, as palavras de gratidão que devo à minha família, embora ficando sempre em dívida.

Aos meus tios, Miguel e Paulo, por serem presença constante na minha vida e a enriquecerem todos os dias. Estou profundamente grata pela vossa generosidade, interesse e carinho e sobretudo pela boa companhia. Senti-me sempre em casa, graças a vocês.

À minha irmã, por desde cedo ser a minha maior inspiração e guia, por ser a primeira força impulsionadora por detrás do meu percurso académico. Obrigada por me ensinares tanto sobre tanta coisa e coisa nenhuma, pelos interesses que partilhamos, e por estares presente com as palavras francas e sensatas que tantas vezes te exigo e das quais preciso sempre, sempre. Pela nossa amizade que é amor, obrigada Sis!

Aos meus pais, pelo infinito alento, pela vontade insaciável de me verem feliz e concretizada, por toda a confiança que em mim depositam. Sempre presentes, sempre incansáveis. Obrigada por me ouvirem, por se interessarem e por me encorajarem a cada passo. O que hoje conquisto e todos os meus sucessos são também vossos, e fruto do vosso amor e profunda dedicação. Nenhum gesto passa despercebido. E nenhuma palavra chega para agradecer uma vida, por isso ficam estas, com amor.

Finalmente, merecedores de uma profunda homenagem, aos meus avós. A todos, porque são pedra basilar na construção da pessoa que sou hoje, e porque orgulhosamente reconheço um pouco de todos em mim. Por todo o amor e carinho. Os vossos ensinamentos perduram, eternizando e celebrando a vossa memória a cada passo. Ao meu avô Joaquim, que partiu antes que pudesse responder-lhe à pergunta que mais me fazia. Hoje a pergunta ganha especial sentido e, finalmente, resposta.

A todos, o meu sentido bem-haja.

“Where is the Life we have lost in living?

Where is the wisdom we have lost in knowledge?

Where is the knowledge we have lost in information?”

T. S. Eliot

Resumo

A barreira epitelial do intestino abriga um conjunto de microorganismos comensais e patogénicos e também um vasto leque de antigénios alimentares. Os linfócitos intraepiteliais (IEL) são células T residentes no epitélio intestinal e constituem uma primeira linha de defesa contra infeções, preservando assim a integridade da barreira epitelial, assegurando a homeostase e reparação dos tecidos.

A ativação desproporcionada de linfócitos pode produzir efeitos nefastos, justificando assim a necessidade de existir um mecanismo de ativação estritamente regulado. Enquanto a maioria dos linfócitos é mantido num estado quiescente, os linfócitos intraepiteliais apresentam-se num estado de ativação elevado, porém controlado, exibindo características de ambas células T efetoras e de memória. Neste estado de ativação elevado, os linfócitos intraepiteliais demonstram prontidão para atuar, no entanto parece existir uma barreira que impede estes linfócitos de executarem em pleno as suas funções efetoras. A ativação de células T convencionais é maioritariamente regulada pelo recetor de células T (TCR), no entanto os sinais que regulam a ativação dos linfócitos intraepiteliais são ainda desconhecidos e o papel do TCR nesta interação permanece controverso. O processo de ativação e subsequentes respostas imunológicas são maioritariamente regulados pela sinalização intracelular que se inicia com a ativação do TCR, que recruta inúmeras moléculas de sinalização onde se incluem as proteínas tirosina fosfatases e as proteínas tirosinas quinases. A ação desfosforilante das PTPs determina a ativação ou a inibição dos seus alvos, conferindo às PTPs um papel fundamental na regulação da sinalização pelo TCR. Deste modo, a desregulação da atividade das PTPs pode resultar numa deficiência nos mecanismos de ação e regulatórios do TCR e consequentemente em patologias de carácter autoimune.

Este estudo procurou investigar o papel das PTPs no estado de ativação dos IELs e pretende avaliar se as PTPs representam um fator determinante no controlo da ativação destas células.

Em resposta à estimulação do TCR, os IELs apresentam uma transdução de sinal intracelular deficiente, a jusante do TCR. Os resultados mostram que as PTPs são altamente expressas por IELs “naturais”, e uma análise mais profunda revela níveis muito elevados das proteinas PTPN22 e SHP-2 nestas células, em comparação com células T convencionais. Observou-se também uma maior atividade das PTPs em IELs naturais. Ao analisar a indução de colite em ratinhos, verificou-se que esta doença é prolongada em ratinhos-quimeras deficientes em *PTPN22.* Mais ainda, após a estimulação de ratinhos-quimera *Ptpn22*$^{-/-}$ com α-CD3, os IELs exibem um maior poder citotóxico. Em ratinhos wild-type tratados com um inibidor de PTP,

ortovanadato de sódio (SOV), e estimulados com α-CD3, os IELs proliferam continuamente, aumentam a expressão de PD-1 e sustêm a produção de Granzima B (GzmB).

Em conjunto, o nosso trabalho mostra o papel proeminente das PTPs nos IELs intestinais, e consequentemente esclarece a sua importância para a função e regulação destas células.

Palavras-Chave: Linfócitos intraepiteliais (IELs); Proteínas Tirosina Fosfatases (PTP); Ativação de IELs; Células T $CD8^+$; Sinalização pelo Recetor de Células T (TCR)

Abstract

The intestinal epithelial barrier is home to an array of commensal and pathogenic microorganisms as well as a variety of food antigens. Intraepithelial lymphocytes (IELs) are highly specialized T cells, which reside within the intestinal epithelium, constituting a first line of defence against infection and ensuring tissue homeostasis. The potential detrimental effects of aberrant lymphocyte activation support the necessity for a strictly regulated lymphocyte activation mechanism. While most lymphocytes are kept in a quiescent state, intriguingly, IELs are sustained in a highly activated yet resting state, sharing many features with both effector and memory T cells. IELs are halted in a poised activation status, which hints at the presence of a cue for activation but also a blockade preventing IELs from mounting a fully-fledged effector response. Indeed, conventional T cell activation is mainly regulated by the T cell receptor (TCR) whereas the cues that regulate IEL activation status are still unknown and the role of the TCR remains controversial. Upon TCR ligation, T cell activation is regulated by signal transduction downstream of the TCR, engaging several intracellular signalling molecules such as Protein Tyrosine Phosphatases (PTPs) and Protein Tyrosine Kinases (PTKs). The dephosphorylation action of PTPs determines the enhancement or inhibition of their specific targets, granting PTPs with a critical role in the regulation of TCR signalling. The dysregulation of PTP function could therefore result in the impairment of the TCR mechanisms of action and regulation and consequently, in T cell-mediated autoimmune disease. This study investigates the role of PTPs in the heightened but poised activation status of IELs and intends to ascertain whether PTPs are a key factor in the control of IEL activation.

The analysis of IEL response to TCR stimulation has revealed that signal transduction is hampered downstream of the TCR. We found that PTPs are highly expressed in natural IELs and further analysis showed increased protein levels of the PTPs *PTPN22* and SHP-2 in these cells, compared to peripheral T cells. Furthermore, we could show increased PTP activity in natural IELs. Analysis of an induced-colitis mouse model has shown that the disease is prolonged in *Ptpn22*$^{-/-}$ Bone Marrow (BM) chimeric mice. We also report that in *Ptpn22*$^{-/-}$ BM chimeras stimulated with α-CD3, IELs show increased cytotoxic potential. Furthermore, in WT mice treated with a general PTP inhibitor, Sodium Orthovanadate (SOV), and stimulated with α-CD3, IELs show continuing proliferation, increased PD-1 expression, and sustained Granzyme B (GzmB) production.

Taken together, our work reveals that PTPs are prominent in intestinal IELs, suggesting they may make an important contribution to the function and regulation of these cells.

Keywords: Intraepithelial lymphocytes (IEL); protein tyrosine phosphatases (PTP); IEL activation; CD8^{+} T cells; T cell receptor (TCR) signalling

Table of Contents

List of Tables

List of Figures

Abbreviations

AhR	Arylhydrocarbon receptor
AP-1	Activator protein 1
APC	Antigen presenting cell
BM	Bone Marrow
BSA	Bovine Serum Albumin
Btnl	Butyrophilin-like molecules
CCL25	Chemokine ligand 25
CCR9	CC-chemokine receptor 9
CD	Crohn's disease
CSK	Cytoplasmic C-terminal Src kinase
DC	Dendritic cell
DGAV	Direção Geral de Alimentação e Veterinária
DSS	Dextran-Sulfate Sodium
DTT	Dithiothreitol
DUSP22	Dual-specificity protein phosphatase 22
FAE	Follicle-associated epithelium
FAK	Focal adhesion kinase
FBS	Fetal Bovine Serum
FOXP3	Forkhead-box protein 3
GALT	Gut-associated lymphoid tissue
GIT	Gastrointestinal Tract
Gzm	Granzyme
GzmB	Granzyme B
IBD	Inflammatory bowel disease
IECs	Intestinal epithelial cells
IEL	Intraepithelial lymphocyte
ILCs	Innate Lymphoid Cells
ILFs	Isolated lymphoid follicles
ITAMs	Immunoreceptor tyrosine-based activation motifs
ITK	IL-2 inducible T cell kinase
IVC	Individually ventilated cages
LAT	Linker for activation of T cells
LCK	Lymphocyte-specific protein tyrosine kinase
LP	Lamina propria

LYP	Lymphoid phosphatase
M cells	Microfold cells
MALT	Mucosa-associated lymphoid tissue
MAPK (ERK)	Mitogen-activated protein kinase
MFI	Mean Fluorescence Intensity
MHC	Major Histocompatibility Complex
MLNs	Mesenteric lymph nodes
NF- κB	Nuclear factor-κB
NFAT	Nuclear factor of activated T cells
NOD	Nucleotide-binding oligomerization domain-containing protein
PBS	Phosphate Buffered Saline
PEP	PEST domain-enriched tyrosine phosphatase
PLCγ1	Phospholipase C gamma 1
PPs	Peyer Patches
PRR	Pattern recognition receptors
PTK	Protein Tyrosine Kinase
PTP	Protein Tyrosine Phosphatase
PTPN	Protein Tyrosine Phosphatase Non-receptor
RA	Rheumatoid Arthritis
RPTPs	Receptor-type PTPs
SD	Standard Deviation
SEM	Standard Error of the Mean
SFK	Src family of protein tyrosine kinases
SH2	Src homology region 2
SHP-1	SH2 domain-containing phosphatase 1
SHP-2	SH2 domain-containing phosphatase 2
SLE	Systemic lupus erythematosus
SNP	Single-nucleotide polymorphism
SOV	Sodium Orthovanadate
SPF	Specific Pathogen-free
T1D	Type-1 Diabetes
TBST	Tris-Buffered Saline with Tween-20
TCPTP	T cell protein tyrosine phosphatase
TCR	T cell receptor
TGFβ	Transforming growth factor-beta

Th1	Type 1 T helper
Th2	Type 2 T helper
TL	Thymus Leukaemia
TLR	Toll-like receptors
Treg	Regulatory T cell
Tyr	Tyrosine
UC	Ulcerative colitis
ZAP70	Zeta-chain-associated protein of 70kDa
α-CD3	Anti-CD3

1. Introduction

1.1. The Mucosal Immune System

The mucosal immune system constitutes a prime line of defence acting at the interface between the host and the external environment.

Epithelial barriers such as the skin and the gastrointestinal, respiratory, and genitourinary tracts are a primary port of entry for pathogens and therefore particularly vulnerable to disease. Whether by ingestion, inhalation, or sexual contact, most of the exogenous threats the body faces are found at mucosal surfaces where the immune system interacts with pathogens and a variety of environmental antigens. Here, immunologic defence is crucial [1, 4, 5].

Although mucosal membranes are a physical barrier against pathogens, they are not stagnant or passive. On the contrary, they are heterogeneous structures that harbour specialized innate and adaptive immune cells. Several immune populations, including macrophages, dendritic cells (DCs), T and B lymphocytes and innate lymphoid cells (ILCs) form a highly diverse and complex network that patrols the tissue and ensures its integrity. These cells safeguard the mucosal barriers while also preventing exacerbated or aberrant immune responses resulting from overstimulation of the immune system or responses against innocuous antigens [4, 5]. The complex and diverse antigenic load present in these surfaces poses a significant challenge for the immune system, which can react to innocuous antigens derived from the intestinal microbiota or food and trigger tissue impairment and severe inflammation disorders. As such, these highly specialized populations of immune cells together with an organized structural setup promote the induction of tolerogenic responses. Nevertheless, immunological tolerance at mucosal barrier sites is not the only route followed by the mucosal immune system since a basal activation state enables protective immune responses and reinforcement of the barrier function at these sites. Despite being continuously exposed to foreign antigens and threatened by invading microorganisms, these epithelial barriers also harbour several beneficial microbes that play an essential role in the immune system's function and regulation. The microbiota, a community mostly composed of bacteria, plays a fundamental role both locally and systemically, contributing to the induction, education and functional tuning of the host's immune system as a whole [6].

In order to grasp the complexity of mucosal immune responses, it is first necessary to understand the anatomy and physiology of mucosal tissues.

1.1.1. Intestinal anatomy and physiology

The mucosal immune system interacts with most of the pathogens and environmental threats that enter the body. Fortunately, it also holds the largest reservoir of immune cells in the body. The gastrointestinal tract (GIT) is the predominant site of microbiome-host interaction and the mucosal surface with the highest exposure to the environment. The GIT is in direct contact with pathogens, environmental antigens and a diverse microbiota and its respective products, constituting a largely reactive environment [1, 7].

The mammalian intestine is a tube-like structure divided into the small and large intestine and comprises most of the GIT lymphoid tissue. The segments composing the intestine are heterogenous, showing distinct morphology, different specialized structures and exerting different physiological functions.

The small intestine is divided into three segments with different characteristics: the duodenum, which starts at the stomach's pylorus, followed by the jejunum, and finally, the ileum, which ends at the ileocaecal valve connecting the small intestine with the large intestine. The upper small intestine, mostly duodenum and jejunum, presents, in its epithelial cell monolayer, long thin projections of the epithelial tissue, named villi (Figure 1a), that extend into the lumen providing a larger surface area for an optimised digestion process and nutrient absorption.

The large intestine starts at the caecum, leading to the proximal colon, transverse colon, distal colon, and the rectum, finally terminating at the anus. In the large intestine, villi and microvilli are absent (Figure 1b), as no intrinsic digestion function takes place in these sections of the intestine, whose central role is the reabsorption of water, absorption of any remaining nutrients and elimination of undigested waste products. Accordingly, the immune cell composition also varies within the intestine, where different segments harbour several innate and adaptive immune cells (Figure 1) [8]. Furthermore, the large intestine is also the main reservoir of commensal bacteria that act in the fermentative digestion of complex carbohydrates that cannot be processed in the small intestine [9].

There are estimated to be between 500 to 1000 different species of bacteria populating the human intestine, the most prevalent ones being Firmicutes, Bacteroidetes, Proteobacteria and Actinobacteria. Remarkably, bacterial numbers generally increase while moving down the gastrointestinal tract, reaching numbers as high as 10^5 per mL in the upper small intestine and 10^{12} per mL in the colon. Intestinal epithelial cells (IECs) actively participate in immunological surveillance and in directing inflammatory responses, since they can express several pattern recognition receptors, such as toll-like receptors (TLR), while also producing chemotactic factors for both myeloid and lymphoid cells [10]. Interspersed in the intestinal epithelium resides a population of lymphocytes, referred to as intraepithelial lymphocytes (IELs) (Figure

1a), a highly specialized class of T cells that are in direct contact with IECs and, evidently, close to an antigen packed gut lumen.

Underlying the epithelial barrier is the lamina propria (LP) (Figure 1) and immediately below, the muscularis mucosa. Together they make up the mucosa, which is proximal to the lumen of the gut and where most immunological processes occur. The epithelial layer and the lamina propria are two very distinct mucosal compartments, although only separated by a thin basement membrane. Notably, the lamina propria also comprises several cell populations of innate and adaptive nature within organized lymphoid structures [9].

1.1.2. Lymphoid structures of the intestine

Immune responses at mucosal barrier sites are mediated by a specialized arm of the immune system, known as the mucosal immune system. The maintenance of mucosal homeostasis relies on the crosstalk between its structural cells, the microbiome, and the mucosal immune system.

The mucosal immune system can be divided into inductive sites and effector sites. Inductive sites comprise local and regional organized mucosa-associated lymphoid tissue (MALT) and draining lymph nodes, where naïve lymphocytes are stimulated with exogenous antigens retrieved from mucosal surfaces.

In the intestine, the gut-associated lymphoid tissue (GALT) together with the mesenteric lymph nodes (MLNs), the largest lymph nodes of the body, are inductive sites for T and B lymphocytes, and therefore the main sites designed for priming adaptive immune cell responses in the gut [8]. The GALT include Peyer patches (PPs), cryptopatches and isolated lymphoid follicles (ILFs) dispersed throughout the intestinal mucosa (Figure 1). A single layer of epithelial cells, known as the follicle-associated epithelium (FAE), separates these lymphoid structures from the intestinal lumen. The FAE contains distinctive columnar epithelial cells termed microfold cells (M cells) that actively transport soluble antigens from the gut lumen, across the epithelial barrier, into an underlying dendritic cell-enriched area, the subepithelial dome where antigens can be presented to adaptive immune cells (Figure 1).

Peyer patches, the best-described tissues of the GALT, are macroscopically visible lymphoid aggregates found in the submucosa and distributed along the length of the distal small intestine, mostly throughout the jejunum and ileum, being very rare in the duodenum. Peyer patches, comprise numerous large B-cell follicles interspersed with smaller T-cell areas, develop early in foetal life. Unlike the mesenteric lymph nodes (MLNs), PPs are not encapsulated, and even though they always contain germinal centres, these appear only

shortly after birth, suggesting immune stimulation dependency, perhaps of luminal antigen origin [11]. The MLNs drain the small intestine and the upper colon, and whereas in humans they are dispersed along the whole intestine, in mice they consist of 4 or five nodes, each node draining different areas of the gut [12].

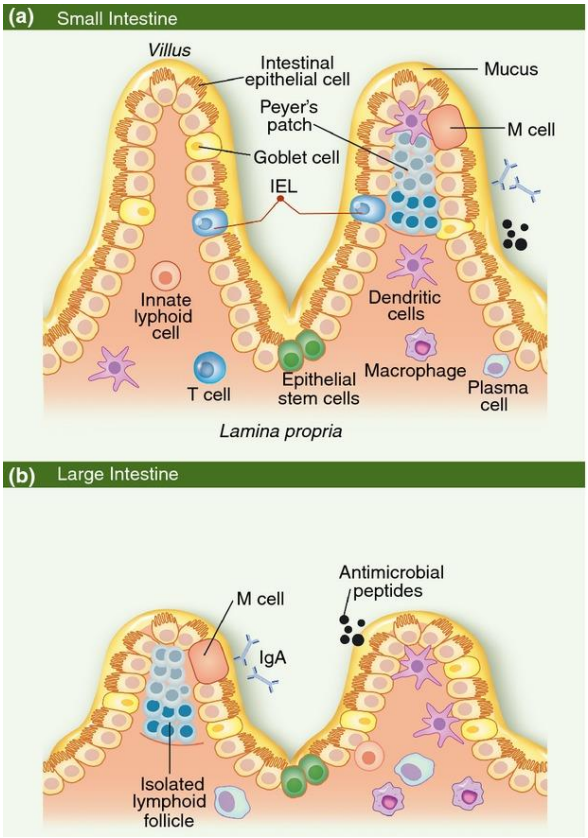

Figure 1 | The cellular and structural composition of the small and large intestinal epithelium. (A) Representative small intestinal epithelium and underlying lamina propria. The mucous layer and the epithelial cell monolayer line the intestine, separating the intestinal lumen from the underlying lymphoid structures. M-cells are located to the follicle-associated epithelium overlying Peyer's patches, and actively transport antigens from the gut lumen to underlying dendritic cells for antigen processing and presentation. At inductive sites, such as Peyer's Patches, lymphocytes are primed and matured and then migrate to effector sites such as the lamina propria to respond to stimulation. Goblet cells also facilitate luminal antigen delivery to underlying dendritic cells. Within the intestinal epithelium resides a highly specialized population of lymphocytes, termed intraepithelial lymphocytes (IELs). **(B)** Organization of the large intestinal epithelium. In contrast to the small intestine, B cells are the predominant lymphocyte population in the lamina propria of the large intestine. Isolated lymphoid follicles can be found both in the small and large intestine, contrarily to Peyer's patches which are not present in the latter. Adapted from McDermott and Huffnagle [1].

Collectively, inductive and effector sites of the mucosal immune system constitute a robust source of immune cells, which mature in mucosal inductive sites and then migrate to mucosal effector sites thus, constituting the basis for the immune response in the GIT [13].

1.1.3. Effector cell distribution throughout the intestine

In the intestinal immune system, there are two very distinct mucosal effector compartments: the gut epithelium and LP.

The LP contains both adaptive and innate immune populations such as B cells, T cells, DCs, macrophages, eosinophils, and mast cells that collectively contribute to intestinal homeostasis.

The LP includes several functionally diverse $CD4^+$ and $CD8^+$ T cell subsets, derived from conventional T cells that have been primed, in secondary lymphoid organs. In the lamina propria, $CD4^+$ T cells are present in higher proportions than $CD8^+$ T cells, in a ratio of 2:1, and both generally display an effector memory phenotype [8]. The LP $CD4^+$ compartment comprises forkhead box protein 3 (Foxp3)-expressing regulatory T cells (T_{reg}), which are a heterogeneous population and essential players in the regulation of the immune response, preventing unrestrained immune responses to harmless stimulus and thus promoting general immune homeostasis and immunologic tolerance, especially in the intestines [9, 14]. Notably, the transforming growth factor-beta (TGFβ) is an essential cytokine for the generation of T_{regs}, and in addition is one of their effector molecules to suppress innate and adaptive immune cells at mucosal sites [15]. Moreover, the IL-17 cytokine family, comprising six members, is also a major player in mucosal immunity and homeostasis, and the IL-17-secreting $CD4^+$ T cell subset, termed Th17 cells, has a central role in ensuring mucosal barrier function and mucosal defence mechanisms [16, 17]. Type 1 T helper (Th1) and type 2 T helper (Th2) cells are also part of the diverse $CD4^+$ T cell compartment of the LP [18, 19].

Some B-cells, initially activated in the GALT, migrate towards the intestinal LP, guided by adhesion molecules and chemokines, where they terminally differentiate into plasma cells. ILCs are another broad population of immune cells present in the LP, which resemble T lymphocytes but do not possess their recombinant antigen receptors. They are thought to take part in early innate immune responses in the intestinal mucosa. Other leukocyte populations can be found in the LP, including innate immune cells including mononuclear phagocytes such as macrophages and DCs, eosinophils, mast cells and plasmacytoid DCs. Macrophages are the largest population of leukocytes in the intestinal LP, where they carry out the vital function of maintaining local homeostasis as critical mediators of immunotolerance in the gut. Macrophages and DCs share the expression of the Major Histocompatibility Complex (MHC) class II and are both linked to the uptake and presentation of antigens in the intestine.

Whereas the LP constitutes a highly heterogeneous environment enriched in different immune cell populations, the epithelial barrier overlying it is mostly composed of IECs interspersed with IELs.

Intestinal IELs are a large heterogeneous population of lymphocytes that reside within the intestinal epithelial layer that lines the lumen of the gut and are therefore in direct contact with IECs and in the vicinity of luminal antigens. In the intestinal epithelium, IELs are present at a frequency of 10-15 IELs per 100 epithelial cells [20]. Murine IELs, composed mainly of $CD8^+$ T cells but also some $CD4^+$ expressing T cells, belong to either the T cell receptor-γδ (TCRγδ) or the TCRαβ lineages. They can be classified as “natural” IELs, indicating they are thymically derived, or as “induced” IELs originating from naïve T cells that acquired their activation phenotype in the periphery. IELs are an intriguing population maintained in a state of semi-activation, expressing activation markers resembling effector cells, but also sharing some characteristics with memory cells [2, 21]. The sophisticated yet complex features of IELs, as well as the critical role they play by acting at effector sites such as the intestinal epithelial barrier, are still not fully understood.

1.2. Inflammatory Diseases of the Intestine

Indeed, the mucosal immune system is an intricate network, and with increased complexity also arise complex pathologies. The proximity to pathogenic microbes at epithelial barrier sites, imbalances in the microbiota and dysbiosis or aberrant immune responses against self are just a few possible prompters of allergies, autoimmune and inflammatory disorders as well as malignant diseases [6].

Among the inflammatory diseases of the intestine, Celiac disease is a chronic inflammatory disorder of the small intestine, an immune-mediated enteropathy caused by dietary gluten in genetically predisposed individuals. Celiac disease affects the duodenum and upper small intestine, and results from a T-cell mediated response to gluten. It is understood that the interaction between gluten and MHC class II HLA-DQ2 and DQ8 molecules is the leading cause of the disease, while it is also acknowledged that, during disease onset, activation of a large population of IELs is necessary to cause tissue damage [22]. Here, the dysregulated activation of IELs, a hallmark of celiac disease, leads to the destruction of the intestinal epithelium and villous atrophy [23].

Moreover, besides celiac disease, there are other inflammatory diseases of the intestine, such as inflammatory bowel diseases (IBDs) which comprise Crohn’s disease (CD) and ulcerative colitis (UC). CD can affect the whole gastrointestinal tract, even though it commonly manifests itself in the distal small intestine, in the ileocaecal region, and frequently appears in the colon.

CD causes chronic inflammation and may lead to chronic abdominal pain, diarrhoea, weight loss, fatigue and obstruction or perianal lesions, a result of an abnormal immune response as well as compromised epithelial barrier function. The cause of CD remains unclear although genetic, immunological, and environmental factors as well as the intestinal microflora are believed to be involved in the onset and development of the disease. Indeed, one of the features of CD is an epithelial barrier dysfunction, where the epithelial monolayer, composed of IECs, presents lesions and superficial injuries. Genetic factors associated with susceptibility to CD have been identified, and mutations in Paneth cell-expressed genes such as NOD2, ATG16L1 and IL-23R genes predominate in CD patients, supported by the fact that in such patients the production of antimicrobial peptides by Paneth cells is decreased. The bacteria-fighting capacity of the mucosal immune system is therefore compromised and may allow the infiltration of pathogens in the lamina propria of the gut leading to the activation of several inflammatory T cell types such as Th1 cells, Th2 cells and Th17 cells. These cells can secrete pro-inflammatory cytokines, for example, IFNγ and TNF. The perpetuation of pro-inflammatory immune responses in this context, by resulting stimulation of other cells such as macrophages, endothelial cells and monocytes and probable inhibition of intestinal regulatory T cells, leads to epithelial injury. [24-26].

UC is a chronic inflammatory disease that is restricted to the colon, mostly characterised by intermittent mucosal inflammation. Similarly to CD, the pathogenesis involves genetic predisposition, environmental factors, epithelial dysfunction, and dysregulation of the immune response [27]. Colonic epithelial cell defects and epithelial barrier and mucous dysfunction are considered major players in the genesis of UC. Additionally, patients with UC have shown decreased microbiota diversity, causing dysbiosis, although to a lesser extent than CD patients. Regarding the immunological scene during UC, several immune cells have been linked to the development of this disease. ILCs seem to increase the expression of cytokines, transcription factors and cytokine receptors. In addition, it appears that there is accumulation of neutrophils in the blood and colonic tissue of UC patients. Furthermore, a novel population of Th cells, Th9 cells, produce IL-9, a cytokine that inhibits cellular proliferation and repair and have been identified as possible contributors to UC [27].

In order to better comprehend the complexity of IBD and the underlying mechanisms of its pathogenesis, several animal models of IBD have been developed, among which is the commonly used dextran-sulfate sodium (DSS)-induced colitis model. DSS chemically induces damage to the epithelium lining the large intestine, disrupting this barrier and allowing the dissemination of bacteria, their products and other inflammatory factors into the underlying tissue. The DSS colitis model is widely used in IBD research due to the simplicity of its use,

the manipulation and administration of the chemical, as well as the reproducibility of the results [28].

1.3. Intraepithelial Lymphocytes

Intraepithelial lymphocytes reside within the epithelial surface of the intestine and are consequently exposed to numerous luminal antigens which can be either pathogen-derived and harmful, or innocuous as the ones derived from food or commensal organisms [29]. Standing at the forefront of the immune defence strategy of the gut, IELs act as sentinels of the mucosal barrier and first immune responders against pathogens while also ensuring the integrity of the epithelial barrier and tissue homeostasis [2]. Conversely, when dysregulated, IELs can also be significant players in inflammatory immune disorders of the gut and other destructive pathologies.

1.3.1. The IEL compartment

The IEL compartment is very heterogeneous as it comprises several distinct IEL populations distributed differently throughout the intestine and carrying out specific functions of both adaptive and innate nature. IELs subsets can be better comprehended if we take into account the pathway by which they acquire memory traits, the nature of the cognate antigens they recognize, as well as the mechanisms involved in their activation and effector functions [29].

Regarding T cell receptor (TCR) expression, IELs can be TCR^+ or TCR^-. Approximately 90% of all IELs are TCR^+ and can be classified as induced (or conventional) or as natural (or unconventional) [7]. Induced IELs comprise $TCR\alpha\beta^+$ $CD4^+$ and $TCR\alpha\beta^+CD8\alpha\beta^+$ T cell subsets that derive from conventional naïve T cells that migrate to the periphery to become antigen-experienced and subsequently home to the intestinal epithelium. Here they usually gain expression of CD8αα, induced upon entry in the intestine. In contrast, natural IELs include $TCR\alpha\beta^+CD8\alpha\alpha^+$ and $TCR\gamma\delta^+$ T cells that undergo thymic differentiation in the presence of self-antigens and home to the intestine immediately after their generation [2, 7].

In the small intestine of mice, most IELs express the non-classical TCRγδ (60-70%) instead of the classical TCRαβ (30-40%). Interestingly, TCRγδ+ IELs are more abundant in the small intestine, whereas $TCR\alpha\beta^+CD4^+$ are the predominant IELs in the colon (Figure 2). Whereas most peripheral tissues, such as the spleen, lymph nodes and blood circulation, comprise approximately identical fractions of major histocompatibility complex (MHC) class I-restricted $CD8^+$ T cells and MHC class II-restricted $CD4^+$ T cells, a large majority of IELs consist of $CD8^+$ T cells, especially in the small intestine [30, 31].

Conventional $CD8^+$ T cells predominantly express the CD8αβ heterodimer, which functions as a co-receptor enhancing signal transduction through the TCR by improving its interaction with MHC class I-peptide complexes. A distinctive feature of IELs is that they acquire expression of the CD8αα homodimer, which is thought to act as a repressor of TCR signalling and consequently of IEL activation, by interacting and binding with higher affinity with the thymus leukaemia (TL) antigen, a non-classical MHC class I protein selectively expressed in the intestinal epithelium [7]. Hence, it is hypothesized that TCR^+CD8aa^+ IELs, which are considered to be in a semi-activated state, express CD8aa to quench the response to high-affinity antigens [7].

In mice, induced $TCR\alpha\beta^+CD8\alpha\beta^+$ T cells comprise about 20-30% of the IEL compartment, and 70-80% in humans, while $TCR\alpha\beta^+CD4^+$ T cells make up around 10-15% of total IELs in both mice and humans. Induced $TCR\alpha\beta^+CD8\alpha\beta^+$ are more enriched in the small intestine, whereas $TCR\alpha\beta^+CD4^+$ T cells are more prevalent in the terminal section of the small intestine, the ileum, and also in the colon, as there is a reduction in their frequency in the duodenum and distal colon [32, 33] (Figure 2).

Conversely, in mice, natural $TCR\gamma\delta^+$ IELs constitute around 40-70% of the IEL compartment, and in secondary lymphoid organs γδ T cells represent around 1%, while in humans this subset composes only 15-20% of the intestinal IEL compartment. Interestingly, in mice, the proportion of $TCR\gamma\delta^+$ IELs decreases from the small to the large intestine, whereas in humans the reverse happens, given that $TCR\gamma\delta^+$ IELs are more enriched in the colon (Figure 2). Natural $TCR\alpha\beta^+CD8\alpha\alpha$ IELs constitute approximately one-third of the total natural $TCR\alpha\beta^+$ compartment and are very rare in adult humans [7, 32, 33].

Disparities in the distribution of IEL populations in the small and large intestine may be explained by the distinct local cues they receive in each compartment. It is well established that, in homeostasis, microbial load in the colon is much higher than in the small intestine; yet, the thicker mucus layer present in the colon is also more effective in stopping microbiota from reaching the epithelium. Additionally, the small intestine is the primary location for food absorption, which dramatically increases the antigen load present and can differentially impact IELs of the small intestine compartment, which are absent in the large intestine [32] (Figure 2).

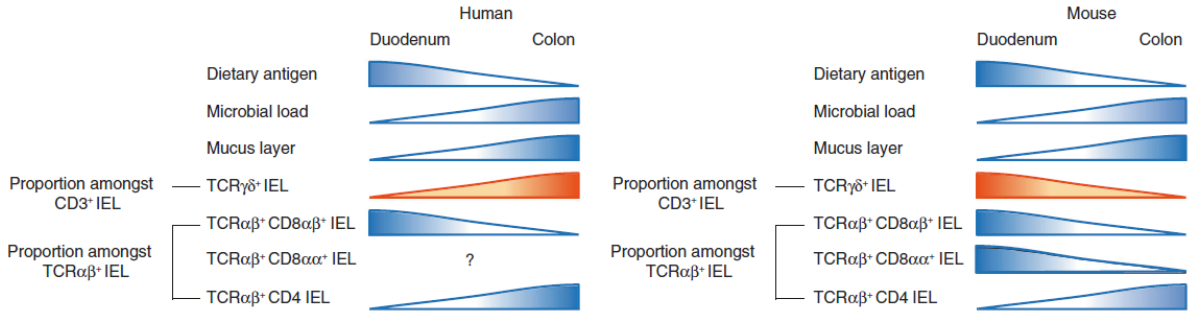

Figure 2 | Regional differentiation of intraepithelial lymphocytes, in human and mice. The small intestine (duodenum) is covered in mucus, creating a large surface area for its principal digestive function. The colon has a higher microbial content and thicker mucous layer as less digestion takes place there and additional anti-microbial action is needed. The two panels show the relative T cell receptor (TCR) αβ+ and TCRγδ+ IEL distribution in the duodenum and colon, and their possible correlation with dietary antigen and microbial load in the two compartments. The comparisons are made directly between the duodenum and colon, therefore the linear depiction of increases/decreases in proportions between the two segments are meant for simplicity and not to illustrate the progression across the other segments of the gut. Adapted from Mayassi et al [32].

Recruitment of IELs to the intestinal epithelium is mediated by the expression of surface receptors such as CC-chemokine receptor 9 (CCR9), a surface receptor which binds with its ligand chemokine ligand 25 (CCL25) expressed in IECs, and therefore crucial for the homing of IELs to the gut. Integrin $\alpha_E\beta_7$, also termed CD103, is expressed in all IELs and interacts with E-cadherin, expressed by enterocytes, enabling entry and retention of IELs in the intestinal epithelial tissues [7, 34]. Unlike lymphocytes in other tissues, IELs are resident on the gut epithelium and do not recirculate, maintaining close interactions with IECs and promoting tissue homeostasis [7].

1.3.2. Development and maintenance of IELs

The T cell lineage is a product of thymic differentiation of bone marrow precursors. Similarly, all IEL subsets undergo differentiation in the thymus; however, the scope of IEL development remains puzzling, and further characterization is needed [2] (Figure 3).

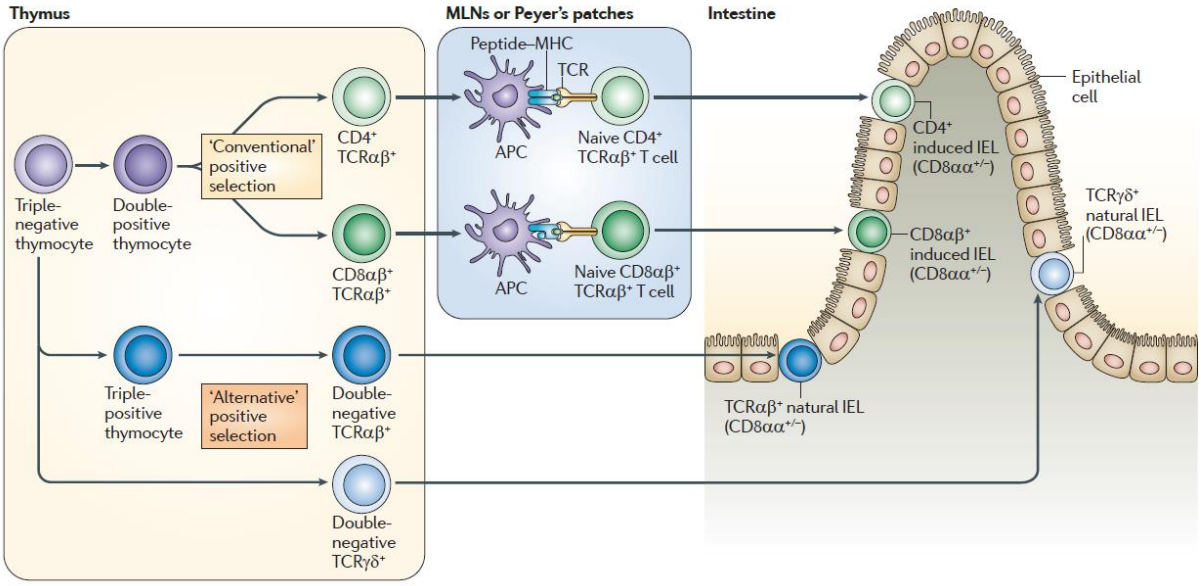

Figure 3 | Development, priming and homing of natural and induced IELs. Overview of thymic selection processes involved in the development of induced and natural IELs. Induced IELs undergo a conventional positive selection in the thymus, are subsequently primed in the periphery, exiting Peyers patches or mesenteric lymph nodes as antigen-experienced T cells which migrate to the intestinal epithelium. Natural IELs undergo a self-antigen driven alternative positive selection and immediately migrate to the intestinal epithelium. Modified from Mucida et al [2].

Induced IELs arise from conventional $CD4^+TCR\alpha\beta^+$ or $CD8\alpha\beta^+$ $TCR\alpha\beta^+$ T cells. In the thymus, $TCR\alpha\beta^+$ double-positive thymocytes ($CD4^+CD8\alpha\beta^+$) undergo conventional positive selection and differentiate into CD4+ or CD8αβ+TCRαβ+ T cells that subsequently migrate to the periphery, entering MLNs or Peyer's patches as conventional naïve T cells (Figure 3). Upon reaching the periphery, they encounter cognate antigens presented by antigen-presenting cells (APCs) and become antigen-experienced T cells, acquiring an effector phenotype (Figure 3). During priming in the periphery, naïve T cells can upregulate intestinal homing receptors, LFA-1, CCR9 and CD103, and acquire gut homing capacity. A fraction of CD4+ and CD8αβ+TCRαβ+ T cells that migrate to the gut acquire expression of the CD8αα homodimer, an activation marker. Likewise, the expression of the early activation marker CD69 is also induced upon entry in the intestine. Interestingly, upon upregulation of CD8αα, CD4+TCRαβ+CD8αα+ cells gain some CD8+ T cell properties such as cytotoxicity. The repertoire of induced IELs is mainly shaped by non-self-antigens encountered in the periphery, which explains why this population is absent at birth and accumulates and expands with age, as exposure to exogenous antigens increases. Induced IELs express characteristic markers of conventional T cells, in a memory-like phenotype, such as CD2, CD5, CD28, LFA-1 and Thy1, unlike natural IELs [2, 7].

Natural IELs comprise TCRαβ+ and TCRγδ+ T cells that migrate to the intestinal epithelium immediately after their development. In the thymus, natural TCRαβ+ IEL precursors undergo an agonist positive selection exiting the thymus as double-negative (CD4-CD8αβ-) TCRαβ+ (Figure 3). In fact, IELs acquire their phenotype in the thymus where they encounter self-antigens, as thymic differentiation is self-antigen driven, which explains why natural IELs are present at birth and decrease with age as well as their propensity for self-reactivity [35]. Indeed, there has been a lengthy discussion regarding the development of natural IELs, but it has become clear that these cells are thymus derived and shaped in the periphery [36]. During thymic development, natural IEL precursors upregulate intestinal homing receptors CD103 and CCR9, resulting in their immediate recruitment to the intestinal epithelium [37, 38]. Most TCRαβ$^+$ and TCRγδ$^+$ T cells acquire expression of CD8αα, as a final stage of their differentiation upon entry into the intestinal epithelium. TGFβ acts as a cue to induce both CD8αα and CD103 expression. These cells exhibit an activated phenotype and express cytotoxicity mediators such as granzyme (Gzm) B, as well as several NK cell receptors [2, 7, 34].

IEL maintenance relies on several factors present at the local epithelial environment. Studies have shown that most IELs seem to be influenced by the intestinal microbiota, as CD4$^+$TCRαβ$^+$CD8αα$^+$ and TCRαβ$^+$CD8αα$^+$ IELs prevalence and cytotoxicity is decreased in germ-free mice [34]. Maintenance and activation of IELs also depend on the interplay between IECs and microorganisms, specifically via Toll-like receptors (TLRs), a group of pattern recognition receptors (PRR) which recognize pathogens. Specifically, TLR2 induces IL-15 production by triggering nuclear factor-κB (NF-κB) signalling. IL-15 signals via the transcription factor T-bet to promote IEL precursor maintenance. Absence of TLR2 results in a decrease of intestinal IEL proliferation and activation [39]. TLRs also induce intracellular signalling through MyD88, an adaptor protein involved in transcriptional activation of cytokine genes. MyD88-deficient mice display a significant decrease in the numbers of TCRαβ$^+$CD8αα$^+$ and TCRγδ$^+$ IELs, as well as a reduced expression of IL-15. These observations come to show that MyD88-dependent signalling is crucial for IEL development and maintenance [40]. Another PRR, nucleotide-binding oligomerization domain-containing protein (NOD) 2 recognizes gut microbiota and senses microbial products. NOD2 signalling triggers IL-15 production, contributing to IEL maintenance [41, 42]. Taken together, these findings suggest that the microbiota may play an important role in IEL maintenance.

Besides the microbiota, IELs are also influenced by the environment and its metabolites. The arylhydrocarbon receptor (AhR), a ligand-activated transcription factor, is a crucial regulator of IEL maintenance, and its deficiency compromises immunoregulation and epithelial barrier integrity [43]. Intestinal immune cells also rely on specific metabolites derived from the

microbiota, environment and diet, such as AhR ligands, which are dietary antigens. AhR ligands can determine the span of the immune response as well as T cell differentiation, maintenance, and function in the intestinal epithelium [21, 34].

1.3.3. IEL activation, regulation, and dysregulation

The activation status of IELs is widely studied yet still poorly understood. Most IELs share characteristics with effector and memory cells. Under steady-state conditions, IELs express activation markers such as CD69 and CD44, contain cytoplasmic granules for cytotoxic activity and can express NK surface receptors, corroborating their effector-like phenotype. IELs can secrete cytokines, yet do not contain transcripts for cytokine expression during steady-state, which they present during inflammation [42]. Resembling memory T cells, IELs do not secrete large amounts of immune mediators or undergo clonal expansion; they are long-lived and arrested in a heightened activation state [21, 44]. IELs display an increased metabolic potential, expressing high levels of transcripts for metabolic enzymes, thus substantiating their poised activation status and effector-like phenotype [44]. Transcriptional analysis has revealed that IELs constitutively express transcripts of genes associated with cytotoxic activity, such as Fas ligand, GzmA and GzmB, CCL5, and with immunoregulatory function, such as PD-1 [42]. IELs seem to be under strict regulation, as their poised yet halted activation status suggests that some factors are preventing a full activation, but also that upon exogenous insult, their activation is accelerated [21]. The factors implicated in the semi-activation state of IELs are still not fully understood, as it is not clear if IELs are stimulated via TCR or if they sense other cues such as inflammation, tissue damage or cell stress [42].

Disease incidence in the intestinal environment as a consequence of pathogen invasion or overstimulation of the immune system can bring about severe consequences, given that aberrant immune responses often occur. In fact, during the onset of IBD or celiac disease, the intestinal mucosa contains persistently high numbers of activated T-cells, featuring IFNγ and IL-17 secreting T cells [45]. In CD, IL-12 is increased in inflammatory lesions [46]. Additionally, induced TCRαβ IELs have been shown to aggravate coeliac disease by causing villous atrophy [47]. The main function of TCRγδ IELs is to safeguard the intestinal epithelium against microorganisms and inflammatory insults, as well as promote healing and epithelial barrier integrity. Compelling evidence shows they execute their protective function through cytokine secretion and production of antimicrobials effectors [48]. However, TCRγδ IELs seem to be highly activated at inflammatory sites of IBD patients, and there seems to be a correlation between IEL numbers and disease severity [49, 50]. Furthermore, TCRγδ IELs are able to

produce IFNγ; notwithstanding, these cells are also capable of controlling the production of IFNγ by other immune cells, which is indicative of TCRγδ IEL ability to protect the epithelium against foreign insults and exacerbated immune responses [2, 7]. Studies in mice demonstrated that the same microbial, dietary and environmental factors that influence IEL development and function are also implicated in the development of IBD [51]. Taken together, there are arguments in support of both the protective function of IELs as well as their pathological role. A better understanding of the immune networks that wire and control different immune responses and functions of IELs is necessary to unveil their role in intestinal pathologies such as IBDs.

1.4. Regulation of T cell receptor signalling by Protein Tyrosine Phosphatases and Kinases

1.4.1. Regulation of T-cell receptor signalling

Expression of a TCR is a distinct characteristic of T cells, and its interaction with a peptide-MHC complex is essential for several cellular outcomes such as T cell activation, proliferation, differentiation, apoptosis, and cytokine release. Individual mature T cells each express a unique TCR, selected by its ability to bind peptides presented by MHC molecules. Thus, the vast TCR repertoire diversity ensures that T cells are capable of recognizing different peptides with a broad range of binding affinities, for example, both self and non-self-peptides [52]. Activation occurs upon T cell encounter of an agonist peptide presented by professional APCs on peptide-MHC complexes, resulting in the formation of the immunological synapse. This interaction triggers a downstream network of signalling cascades that are tightly regulated and determine cell activation, differentiation and effector and memory immune responses [53]. The TCR is a transmembrane receptor complex composed of ligand-binding α and β chains or γ and δ chains, a CD3 complex with ε, γ and δ chains, and two ζ chains subunits that contain immunoreceptor tyrosine-based activation motifs (ITAMs) (Figure 4) [3]. Engagement of the TCR results in the recruitment of co-stimulatory receptors, like CD28, as well as binding of CD4 or CD8 co-receptors. The cytosolic domain of CD4 and CD8 co-receptors binds the protein tyrosine kinase (PTK) lymphocyte-specific protein tyrosine kinase (LCK), a member of the Src family of protein tyrosine kinases (SFK). LCK promotes the phosphorylation of tyrosine (Tyr) residues in the ITAMS of the CD3 ζ chains, leading to recruitment of ζ-chain-associated protein of 70kDa (ZAP70), and its subsequent phosphorylation and activation by LCK [3, 53]. Activation of ZAP70 promotes its kinase activity, leading to the phosphorylation of its target molecules such as the transmembrane adaptor linker for activation of T cells (LAT) (Figure 4). Phosphorylation of LAT Tyr residues by ZAP70 allows the recruitment of multiple downstream

adaptors and signalling molecules leading to the formation of the LAT signalosome and responsible for the activation of several major signalling branches [54]. Whether directly or through binding to adaptors, LAT recruits and activates effector signalling molecules such as phospholipase C gamma 1, (PLCγ1), IL-2 inducible T cell kinase (ITK) and Vav1 [54]. Ultimately, activation of LAT-associated molecules induces signal transmission through three major signalling pathways: the Ca^{2+}-calcineurin, the mitogen-activated protein kinase (MAPK, also known as ERK) and NF- κB (Figure 4). The outcome of this signal propagation is the nuclear translocation of several transcription factors, including activator protein 1 (AP-1), NF-κB and nuclear factor of activated T cells (NFAT) (Figure 4). Along with co-receptor and cytokine signalling, this induces several T cell responses such as T cell proliferation, migration, cytokine production and effector functions [53].

These TCR signalling pathways require molecular mechanisms to limit effector function and avoid immune pathology [55]. Precise control of Tyr phosphorylation by PTK and Tyr dephosphorylation by protein tyrosine phosphatases (PTP) is essential to the establishment of appropriate immune responses.

Phosphorylation and dephosphorylation of LCK kinase's Tyr residues Y394 and Y505 render the conformation of its catalytic domain either active or inactive, this way regulating LCK's kinase activity. Phosphorylation of the Y505 residue by protein tyrosine kinase CSK renders the catalytic domain of LCK inactive, whereas autophosphorylation of the Y394 residue activates LCK [53].

Similarly to PTKs, PTPs also serve a pivotal role in regulating T cell activation, given the control function they exert upon key receptors and intracellular signalling molecules in T cells. In fact, PTPs are the natural counterpart of PTKs, and the balance between kinase and phosphatase activity controls the phosphorylation and dephosphorylation dynamic of the signalling network. Depending on the target site and on the signalling network status, PTPs can either have an enhancing or inhibitory role upon their target molecules, shaping TCR signalling and consequently its activation [3, 56]. PTPs can be subdivided into two categories: receptor-type PTPs (RPTPs) and nonreceptor-type PTPs (PTPNs). RPTPs have extracellular domains and are thought to bind ligands, unlike PTPNs that are located predominantly in the cytoplasm.

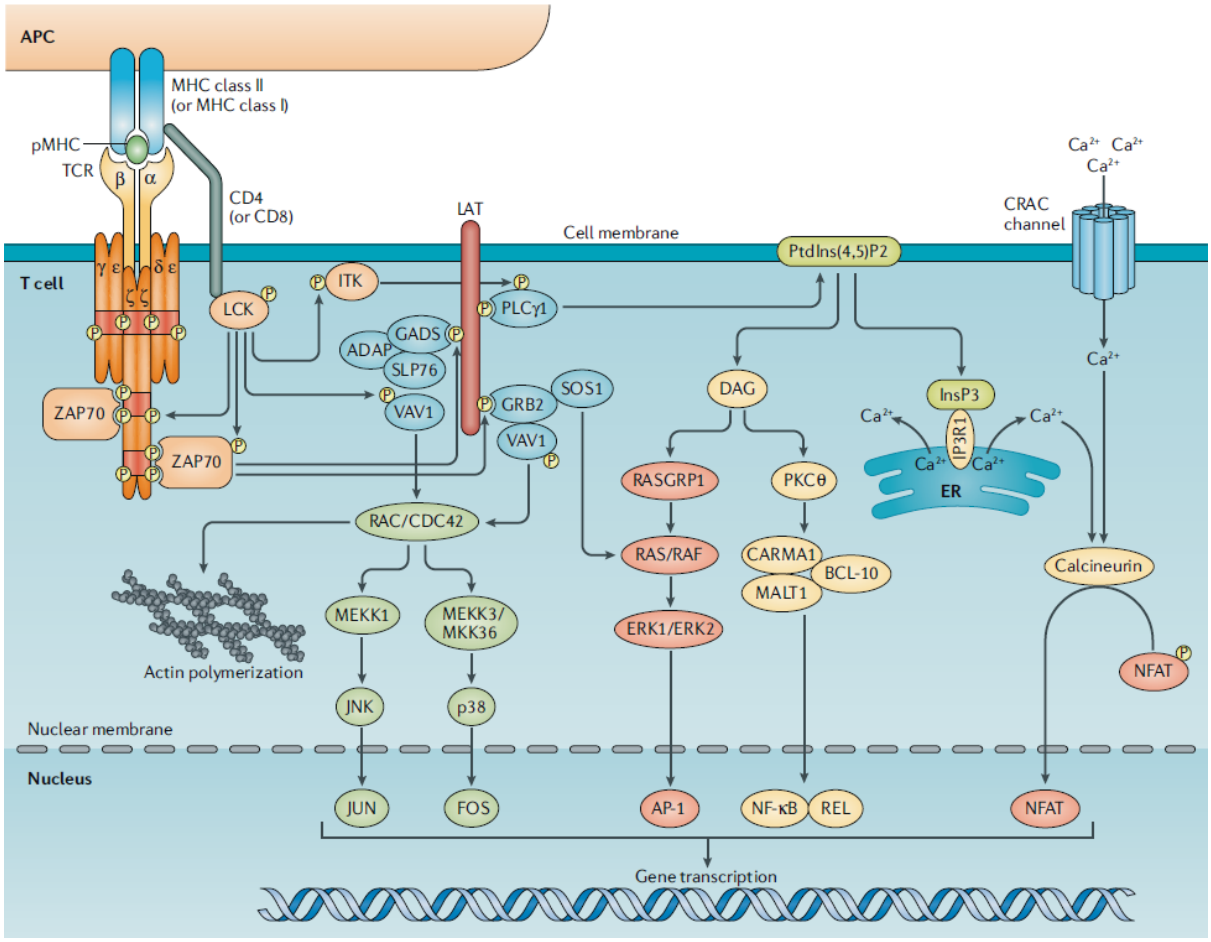

Figure 4 | T cell receptor major signalling pathways. Engagement of the TCR, through binding to a peptide-MHC complex presented by an antigen-presenting cells (APCs), triggers signal transduction through the T cell receptor (TCR). TCR stimulation leads to a downstream cascade of signalling events, where Src family kinases (SFKs) LCK and FYN are activated and bind the intracellular domains of CD4 and CD8 co-receptors. Following recruitment to the TCR, LCK phosphorylates immunoreceptor tyrosine-based activation motifs (ITAMs) in the zeta chains enabling the activation of protein tyrosine kinase ZAP70. ZAP70 then phosphorylates adaptor protein linker for activation of T cells (LAT) which enables recruitment of several effector molecules triggering signal transduction through different signalling pathways. Major signalling pathways such as the Ca^{2+}-Calcineurin, the NF-κB pathway, and the mitogen-activated protein kinase (MAPK) pathway result in T cell proliferation, migration, cytokine release and effector functions. Adapted from Gaud et al [53].

In the context of T cell activation, CD45 and CD148 are widely studied RPTPs. CD45 dephosphorylates both Y394 and Y505, hence, being able to positively or negatively regulate the activity of LCK. In addition, several cytoplasmatic phosphatases are reported to dephosphorylate the Y394 residue, consequently inactivating LCK [53].

Several PTPNs are reported to act on TCR signalling in lymphocytes, by dephosphorylating Y394, therefore causing LCK inactivation, including PTPN2, PTPN22, SH2 domain-containing

phosphatase 1 (SHP-1; also known as PTPN6), PTPN12 and dual-specificity protein phosphatase 22 (DUSP22) (Figure 4). Conversely, other PTPNs such as SHP-2 can positively regulate TCR signalling. Therefore, some PTPNs are believed to be key players in the dampening of TCR signalling and subsequent lymphocyte activation. Additionally, increasing evidence has shown that alterations to the genetic makeup of PTPs are linked to human autoimmune diseases, as we will discuss further along [53].

1.4.2. TCR signalling in IELs

The TCR has a central role in the activation of conventional T cells and the spurring of subsequent functional responses as well as in the survival of some T cell populations [57-59]. Interestingly, it is still unclear whether IELs require functional TCRs and TCR inherent signal transduction machinery for IEL activation, development, and differentiation.

T cell activation can be perceived as a polarised on-off switching mechanism in peripheral T cells; however, in IELs, this concept does not seem to apply. As stated before, IELs are activated yet resting T cells, as they exhibit some but not all properties of activated T cells, showing readiness but also the need for additional immunological cues to achieve full effector potential. Indeed, starting as partially activated cells with cytotoxic potential and expressing some activation markers suggests that IELs are prepared to deliver a full effective immune response as soon as a TCR/CD3 signal is received, in a coordinated co-stimulatory signalling process [60]. The mechanisms by which IELs can regulate suppression or rapid activation remain unclear as selective or activating ligands are still unknown [61]. It is now established that TCR signalling is necessary for agonist positive selection of both αβ IELs and γδ IELs, in the thymus and intestine, respectively. Nevertheless, it is still uncertain whether TCR engagement is vital to fully activate IELs [35]. Full activation might require peptide-antigen presenting, cytokines and co-stimulatory molecules/receptors [61].

IELs present several unconventional innate-like signalling receptors such as CD94 and NKG2D that indicate a possible TCR independent activation mechanism [35]. Studies using transgenic mice expressing a TCR specific for an MHC-I- restricted ovalbumin peptide (OT-I) have revealed that IELs are activated even in the absence of cognate antigen priming [60, 62]. Furthermore, γδ natural IELs have also been described to respond to innate-like stimulus, in the absence of TCR ligands and be activated via TLR [63] or AhR pattern recognition receptors [64, 65], as well as NK receptors.

Furthermore, recent studies identified butyrophilin-like (Btnl) molecules, expressed constitutively in the gut, to contribute to development and homing of TCRγδ IELs to the gut

and skin epithelium. TCR ligands such as Btnl1, Btnl6, Skint1 and Skint2 are required for normal γδ IEL development, expansion, and retention in the gut, shaping TCR repertoires of $γδ^+$ IELs in gut and skin, respectively [66]. Nonetheless, Btnl ligands seem to be downregulated in both chronic inflammatory diseases and colorectal cancer, suggesting that they do not regulate IEL activation in the gut [35].

Similarly to peripheral T cells, most IELs require a CD3-derived signal, engaging the TCR-CD3 complex, to initiate immune activation and a proliferative response [60, 61]. Use of anti-CD3 antibodies allows for direct stimulation of the CD3 signalling complex, bypassing TCR ligation, and is often a strategy used to stimulate IELs in mice. Following anti-CD3 stimulation, IELs acquire features of fully activated effector cells such as the expression of CD44, Ly-6C, OX40, FasL and CD25, together with the expression of cytotoxic mediators and cytokines [67, 68]. Anti-CD3 *in vivo* administration triggers systemic activity, indiscriminately stimulating T cells throughout all tissues, consequently resulting in a cytokine storm release with increasing levels of TNF and IFNγ and causing a diarrhoea pathology [69]. Upon anti-CD3 stimulation release of GzmB is also prompted, increasing the cytotoxic potential of IELs. Altogether, this indicates that the TCR-CD3 complex in IELs is functional as anti-CD3 stimulation induces cytokine production and cytolytic potential [42, 60, 61]. Notably, several functional studies have relied on anti-CD3 costimulation.

Additionally, studies have reported that blocking TCR signalling using anti-TCRγδ-blocking antibodies or with a Syk-ZAP70 kinase inhibitor did not produce any changes in the migration and functionality of γδ IELs during infection [35, 70]. IELs differ from conventional T cells found in the periphery, exhibiting an activated yet resting phenotype, and appear hyporeactive in response to TCR stimulation [71]. In fact, the γδ TCR and the αβ TCR carried by natural IELs have shown to be refractory to agonistic TCR antibodies, such as α-CD3, in ex vivo stimulation assays [71, 72]. Therefore, given that specific agonistic antibodies for both TCRγδ and TCRαβ IELs did not trigger signalling of the TCRs, IELs appear to undergo activation through other mechanisms [71, 72]. Studies intended to assess TCR function measured intracellular free calcium concentration in response to TCR cross-linking [71]. High basal calcium levels were observed in both TCRγδ and TCRαβ IELs, and cells were shown to be refractory to TCR-dependent calcium influx induction. When administrating *in vivo* specific TCRγδ-blocking antibodies, a decrease on basal calcium levels was detected on TCRγδ IELs, altogether suggesting that the TCR is constantly triggered and functional *in vivo* [71]. Thus, it seems that TCR triggering does not induce calcium flux increase or phosphorylation of downstream signalling molecules hence the necessity for the elucidation of the intricate signalling network in IELs.

The question of how IELs are activated remains, although understanding what drives their activation and what restrains them brings us one step closer to unveiling new strategies against inflammatory intestinal diseases.

1.4.3. Receptor and Non-receptor Protein Tyrosine Phosphatases in TCR signalling

Immune cell development and function relies on the equilibrium between PTK and PTP activity, which enables the precise regulation of Tyr phosphorylation (Figure 5). Conversely, the disruption of this equilibrium may compromise immune cell function and cause autoimmunity, immunodeficiency or malignancy [73]. The receptor-type phosphatase CD45, encoded by the *PTPRC* gene, is expressed among all nucleated hematopoietic cells. It comprises an extracellular segment and two cytoplasmic PTP domains. Several studies with loss of function *in vitro* and *in vivo* models have confirmed this phosphatase's dual role in T cell activation. CD45 enables a positive regulation of T cell activation by dephosphorylating inhibitory Tyr residues of SFKs, such as LCK and FYN. However, it also restricts activation by dephosphorylating activating Tyr residues of LCK (Figure 5). Considering the central role of CD45 to enhance T cell activation, T cells carrying mutations of the *PTPRC* gene could favour hyperactivation and contribute to autoimmunity.

The lymphoid phosphatase (LYP), encoded by the *PTPN22* gene, is a cytosolic PTP belonging to the PEST family (Figure 5). LYP, and its murine orthologue PEST domain-enriched tyrosine phosphatase (PEP), are constituted by an N-terminal domain, an interdomain and a C-terminal domain that contains four proline-rich motifs. *PTPN22* is expressed solely on hematopoietic cells, including T and B lymphocytes as well as myeloid cells, and is predominantly located in the cytoplasm although occasionally also present in the nucleus.

PTPN22 has a powerful negative regulatory role in T cell activation, by inhibiting early signalling downstream of the TCR. Enforcement and overexpression of *PTPN22* in early cell studies indicated its inhibition of TCR signalling by dephosphorylation of Tyr residues in LCK, FYN and ZAP70 [74-76]. PTPN22 was found to form a complex with cytoplasmic C-terminal Src kinase (CSK), a suppressor of T cell activation through phosphorylation of the inhibitory Tyr residues of LCK and FYN. Additional putative targets of PTPN22 were identified resorting to substrate trapping experiments. These showed that PTPN22 might act by dephosphorylating positive Tyr residues of SFKs and also their substrates, including LCK, ZAP70, CD3 ζ chain, VAV and CD3ε [3, 73, 77].

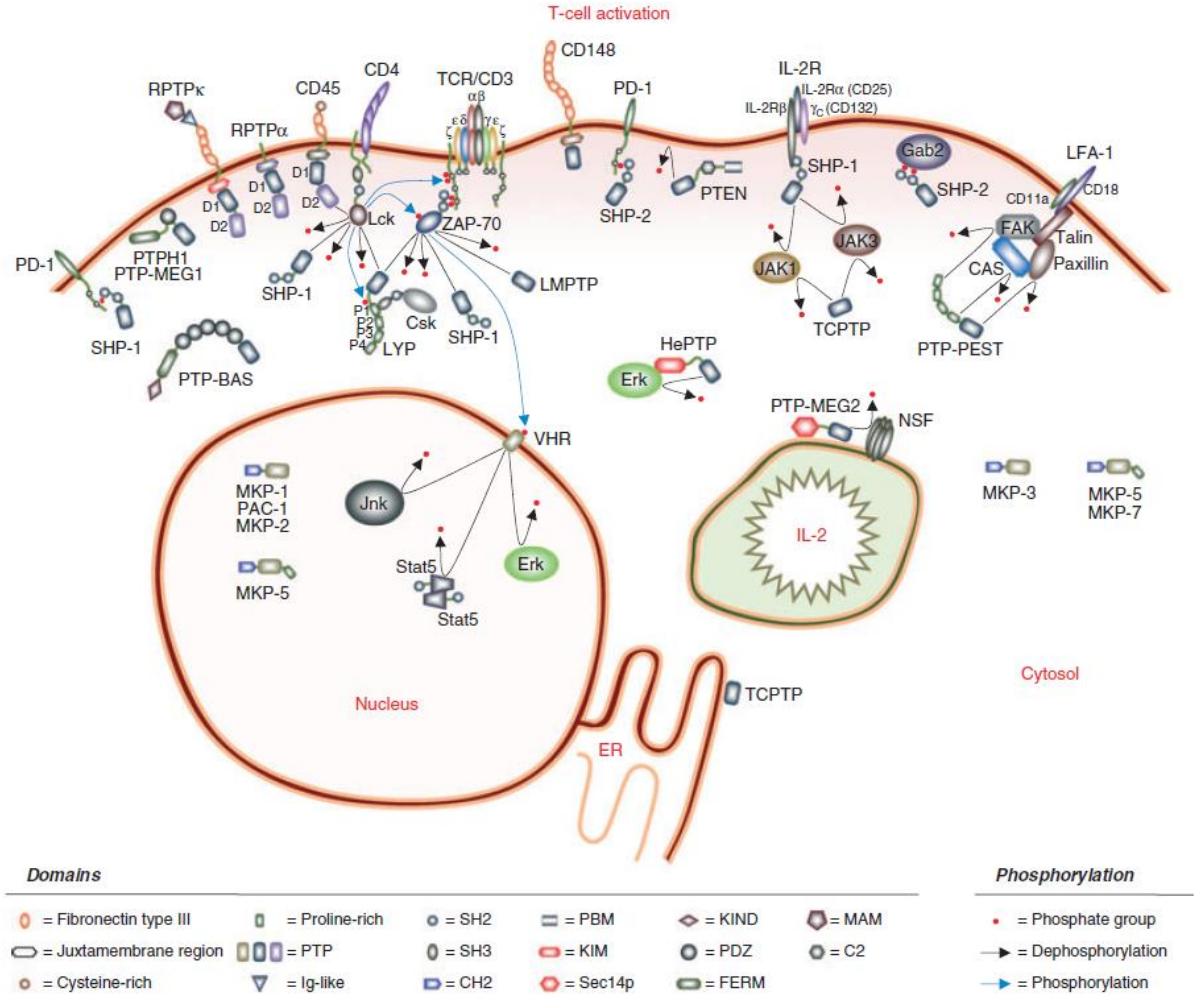

Figure 5 | Protein tyrosine phosphatase regulation of T cell activation. Schematic representation of T cell activation that involves tyrosine phosphorylation at multiple levels. Both receptor and nonreceptor protein tyrosine phosphatases (PTPs) play multiple roles in the regulation of T cell activation, mediating both positive and negative regulation of intracellular signalling events. Upon T cell receptor engagement with antigen, waves of phosphorylation and dephosphorylation follow. This dynamic signalling cascade is controlled by the interplay between PTPs and protein tyrosine kinases (PTKs). PTPs act on Src family kinases (SFKs), on the ζ chains of immunoreceptor tyrosine-based activation motifs (ITAMs) and ZAP70, regulating their phosphorylation status and consequently their activity. PTPs also regulate the function of several cell receptors. Further downstream, PTPs control T cell migration, post-transcriptionally induced cytokine secretion, proliferation, and function. Adapted from S. M. Stanford et al [3].

Additionally, PTPN22 importance in TCR signalling was highlighted in a study where PTPN22-deficient mice were generated. These mice presented an accumulation of effector and memory $CD4^+$ and $CD8^+$ T cells and developed lymphadenopathy and splenomegaly [78]. Data revealed increased positive selection in the thymus, which resulted in the expansion of these compartments, suggesting that PTPN22 controls proliferation. Also, when *Ptpn22*$^{-/-}$ T cells were adoptively transferred, an increase in proliferation was noted when compared to

controls. In this study, it was also revealed that PTPN22 deficiency did not affect naïve T cell proliferation, however in *Ptpn22*$^{-/-}$ effector/memory T cells TCR signalling, expansion and function was enhanced. Adoptive transfer of *Ptpn22*$^{-/-}$ T cells showed enhanced proliferation comparing to controls, indicating that the increased T cell expansion and function is T cell intrinsic [78, 79]. Leading from the fact that PTPN22 regulates LCK autophosphorylation, mediated by Tyr^{394}, the phosphorylation of its positive and negative Tyr residues was analysed. Wild-type effector T cells, upon stimulation with anti-CD3 (α-CD3), showed TCR-induced phosphorylation of LCK Tyr^{394}, whereas this was augmented and sustained in *Ptpn22*$^{-/-}$ effector T cells, consequently enhancing phosphorylation of ZAP70 and ERK. Therefore, it can be concluded that the absence of PTPN22 induces hyperresponsiveness of effector cells upon TCR engagement. These observations endorse the belief that PTPN22 controls the function of activated effector T cells by dephosphorylating LCK autoregulatory site, suppressing T cell activation. Additionally, this data also suggests PTPN22 shapes proliferation of effector and memory T cells [78].

Recent studies using transgenic OT-1 mice reveal that PTPN22 can distinguish between weak and strong agonist peptides. In both naïve and effector T cells, PTPN22 limits signalling via the TCR when responding to weak agonist peptides and self-peptides, but not when presented with strong agonist antigens. T cell activation is arrested by PTPN22-mediated dephosphorylation of LCK and ZAP70 kinases, and consequently, *Ptpn22*$^{-/-}$ cells have a lower threshold for activation. These findings render PTPN22 as a key regulator of T cell responses to low-affinity antigens [79, 80]. PTPN22-deficient CD8+ cytotoxic T cells became self-reactive and triggered inflammatory cytokine release in response to self-peptide, supporting the notion that PTPN22 acts as a break on responses to weak antigens [81].

PTPN22 has been associated with multiple human autoimmune diseases. A missense single-nucleotide polymorphism (SNP) C1858T in the *PTPN22* gene was reported to increase predisposition to Type-1 Diabetes (T1D), rheumatoid arthritis (RA) and systemic lupus erythematosus (SLE). C158T leads to a substitution of tryptophan for arginine at the position 620 (PTPN22-R620W), which impairs the ability of PTPN22 to interact with CSK. Reports are somehow controversial regarding the functional effects of this substitution, and several models have been proposed to assess the effect of PTPN22-R620W in the variation in TCR signalling. Even though some authors point to a PTPN22-R620W gain of function model in T cell activation, supported by reduced basal levels of ERK activation and IL-2 production in PTPN22-R620W carriers, other authors report it as a loss-of-function model where carriers of PTPN22-R620W display increased anti-CD3 induced ERK phosphorylation and cell proliferation. Many reports have emerged, and the functional effects of this mutation are still

not fully described [79]. Nonetheless, strong epidemiological evidence links PTPN22-R620W to autoimmune diseases, therefore making *PTPN22* a possible therapeutic target.

The Src homology region 2 (SH2)-containing PTPs, SHP-1 and SHP-2, are structurally very similar. However, their expression patterns and regulatory mechanisms and most importantly, their physiological functions differ [3, 82].

SHP-1, encoded by the *PTPN6* gene, is expressed in all hematopoietic cell lineages at all stages, and also in epithelia at lower levels. SHP-2, encoded by the *PTPN11* gene, is ubiquitously expressed. Both SHPs are cytosolic PTPs containing two N-terminal SH2 domains, followed by a central catalytic PTP domain and a C-terminal tail containing two tyrosyl phosphorylation sites. SHP-1 and SHP-2 are both regulated by phosphorylation of the C-terminal region [3, 56].

In T cells, both ZAP70 and LCK have been indicated as possible substrates of SHP-1, which acts as an early inhibitor of TCR signalling and a regulator of T cell activation threshold. In SHP-1-deficient thymocytes and peripheral T cells, a stronger TCR stimulation response, reflected in IL-2 production and proliferation, was recorded, due to the increase in SFKs activation [83, 84]. Upon TCR engagement, SHP-1 is phosphorylated by LCK and recruited to the TCR where it can in turn dephosphorylate signalling molecules such as ZAP70, LCK, PI3K, VAV, SLP-76 and CD3ζ suggesting that SHP-1 acts as a negative regulator of T cell activation (Figure 5). It has been demonstrated that weak antagonistic signals lead to faster recruitment of SHP-1 to the TCR, entering a negative feedback loop where LCK phosphorylates SHP-1, which in turn dephosphorylates LCK [85]. In the case of strong agonistic TCR stimuli, ERK is activated, and a conformational change is induced on LCK, resulting from its phosphorylation on a serine residue. Hence, this prevents LCK from binding to SHP-1 and leads to inactivation of LCK, allowing for a sustained TCR signal.[3]

Recently, a study resorting to a conditional knockout of SHP-1 in mature single-positive cells allowed for a better understanding of the cell-intrinsic consequences of SHP-1 deficiency. Results showed that SHP-1 deficiency reduces the numbers of short-lived $CD8^+$ effector cells without compromising the long-lived memory cell pool [86].

SHP-2 is perceived as a key regulator of receptor-mediated signalling and essential for embryonic development, haematopoiesis and lymphoid development. SHP-2, unlike SHP-1, is deemed a positive regulator of TCR signalling. This is supported by the fact that conditional deletion of SHP-2 in T cells is shown to inhibit T cell activation, by compromising TCR-induced ERK activation and proliferation. Conversely, opposing its role as a positive regulator of T cell activation, SHP-2 mediates the inhibitory effects of receptors such as PD-1, PECAM-1 and BTLA (Figure 5) [3, 56].

PTPN2, also referred to as T-cell protein tyrosine phosphatase (*TCPTP*), is a ubiquitously expressed cytosolic PTP involved in the regulation of several signalling pathways, mainly via cytokine receptors and Jak-STAT. Observations of mice with conditional *PTPN2* deficiency suggest that *PTPN2* acts as a regulator of early TCR signalling by dephosphorylating LCK and FYN (Figure 5). *PTPN2*-deficient mice also present increased thymocyte positive selection and accumulation of effector-memory T cells in the periphery. PTPN2-deficient T cells display higher phosphorylation of Tyr residues and increased proliferation. Additionally, a non-coding polymorphism of *PTPN2* has been linked to human autoimmune diseases such as T1D, RA, Crohn's disease and CD. [56]

PTP-PEST, encoded by the *PTPN12* gene, is a ubiquitously expressed cytosolic PTP, which belongs to the PTPN22 family and is highly expressed in immune cells. Similar to PTPN22, it appears that PTPN12 negatively regulates TCR signalling and binds CSK. PTPN12 regulates signalling proteins such as focal adhesion kinase (FAK), Cas and Pyk2, a PTK involved in adhesion and migration (Figure 5). In fact, PTPN12 induces dephosphorylation of Tyr phosphorylation substrates including Shc, Cas, Pyk2 and Fak, inhibiting the Ras pathway [87]. Studies where an allele of PTPN12 was conditionally deleted proved that PTP-PEST is not essential for T cell development or primary responses. Nonetheless, PTPN12 deficiency caused a selective increase in Pyk2 phosphorylation, correlating to a decrease in T cell adhesion following secondary T cell activation [88]. Additionally, the study, using a mice model of multiple sclerosis, also showed that PTP-PEST-deficient mice are less susceptible to develop T cell-dependent immunopathology [87, 88]. Therefore, PTPN12 may contribute to the development of such diseases through a T cell-mediated process.

PTPH1, encoded by the *PTPN3* gene, is widely expressed including in hematopoietic tissues. When overexpressed, PTPN3 inhibits TCR signalling through the dephosphorylation of ITAMs in the CD3ζ chains of the TCR (Figure 5) [3].

PTP-MEG1 encoded by the *PTPN4* gene is expressed in most tissues, including the lymphoid tissue. Overexpression of PTPN4 inhibits TCR-induced T cell activation (Figure 5) [3].

PTP-MEG2, encoded by the *PTPN9* gene, is widely expressed, including in T cells and is necessary for vesicle formation (Figure 5) [3].

PTPD1, encoded by the *PTPN21* gene, is a cytosolic phosphatase activated by SFKs. In response to growth factor stimulation PTPN21 in turn dephosphorylates a negative Tyr residue of Src, reducing its activity. Through the formation of a complex with actin, Src and FAK, PTPN21 regulates adhesion, scattering and migration [89].

Taken together, abundant data supports the importance of PTPs and of their role in the regulation of TCR signalling networks and consequently on the activation of T cells and T cell homeostasis. Through the dephosphorylation of Tyr residues, PTPs modulate the interaction between signalling molecules and shape T cell responses to several stimulus. Modifying the sensitivity of the TCR through the inhibition of PTPs, one of its major regulatory mechanisms, allows for a better comprehension of the impact of these molecules in TCR signalling transduction and subsequent T cell activation and function. Sodium orthovanadate (SOV) and pervanadate are general PTP inhibitors which are known to suppress phosphatase activity and increase phosphorylation of Lck positive Tyr residues and can therefore be used to simulate the absence of PTPs and study their role in T cell responses [90, 91].

It is of uttermost importance to ensure appropriate immune responses in order to prevent autoimmunity. Indeed, there are several studies investigating the contribution of PTPs for autoimmune disease. For example, the role of SHP-2 in T cells during induced-colitis and associated carcinogenesis was assessed in SHP-2 conditional knock-out mice models, and it was found that SHP-2 deficiency in T cells aggravated colitis and increased pro-inflammatory cytokine levels [92].

Additionally, mutations in PTPN22 have been linked with several autoimmune disorders even though their contribution to these pathologies remain unclear. Specifically, some PTPs have already been associated with IBDs, and two genetic variants of PTPN22, loss of function polymorphism PTPN22-R263Q and gain-of-function PTPN22-R620W, have been associated with reduced risk of UC and CD, respectively [93, 94]. Indeed, loss-of-function mutations in PTPN22 are associated with lymphoproliferative disease and accumulation of memory-phenotype T cells with time, yet do not culminate in spontaneous autoimmunity [78]. Further studies, then followed to show that the lack of spontaneous autoimmunity might be due to an increase in regulatory T cell and enhanced efficiency of this population. In this study, transfer of PTPN22 deficient T cells into a lymphopenic recipient resulted in a more severe colitis phenotype [95]. Therefore, further studies are necessary to determine if the effects of PTPN22 variants in intestinal T cell homeostasis contributes to IBD.

Thus far, in this context, the role of PTPs in IELs has not been addressed creating a knowledge gap in what regards the roles and actions mechanisms of PTPs in IEL activation and their involvement in IBDs.
Therefore, this master thesis intends to clarify PTP contribute to IEL activation status and unravel their complex interaction, highlighting its relevance to IBD pathologies.

2. Aim of the study

The integrity of the intestinal barrier is relentlessly challenged by the presence of commensal and pathogenic microbiota, as well as an array of different antigens. IELs are embedded in the intestinal epithelium and are critical for the preservation of the intestinal barrier integrity by ensuring the equilibrium between immune tolerance and protection of the epithelium [42]. The regulation of IEL protective function and cytotoxic effector responses is essential to keep these cells in check and prevent aberrant and potentially damaging immune responses, as well as conserve their protective function. In fact, it has been shown that dysregulated activation and function of IELs is critically involved in the exacerbation of intestinal damage in the onset of IBDs, such as CD and coeliac disease [23, 49, 50]. Intriguingly, IELs share characteristics with both effector and memory T cells presenting an activated yet resting phenotype. The heightened activation state of IELs, which is thought to facilitate a swifter cell activation, is suggestive that a cue for activation is received and sets them apart from conventional T cells [21]. Contrastingly, IELs are arrested in a poised activation status which indicates that a blockade preventing full activation might be in place, keeping these cells from achieving full effector function [21]. The cues that regulate IEL effector function are still largely unknown, and whereas in conventional T cells the TCR is essential to activate effector responses, the involvement of the TCR for the activation of IELs is still controversial. Indeed, T cell activation is mediated by signal transduction downstream of the TCR in a tightly regulated cascade of signalling events, requiring the engagement of several downstream signalling molecules. PTKs and PTPs regulate the dynamic wave of phosphorylation generated downstream of the TCR and through dephosphorylation of signalling molecules, PTPs can determine the enhancement or reduction of the function of their targets. Hence, PTPs are critical for the regulation of TCR signalling and impairment of their function can be potentially hazardous and cause T cell related pathologies.

This work aims to determine the impact of PTP on the activation of IELs and establish a connection between their heightened, yet poised activation state. In order to address this question, we defined several goals:

1. Determine the TCR responsiveness of IELs

2. Assess the expression and activity of PTP in IELs

3. Establish whether the inhibition/deletion of certain PTPs, both *in vitro* and *in vivo,* has an impact on TCR signal transduction in IELs

3. Material and Methods

3.1. Material

3.1.1. Equipment

All equipment used are specified below.

Table 3.1 | Equipment and devices.

Equipment	Manufacturer
Agitorb 200	**Agitorb**
Agitorb 200 ICP	
7500 Fast Real-time PCR System	**Applied Biosystems**
FACSAria III	**BD Biosciences**
FACSAria IIu	
LSRFortessa X-20	
Mini-PROTEAN Tetra Vertical Electrophoresis	**Bio-Rad**
Mini Trans-Blot Electrophoretic Transfer Cell	
PowerPac Basic	
T100 Thermal Cycler	
Centrifuge 5430 R	**Eppendorf**
Centrifuge 5810	
Centrifuge 5810 R	
GE Healthcare Life Sciences Amersham Imager	**GE Healthcare**
Precision Balance EMS	**KERN**
Labnet International Accublock Digital Dry Bath	**Labnet International**
autoMacs Pro Separator	**Miltenyi**
MACSMix Tube Rotator	
pH Meter Lab 855	**SI Analytics**
Analogue Tube Roller Mixer SRT9	**Stuart Equipment**
Infinite M200 Microplate reader	**Tecan**
NanoDrop 2000	**Thermo Scientific**
ARE Hot Plate Stirrer	**VELP Scientifica**
Micro Star 17	**VWR**
Micro Star 17R	
Primovert	**ZEISS Primovert**

3.1.2. Consumables

Table 3.2 | Consumables.

Product	Manufacturer
Falcon Centrifuge Tube (15mL, 50mL)	**Corning**
Polystyrene round-bottom tubes (5mL)	
Cell Strainer (100µm)	
Costar 96 Well Cell Culture Plate	
Cell culture OrDish	**Orange Scientific**
Filter Tips (20µL, 200µL, 1000µL)	**Greiner bio-one**
96 Well Flat-bottom Clear Microplate	
uTIP Universal Fit Pipette Tips (10µL)	**Biotix**
CellTrics Strainer (50µm)	**Sysmex**
autoMACS Columns	**Miltenyi**

3.1.3. Reagents

All reagents used in this thesis were purchased from the companies shown below, unless otherwise specified in the text.

Table 3.3 | Reagents used for tissue and cell isolation procedures and molecular assays.

Reagents	CAT	Company
30% Acrilamide/Bis	1610158	Bio-Rad
30x DTT	14265	Cell Signalling
3x Blue Loading Buffer	56036	Cell Signalling
Ammonium Chloride (NH4Cl)	9724	Sigma Life-Science
Ammonium Persulfate (APS)	A3678	Sigma Life-Science
Bovine Serum Albumine (BSA)	A7906	Sigma-Aldrich
Dextran-Sulfate Sodium	130110	MP Biomedicals
Dulbecco's Modified Eagles Medium Complete	D5030	Sigma-Aldrich
EDTA	3690	Sigma-Aldrich
EDTA	3690	Sigma-Aldrich
Fetal Bovine Serum (FBS)	F9665	Sigma Life Science
Fixation/Permeabilization Concentrate	00-5123-43	Invitrogen
Fixation/Permeabilization Diluent	00-5223-56	Invitrogen
Glycine	G8898	Sigma Life-Science
HCl	3044174	Sigma-Aldrich

HEPES	H0887	Sigma-Aldrich
***InVivo*MAb Anti-mouse α-CD3ε**	BE0001-1	BioXCell
Methanol	322415	Sigma-Aldrich
Na2EDTA	E5134	Sigma-Aldrich
PBS 10x	MB18201	NZYTech
Penicillin-Streptomycin	15140-122	Gibco
Percoll	17-0891-01	GE Healthcare
Permeabilization Buffer 10x	833356	Invitrogen
Phosphate Buffered Saline (PBS) 1x	A1286301	Gibco
Pierce ECL Western	32106	Thermo-Scientific
Polymyxin B	P6902	Sigma
Potassium Bicarbonate (KHCO3)	60339	VWR Chemicals
RnaLater	494623	Invitrogen
SDS solution 10%	1610416	Bio-Rad
SHP1/2 Inhibitor	565851	Sigma-Aldrich
Sodium Chloride	AM9760G	Ambion
Sodium dodecyl sulfate pellets	P4417	Gibco
Sodium Orthovanadate	S6508	Sigma-Aldrich
Sodium Pyruvate	S8636	Sigma-Aldrich
N,N,N′,N′-Tetramethylethylenediamine (TEMED)	T9281	Sigma Life-Science
Trizma Base	T1503	Sigma Life-Science
Tween-20	P1379	Sigma Life-Science

3.2. Methods

3.2.1. Mice

C57BL/6J mice were obtained from Charles River Laboratories. TCRδ-eGFP, C57BL/6 Ly5.1 and Rag2-deficient ($Rag2^{-/-}$) mice were bred at the Instituto de Medicina Molecular, Lisbon, Portugal. PTPN22-deficient mice ($PTPN22^{-/-}$) were kindly provided by the Zamoyska Lab at the University of Edinburgh.

Mice were kept under specific pathogen-free (SPF) conditions and housed in individually ventilated cages (IVC) in a temperature-controlled environment with a 12h-hour light/dark cycle. All mice had free access to drinking water and food. Unless otherwise stated, male and female mice were used at 5 to 15 weeks old. All animal experiments were conducted according

to regulations of the Direção-Geral de Alimentação e Veterinária (DGAV) and institutional guidelines approved by the local ethics committee.

For α-CD3 stimulation *in vivo* anti-mouse α-CD3ε monoclonal antibody was administrated intraperitoneally at 25µg/200µL/mouse in PBS.

For SOV-induced inhibition of PTPs *in vivo,* mice received by intraperitoneal injection SOV at 200µg/mouse in PBS.

3.2.2. T cell isolation

Intestinal intraepithelial lymphocytes were isolated by removing the small intestine or colon. Organs were flushed with PBS, opened longitudinally and sectioned into 1cm fragments. The fragments were immersed in IEL buffer and shaken at 37ºC for 15 minutes at 220 rpm, followed by 15 minutes at 150rpm. Single-cell suspensions were obtained by filtering the intestine fragments through a 100µm strainer and further purified by isotonic 37,5% Percoll density gradient centrifugation. Splenocytes for MACS purification were isolated by mashing spleens through a 50µm or 100µm strainer and washing with PBS. Splenocytes for downstream FACS analysis were isolated by mashing spleens in ACK, through a 40µm strainer, for red blood cell lysis. Cells were analysed or sorted further through FACS.

3.2.3. Fluorescence Activated Cell Sorting

Following T-cell isolation, IELs and splenocytes were resuspended MACS buffer. To further purify single-cell suspensions, IELs were stained for CD8α APC and similarly splenocytes were stained for Thy1.2 (CD90.2) APC for 5min at RT. Posteriorly, APC-binding magnetic beads were added and left to incubate for 20min at 4ºC. Cells were filtered through a cell strainer and by immunomagnetic cell separation, cells were positively selected in an autoMACS Pro Separator (Miltenyi) and then surface stained for further cell sorting. Cell sorting was performed by BD FACSAria III (BD Biosciences) and FACSDiva Software 8.0. Sorted cells were preserved in RNAlater for subsequent RNA extraction or in loading dye for Western blotting. Cells for *in vitro* T cell stimulation were stimulated immediately after sorting.

3.2.3.1. Buffers and solutions for tissue and cell isolation and purification

IELs were isolated from the tissues in IEL buffer prepared in PBS (1mM Sodium Pyruvate; 20mM HEPES; 10mM EDTA; Pen-Strep; 10% (v/v) FBS; 10µg/mL Polymyxin B). A 37,5% Percoll gradient solution was prepared in water (37.5% (v/v) Percoll; PBS (1x); adjusted to pH

7.5) for gradient separation of IELs. MACS buffer was prepared in PBS (0.5% (v/v) FBS; 2mM EDTA) and used for further cell purification. Erythrocytes Lysing Buffer 10x ACK (1.5M NH4Cl ; KHCO3 100mM; 10mM Na2EDTA; adjusted to pH 7.2) was prepared in water and diluted before use to 1x ACK, for erythrocyte lysis.

3.2.4. Quantitative PCR

Cells were FACS sorted as described above and immediately stabilised in RNAlater (Invitrogen). RNA was extracted using the RNeasy Mini Kit or Micro Kit (Qiagen) and reverse-transcribed using the High-capacity RNA-to-cDNA kit (Applied Biosystems), according to the manufacturer's protocol. Resulting cDNA was diluted 1:4. Quantification of mRNA expression of the genes of interest by qPCR was performed using the SYBR Select Mastermix (Applied Biosystems) or NZYSpeedy qPCR Green Master Mix (NZYTech), according to the manufacturer's protocol. Specific QuantiTect Primer Assays (Qiagen) were used for the following genes of interest: PTPN1, PTPN3, PTPN4, PTPN5, SHP-1, PTPN9, SHP-2, PTPN12, PTPN21, PTPN22 (PEP), as shown on Table 3.4. Gene expression was normalized to the housekeeping gene Rn18s (Qiagen). qPCR reactions were performed in a 7500 Fast Real-Time PCR System (Applied Biosystems), according to the following protocol: holding stage at 95°C for 2min; cycle stage of 40 cycles at 95°C for 5s followed by 60°C for 30s and acquisition of fluorescence; 95°C for 15s; 60°C for 1 min and increase of temperature by 1% up to 95°C continuous acquisition for melting curve; 60°C for 15s. Results were analysed using the 7500 Software 2.3v provided.

Table 3.4 | Primers used for qPCR analysis.

Gene	Primer Assay	CAT	Detection System	Company
PTPN1	Mm_Ptpn1_1_SG	QT00166418	SYBRGreen	Qiagen
PTPN3	Mm_Ptpn3_2_SG	QT01550031		
PTPN4	Mm_Ptpn4_1_SG	QT00149457		
PTPN5	Mm_Ptpn5_1_SG	QT01063580		
PTPN6	Mm_Hcph_1_SG	QT00155967		
PTPN9	Mm_Ptpn9_1_SG	QT00170520		
PTPN11	Mm_Ptpn11_1_SG	QT00103362		
PTPN12	Mm_Ptpn12_1_SG	QT00168126		
PTPN21	Mm_Ptpn21_1_SG	QT00197862		
PTPN22	Mm_Ptpn8_1_SG	QT00103943		
Rn18s	Mm_Rn18s_3_SG	QT02448075		

3.2.5. *In vitro* T cell stimulation

Cells were FACS sorted, pelleted and supernatant was removed. For T cell stimulation, α-CD3 and HamIgG antibodies were used *in vitro*. Cells for stimulated samples were resuspended and incubated in 25µL of α-CD3 (5µg/mL) for 10min at RT, posteriorly 25µL of HamIgG (20µg/mL) were added and cells incubated for 2min at 37ºC. For unstimulated control samples, 50 µL of PBS were added to the cells and incubated for 10min at RT, followed by 2 min at 37ºC. In H_2O_2 control samples, 50µL of H_2O_2 (10mM) were added and cells were incubated for 2min at 37ºC. Afterwards, 25µL of 3x Loading buffer was added to all samples and they were immediately placed on ice. Samples were stored at -20ºC.

3.2.6. Western Blotting

Cells were previously FACS sorted and whole cell extracts were prepared and stored in Blue loading buffer 1x at -20ºC. Whole cell extracts were sonicated, heated to 95ºC for 5min and centrifuged at 17000g for 3 minutes. Samples were then loaded on a 10% gel alongside a protein standards ladder (Kaleidoscope Precision Plus Protein Ladder, Bio-Rad) and fractioned by SDS-PAGE. Electrophoresis was ran at 50V for 30 minutes and afterwards at 150V for approximately 1 hour in a Mini-PROTEAN Tetra Vertical Electrophoresis Cell. Membranes were activated in methanol and rinsed with Transfer Buffer. Proteins were transferred from the gel matrix to PVDF membranes (Bio-Rad) using a Mini Trans-Blot Electrophoretic Transfer Cell, during 1 hour at 100V, at constant 350mA. Membranes were incubated in Blocking solution for 60min and washed with TBST (Tris-Buffered Saline with Tween-20). Membranes were incubated with primary antibodies, diluted in 2% BSA in TBST and 0.002% Sodium Azide, according to antibody dilutions specified on Table 3.5., on a tube roller overnight, at 4ºC. Membranes were rinsed and washed once for 10 minutes in TBST and then incubated with a secondary antibody, an anti-rabbit-Horseradish peroxidase-conjugated antibody (antibody diluted 1:2500 in Blocking Buffer) for 1 hour. After incubation, the membranes were washed 3 times for 10min with TBST. Membranes were developed with ECL and signal acquired in an Amersham Imager 680, according to manufacturer's protocols.

3.2.6.1. Western Blot stock solutions and buffers

Whole cell extracts were preserved in 1x Blue loading buffer with Dithiothreitol (DTT) (10% (v/v)). Samples were loaded in a 10% gel, separated by electrophoresis in Running Buffer (25mM Tris Base; 192mM Glycine; 0.1% SDS), and the proteins were transferred to the

membrane in Transfer Buffer (25mM Tris Base, 192mM glycine). TBST (20mM Tris Base; 150mM NaCl; 0.1% (v/v) Tween) rinsing and washing membranes. A Blocking solution (5% (w/v) Powder Milk in TBST) was used to incubate the membranes after transfer.

Table 3.5 | Antibodies used for Western Blot analysis.

Specificity	Host/Clonality	Dilution	CAT nº	Company
ZAP70	Rabbit monoclonal	1:1000	2705S	Cell Signalling
PLCγ1	Rabbit monoclonal	1:1000	5690T	Cell Signalling
ERK	Rabbit monoclonal	1:2000	4695T	Cell Signalling
pZAP70	Rabbit monoclonal	1:1000	2717	Cell Signalling
pPLCγ	Rabbit monoclonal	1:1000	14008	Cell Signalling
pERK	Rabbit monoclonal	1:2000	4370T	Cell Signalling
PTPN22	Rabbit monoclonal	1:1000	14693	Cell Signalling
SHP-1	Rabbit monoclonal	1:1000	3759	Cell Signalling
SHP-2	Rabbit monoclonal	1:1000	3752	Cell Signalling
α-Tubulin	Rabbit monoclonal	1:1000	9099S	Cell Signalling
B-Actin	Rabbit monoclonal	1:1000	12620S	Cell Signalling

3.2.7. Bone Marrow Chimeras generation

Bone marrow chimeras were generated by transplantation of congenitally labelled bone marrow progenitor cells of PTPN22$^{-/-}$ or WT donor mice into a Rag2$^{-/-}$ recipient mouse. Recipient mice were subjected to sub-lethal irradiation (450rad) 24h before bone marrow transplantation.

Bone marrow was isolated from the hind legs of donor mice. Muscle and connective tissue were removed, and femur and tibia were flushed with DMEM medium to extract the cells. Cells were filtered through a 100µm strainer. Cell numbers and viability were determined manually using a haemocytometer and Trypan Blue staining. Cells were resuspended in PBS at a concentration of 2.5x10^7/mL and subsequently injected intravenously, 200µL per recipient mouse.

Mice were checked for chimeric reconstitution after 6 weeks by flow cytometric analysis of blood samples. Blood was collected from the tail vein and the samples were centrifuged at 4ºC and 500g for 5 minutes and incubated in ACK buffer for 3 minutes. Afterwards, PBS was added, and cells were centrifuged, washed again, and resuspended in PBS. Cells were surface-stained for 30 minutes at 4ºC with fluorescence-conjugated monoclonal antibodies for

CD45.1, CD45.2, TCRβ, TCRδ, GR-1, CD11b, CD19, and LIVE/DEAD. After surface staining, cells were washed with PBS, centrifuged at 300g at 4ºC for 5 minutes. Finally, cells were resuspended in PBS and acquired in a BD LSRFortessa™ X-20 flow cytometer. Flow cytometry data was analysed in FlowJo™ (FlowJo Software for Windows, Version 10.7.0, Ashland, OR: Becton, Dickinson and Company; 2019).

3.2.8. DSS-induced colitis model

DSS was administered in the drinking water at 2,5% (w/v) solution for 6 days, and then replaced with regular drinking water until experiment endpoint. The weight of individual mice was monitored frequently, and body condition was examined and scored in order to assess animal health. Mice presenting a weight loss of more than 20% of initial body weight were sacrificed, according to ethical guidelines. Mice were sacrificed and small intestines and spleens were collected at day 7 after initial DSS treatment. In order to determine disease severity 4 parameters were evaluated including body weight loss, blood loss, stool consistency and general appearance of mice. Each parameter was scored appropriately according to the symptoms manifested, as seen on Table 3.6.

Table 3.6 | Disease severity score for assessment of DSS-induced colitis in mice.

Body Weight Loss		**Occult/Gross Blood Loss**	
No weight loss	0	No visible blood	0
0% - 5%	1	No visible blood and positive hemacult test	1
5 - 10%	2	Slight traces of blood on stools	2
10 - 20%	3	Bloody stools, no blood-stained perineum	3
> 20%	4	Rectal hemorrhage, blood-stained perineum	4
Stool Consistency		**General Appearance**	
Well-formed/normal stools	0	Normal	0
Pasty semi formed stools	1	Piloerection only	1
Soft stools	2	Piloerection and lethargy	2
Diarrhea and no stained perineum	3	Persistently hunched, lethargy and piloerection	3
Watery diarrhea and stained perineum	4	Motionless, sickly, sunken-eyed, ataxic	4

3.2.9. Protein Tyrosine Phosphatase Activity assay

Cells were previously sorted by MACS and FACS sorting, stabilized in PTP assay buffer with DTT and homogenized. PTP activity was determined using a Protein Tyrosine Phosphatase Assay Kit (Abcam). Fluorescence standards were prepared by diluting the 5mM stock in PTP Assay Buffer at a final 100µM concentration, yielding a series of Fluorescence Standards (0, 200, 400, 600, 800, 1200, 1600, 2000 pmol/well). Fluorescence standards were added to the test 96-well plate.

Cells were incubated in ice for 5 minutes and centrifuged at 10,000 x *g* and 4ºC for 15 minutes. Supernatants were collected and kept on ice until further use. Test samples were incubated in the test plate with PTP Assay Buffer ($1.5x10^5$ cells/well). As a negative control another set of test samples was incubated with PTP Assay Buffer and Suramin (2mM). As a background control a well containing only the PTP assay buffer was setup, and as a positive control the PTP provided with the kit was added to a separate well. The plate was preincubated for 10 minutes at 25ºC. The reaction was initiated by adding a PTP substrate to each reaction well. Fluorescence was measured at Ex/Em= 368/460 nm in kinetic mode for 45 minutes at 25ºC, in a Tecan Infinite M200. A fluorescence standard curve was calculated and plotted by correlating the emitted fluorescence, expressed in relative fluorescence units, with the corresponding standard concentrations. Reaction kinetics were plotted and PTP specific activity determined and expressed in pmol/minute/$1x10^5$cells. All standards, controls and samples were assayed in duplicate.

3.2.10. Flow Cytometry

After T cell isolation, splenocytes and IELs, cells were briefly washed with PBS, and transferred to a plate. Cells were resuspended in 200µL of PBS, washed and supernatant was removed. IELs and splenocytes were surface stained for 15 minutes at 4ºC, with fluorescence-conjugated monoclonal antibodies for CD8α, CD8β, TCRδ and TCRβ, CD45.2 or CD45, PD-1, GzmB and LIVE/DEAD Fixable Near-IR staining. Cell were washed and resuspended in Fixation/Permeabilization solution (1:4 of Fixation/Permeabilization concentrate in Fixation/Permeabilization diluent) for 30 minutes, at 4ºC. Cells were washed twice in Permeabilization Buffer (1:10 Permeabilization Buffer in ddH_2O). Intracellular staining was prepared in Permeabilization Buffer, and cells were stained for Ki67 for 30 minutes at 4ºC, followed by one wash with Permeabilization Buffer and another with PBS. Finally, cells were

resuspended in PBS and acquired in a BD LSRFortessa X-20 flow cytometer. Flow cytometry data was analysed in FlowJo™ (FlowJo Software for Windows, Version 10.7.0, Ashland, OR: Becton, Dickinson and Company; 2019).

Table 3.7 | Antibodies used for flow cytometric analysis and FACS sorting.

Specificity		Dilution	CAT	Company
Anti-APC MicroBeads		300	130-090-855	Miltenyi Biotec
CD4	Pe-Cy7	1000	100528	Biolegend
CD4	PerCpCy5.5	500	100540	BioLegend
CD8α	BV605	300	63-0081-82	Invitrogen
CD8α	Pe	500	100708	BioLegend
CD8α	APC	500	17008183	eBioscience
CD8β	FITC	500	126606	BioLegend
CD8β	PerCpCy5.5	500	126610	BioLegend
CD11β	PeCy7	1500	101216	BioLegend
CD19	BV605	200	115540	BioLegend
CD44	AF700	300	103026	BioLegend
CD45	BV605	300	103140	BioLegend
CD45.1	PacBlue	1000	110722	BioLegend
CD45.2	AF700	500	109822	BioLegend
CD45.2	APC	500	109818	BioLegend
CD90.2 (Thy1.2)	APC	400	140312	BioLegend
GR-1	PerCpCy5.5	500	108428	BioLegend
GrzB	PacBlue	500	515408	BioLegend
IFNγ	APC/AF647	200	505810	BioLegend
Ki67	AF647	300	558615	BD Biosciences
Live/Dead Near-IR	APC-Cy7	1000	L34976	Invitrogen
PD1	Pe	500	135206	BioLegend
TCRβ	BV785	500	109249	BioLegend
TCRβ	Pe	300	109208	BioLegend
TCRδ	FITC	200	118106	BioLegend
TCRδ	FITC	200	107504	BioLegend
TCRδ	Pe	200	107508	BioLegend
TCRδ	APC	200	118116	BioLegend
TNFα	PacBlue	200	506318	BioLegend

3.2.11. Statistical Analysis

In the present work, statistical analyses were performed using GraphPad Prism Software (GraphPad Prism version 6 for Windows, GraphPad Software, San Diego, California USA) and is expressed in ±SD or ±SEM, described in each figure legend, where applicable. P values were determined using one-way ANOVA and the Holm-Sidak's post-hoc multicomparison test. Differences were considered statistically significant where $P<0.05$ and significance is expressed as follows: *$P < 0.05$, **$P < 0.01$, ***$P < 0.001$, ****$P < 0.0001$.

4. Results

4.1. TCR stimulation of intraepithelial lymphocytes does not show phosphorylation of downstream molecules

It remains unclear if TCR engagement is crucial for the activation of IELs. Therefore, we first focused on assessing how IELs respond to TCR stimulation. CD8⁺ splenic T cells and small intestinal CD8αα⁺ IELs were flow sorted and incubated with α-CD3 antibodies, which was subsequently crosslinked with anti-HamIgG. Western blot analysis allowed us to evaluate signal transduction downstream of the TCR, by targeting proteins of the signalling cascade and evaluating their phosphorylation status (Figure 6).

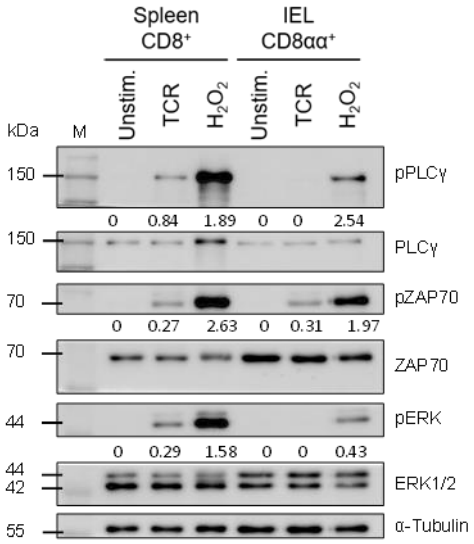

Figure 6 | Upon TCR stimulation, intraepithelial lymphocytes do not exhibit phosphorylation of downstream molecules. Murine CD8⁺ splenocytes and CD8αα⁺ IELs were isolated and purified by MACS and Flow sorting. Cells were stimulated in vitro with 5µg/mL α-CD3 and 20µg/mL α-Hamster IgG (α-CD3 and α-HamIgG crosslinking). Unstimulated cells received only PBS. As a positive control of phosphorylation, cells were incubated with 10mM H_2O_2, inducing overall phosphorylation. Cell lysates were separated by SDS-PAGE, followed by an electrophoretic transfer. The phosphorylation state of PLCγ, ZAP70 and ERK was assessed by immunostaining of PLCγ, ZAP70, ERK and of their phosphorylated counterparts pPLCγ, pZAP70 and pERK. The marker (M) used for reference and the molecular weights of the detected proteins are indicated on the left. The blot was reprobed for α-Tubulin and normalised to its protein expression level, to demonstrate equal protein loading. Relative fold changes were normalised to total protein levels of PLC, ZAP70 and ERK, and are shown below each panel.

We verified that upon TCR ligation, the phosphorylation levels of Tyr319, a tyrosine residue of TCR proximal signalling molecule ZAP70, were similar between CD8⁺ splenocytes and CD8αα⁺ IELs (Figure 6). Additionally, ZAP70 phosphorylation was enhanced in the positive

control H_2O_2-incubated $CD8^+$ splenocytes when comparing to $CD8\alpha\alpha^+$ IELs in the same condition and both at much higher levels than TCR-stimulated cells. However, upon TCR stimulation, distal signalling molecules PLCγ and ERK were phosphorylated in splenic CD8+ T cells, whereas in $CD8\alpha\alpha^+$ IELs, no phospho-PLCγ or phospho-ERK was observed. Similarly, upon H_2O_2 treatment both pPLCγ and pERK were detected in splenocytes and IELs; but at much lower in IELs. Altogether, these data suggest that in IELs only ZAP70, an early TCR signalling molecule, is phosphorylated upon stimulation. The signal transduction does not appear to progress further downstream as the more distal proteins are not phosphorylated. These data indicate that, unlike peripheral $CD8^+$ splenocytes, $CD8\alpha\alpha^+$ IELs do not respond to TCR stimulation in the same way.

4.2. IELs express high levels of protein tyrosine phosphatases

The finding that IELs do not respond to TCR stimulation, as there is no phosphorylation of signalling molecules downstream of ZAP70, suggested that the signalling cascade might be interrupted. We hypothesised that PTPs could be involved in dampening the signal transduction. To assess this, we determined the abundance of cytosolic PTPs in IELs and splenocytes. Firstly, we focused on determining the mRNA expression of PTPN-encoding genes of 10 non-receptor PTPs (*PTPN1*, *PTPN3*, *PTPN4*, *PTPN5*, *PTPN6*, *PTPN9*, *PTPN11*, *PTPN12*, *PTPN21*, *PTPN22*) (Figure 7). Expression of mRNA was measured by quantitative real-time RT-PCR in $CD4^+$, $CD8^+$ and TCRδ T cells from the spleen and two subsets of IELs from the small intestine, CD8αα and CD8αβ.

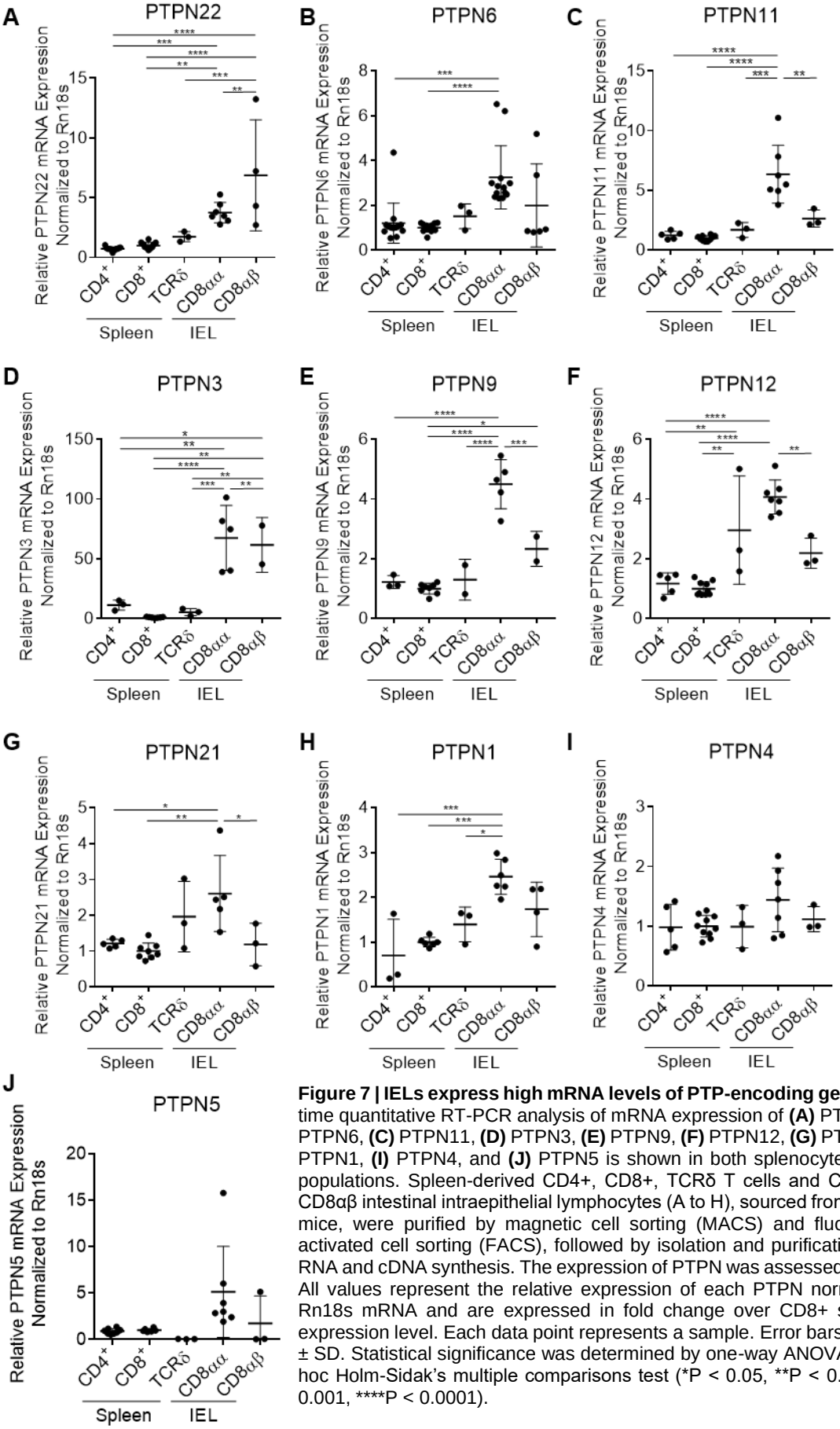

Figure 7 | IELs express high mRNA levels of PTP-encoding genes. Real-time quantitative RT-PCR analysis of mRNA expression of **(A)** PTPN22, **(B)** PTPN6, **(C)** PTPN11, **(D)** PTPN3, **(E)** PTPN9, **(F)** PTPN12, **(G)** PTPN21, **(H)** PTPN1, **(I)** PTPN4, and **(J)** PTPN5 is shown in both splenocytes and IEL populations. Spleen-derived CD4+, CD8+, TCRδ T cells and CD8αα and CD8αβ intestinal intraepithelial lymphocytes (A to H), sourced from C57BL/6 mice, were purified by magnetic cell sorting (MACS) and fluorescence-activated cell sorting (FACS), followed by isolation and purification of total RNA and cDNA synthesis. The expression of PTPN was assessed by qPCR. All values represent the relative expression of each PTPN normalised to Rn18s mRNA and are expressed in fold change over CD8+ splenocyte expression level. Each data point represents a sample. Error bars represent ± SD. Statistical significance was determined by one-way ANOVA and post hoc Holm-Sidak's multiple comparisons test (*P < 0.05, **P < 0.01, ***P < 0.001, ****P < 0.0001).

We found that, generally, most of the PTPNs analysed were differentially expressed in splenic T cells and IELs. For the purpose of this analysis, we show mRNA expression data in fold change over splenic $CD8^+$ T cells. We observed that in comparison to CD8+ T cells from the spleen, in CD8αα IELs, the expression of *PTPN22*, *PTPN6* and *PTPN11* was substantially increased. There was an approximately 3 to 4-fold increase in *PTPN22* and *PTPN6* expression in CD8αα (Figure 7, A and B). In CD8αβ IELs, *PTPN22* mRNA levels were variable but significantly increased (Figure 7A) whereas in this subset *PTPN6* expression did not vary significantly from conventional $CD8^+$ T cells. *PTPN11* expression was increased 6-fold in CD8αα IELs compared to $CD8^+$ splenocytes (Figure 7C). In CD8αβ, expression of *PTPN11* was significantly lower than in CD8αα IELs, but not different from the expression of this PTP in splenic $CD8^+$ T cells. We observed high variability in *PTPN3* mRNA levels between splenocytes and IELs, with both IEL subsets markedly expressing more *PTPN3* (Figure 7D). *PTPN9* and *PTPN12* expression were significantly augmented in CD8αα IELs, presenting a 4-fold increase in relation to $CD8^+$ splenocytes (Figure 7, E to F). In CD8αβ, the expression of *PTPN9* and *PTPN12* was significantly lower compared to CD8αα IELs, but still amounting to a 2-fold increase over splenic $CD8^+$ T cells (Figure 7, E to F). *PTPN21* and *PTPN1* were found to be more expressed in CD8αα IELs by a 2-fold increase over the expression of $CD8^+$ splenocytes. The level of expression of *PTPN4* and *PTPN5* expression was similar throughout the T cell subsets analysed, and no significant differences were found (Figure 7I). The data shown here represent basal expression of each phosphatase in each lymphoid population analysed and indicated that PTPN-encoding genes are highly expressed in IELs, surpassing PTPN expression in conventional T cells. Notably, CD8αα IELs high PTPN expression is evident across all the PTPNs analysed, and PTPN22, PTPN6, PTPN11, PTPN9 and PTPN12 are consistently 4 to 6-fold more expressed in CD8αα than in conventional T cells.

In order to assess how the augmented expression of PTPN-encoding genes in IELs would translate in the cellular abundance of the corresponding proteins, we quantified protein expression of PTPN22, SHP-1 (*PTPN6*) and SHP-2 (*PTPN11*) in spleen-derived $CD4^+$, $CD8^+$ and TCRδ T cells and in CD8αα and CD8αβ IELs from the small intestine (Figure 8A). Protein levels were determined by Western Blot.

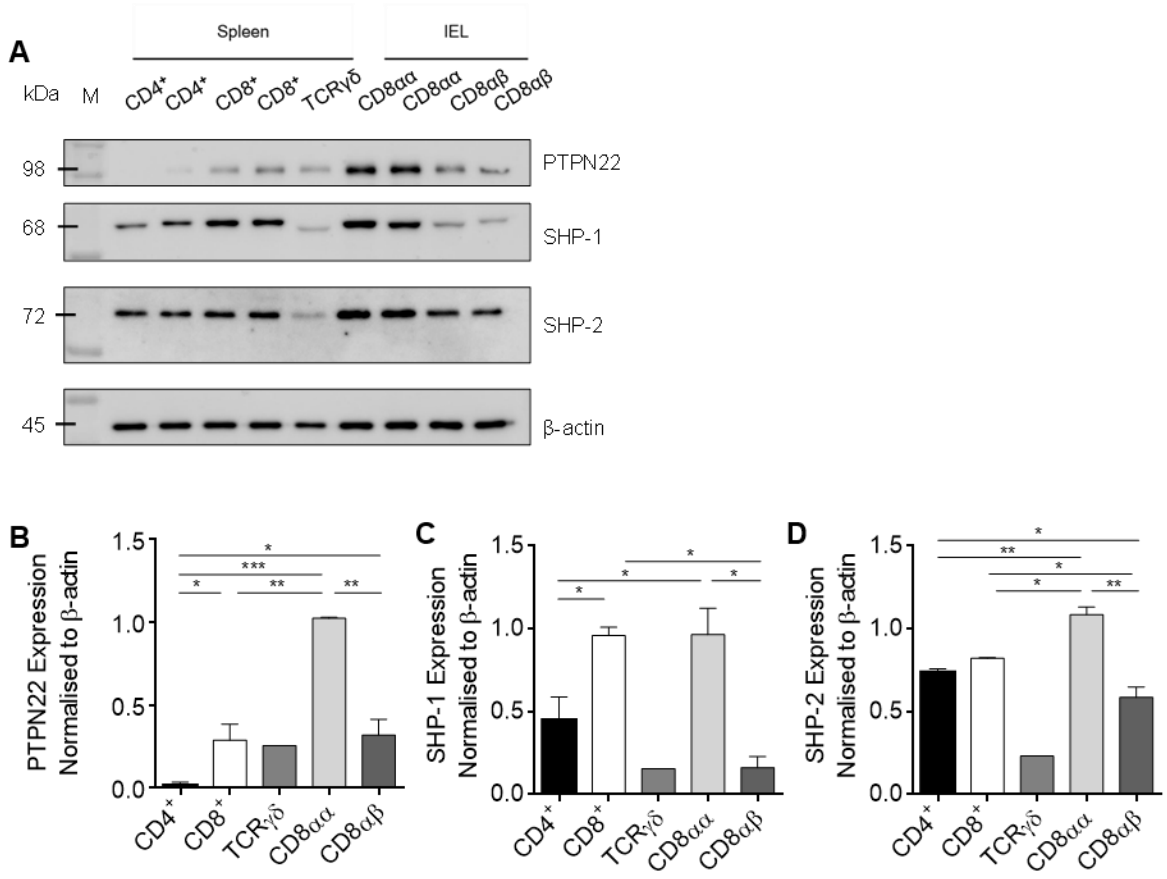

Figure 8 | IELs express high protein levels of PTPN22, SHP-1 and SHP-2. (A) Representative western blot image of the protein expression levels of PTPN22, SHP-1 and SHP-2 in cell lysates of $CD4^+$, $CD8^+$ and TCRδ splenocytes and CD8αα and CD8αβ IELs was determined by Western Blot. Splenocytes and IELs were sourced from C57BL/6 mice and purified by MACS and Flow sorting. Cells were lysed in loading buffer and sonicated. Cell lysates were separated by SDS-PAGE, followed by an electrophoretic transfer. The membrane was probed with antibodies for anti-Ptpn22, anti-SHP-1 and anti-SHP-2. The blot was reprobed for β-actin to demonstrate equal protein loading. Each lane represents one individual sample. The marker (M) used for reference and the molecular weights of the target proteins, expressed in kDa, are indicated on the left. **(B** to **D)** Relative protein expression of **(B)** PTPN22, **(C)** SHP-1 and **(D)** SHP-2 were normalised to β-actin protein expression levels. Average values of biological repeats are plotted (n=2). Error bars represent ± SD. Statistical significance was determined by one-way ANOVA analysis and post hoc Holm-Sidak's multiple comparisons test (*P < 0.05, **P < 0.01, ***P < 0.001).

We evaluated PTPN22 protein levels in the different subsets and found that it was significantly higher in CD8αα IELs compared to other lymphocyte populations analysed (Figure 8A and B). Specifically, PTPN22 protein level was increased significantly in CD8αα IELs compared to splenic $CD8^+$ T cells. In CD8αβ IELs PTPN22 protein level was significantly lower than in CD8αα and closer to levels detected in splenic $CD8^+$ cells. The same was verified in splenic TCRδ T cells, which also showed lower amounts of PTPN22. Consistent with the results for

the mRNA expression, $CD4^+$ T cells from the spleen showed the lowest levels of PTPN22 protein. We also assessed SHP-1 protein levels, which were similar in CD8αα IELs and CD8 splenocytes. SHP-1 was markedly present in both, but no significant difference was found between IELs populations (Figure 8A and C). In addition, SHP-1 protein levels are significantly lower in both TCRδ T cells and CD8αβ IELs. Furthermore, we determined SHP-2 protein levels and observed a significant increase in CD8αα IELs, surpassing the levels of this protein in both spleen-derived populations and CD8αβ IELs (Figure 8A and D). TCRδ T cells exhibit a very low level of this protein. It is noteworthy that natural IELs show higher protein levels of PTPN22 and SHP-2 as well as mRNA expression, these data indicate a potentially higher activity of these PTPs in natural IELs.

Taken together, our findings indicate that IELs exhibit increased PTPN levels, especially the $CD8\alpha\alpha^+$ subset.

4.3. IELs show increased phosphatase activity

After showing PTPNs are increased in IELs, we aimed to clarify the extent of their enzymatic function. Hence, we measured PTP activity in murine intestinal CD8αα and CD8αβ IELs as well as in their $CD8^+$ splenic counterparts. PTP activity was determined by correlating the amount of a specific fluorogenic PTP substrate metabolised with the measurements of fluorescence emitted over time (Figure 9, A and B). A positive control was established by adding a highly active PTP. As a negative control, the general PTP inhibitor suramin was added to $CD8^+$ splenocytes and CD8αα and CD8αβ IELs. For the blank control, no PTPase substrate was added. A fluorescence standard curve was calculated and plotted by correlating the emitted fluorescence of the standards, expressed in relative fluorescence units, with the corresponding standard concentrations (Figure 9A).

The fluorescence readings from the positive control showed high values of detected relative fluorescence. In $CD8^+$ splenocytes and CD8αα and CD8αβ IELs treated with the PTP inhibitor, we observed low levels of relative fluorescence, throughout the whole time of acquisition, similarly to the blank measurements, which suggests that the inhibitor was effective in suppressing phosphatase activity (Figure 9B). Moreover, values of relative fluorescence detected overtime in $CD8^+$ splenocytes, and CD8αβ IELs were similar, indicating that both populations did metabolise the substrate (Figure 9B). In CD8αα IELs however, we observed a much higher value of relative fluorescence, resulting from an increase in substrate metabolism over time and exceeding splenocytes and CD8αβ IELs, as well as the positive control values (Figure 9B). After quantifying PTP specific activity, we indeed verified that in CD8αα IELs, phosphatase activity was highly increased, significantly surpassing PTP activity

in splenic $CD8^+$ and CD8αβ (Figure 9C). Between $CD8^+$ splenocytes and CD8αβ, no significant difference was found in PTP activity. These findings show that steady-state natural CD8αα IELs present a substantially increased phosphatase activity, indicating a possible role for these phosphatases in the modelling of TCR signalling in natural IELs.

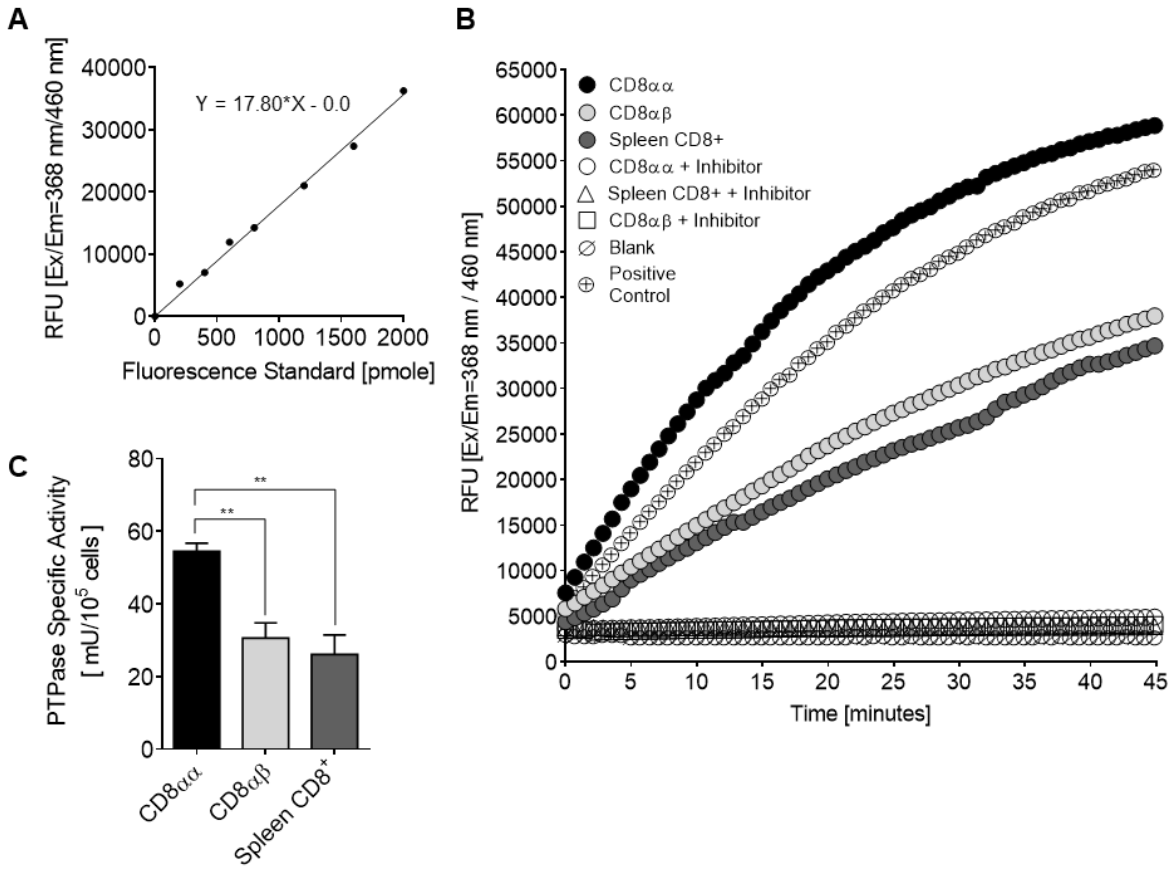

Figure 9 | IELs show increased phosphatase activity. Protein tyrosine phosphatase activity was assessed in CD8+ splenocytes and CD8αα and CD8αβ IELs. Cells were isolated from spleen and small intestine of C57BL/6 mice, purified by MACS and FACS cell sorting and incubated with a fluorogenic protein phosphatase substrate. **(A)** A fluorescence standard curve was used to determine substrate metabolised during the reaction time. One mole of fluorescent standard corresponds to one mole of metabolised substrate and release of one mole inorganic phosphate. Fluorescence was measured in relative fluorescence units (RFU). Standard curve coefficient of the slope b= 17.80 and intercept=0. **(B)** Reaction kinetics of PTP substrate metabolism are represented. A positive control was established using a PTP, and negative controls by incubating cells with suramin, a broad inhibitor of PTP. Fluorescence was measured during 45 minutes at Ex/EM= 368/460nm and **(C)** PTP activity calculated from fluorescence reading applied to the fluorescence standard curve and expressed in pmol/minute/105 cells (µU/105). All standards, controls and samples were tested in duplicate. Data is representative of n=4. Error bars represent ± SEM. One-way ANOVA and post hoc Holm-Sidak's multiple comparisons test was used. **P < 0.01

4.4. Impact of *Ptpn22* on *in vivo* activation of IELs

Our previous data showed that IELs harbour increased phosphatase activity, particularly in the CD8αα subset. We also observed that in CD8αα IELs, *Ptpn22* expression and protein content is significantly increased relative to conventional $CD8^+$ T cells. *Ptpn22,* among other PTPs, is known to inhibit TCR signalling and therefore can negatively regulate T cell activation and function. Given that IELs are arrested in a poised activation status, we hypothesised that PTPs, such as *Ptpn22,* could contribute to this status. Hence, in the absence of PTPs, we could expect to see a stronger activation and functional response of IELs.

In order to investigate the role of *Ptpn22* on the activation status of IELs, we proceeded with *in vivo* studies exploring IELs response in the absence of this phosphatase.

First, we established a model of *Ptpn22* deficiency in lymphocytes by generating *Ptpn22*$^{-/-}$ bone marrow (BM) chimeric mice, as well as WT BM chimeric mice to serve as experimental controls. Recipient Rag2$^{-/-}$ mice were subjected to sub-lethal irradiation, inducing haematopoiesis suppression, and 24h later were transplanted with bone marrow hematopoietic cells of *Ptpn22*$^{-/-}$ adult donor mice or WT control mice (Figure 9A). The mouse strains used express different variants of the common leukocyte antigen (CD45). Donor *Ptpn22*$^{-/-}$ bone marrow cells expressed the congenic CD45.2 surface marker, which allowed for donor cells to be easily distinguished from CD45.1 expressing host cells. Approximately six weeks post adoptive transfer, *Ptpn22*$^{-/-}$ BM chimeras were screened for the presence of donor cells and reconstitution of hematopoietic lineage populations (Figure 9A).

Reconstitution of bone marrow-derived immune populations in chimeric mice was assessed by flow-cytometric analysis of peripheral blood. Cells were stained for CD45.1 and CD45.2 to determine donor and host cell composition and also stained for adaptive immune cells such as TCR$\alpha\beta$ and TCR$\gamma\delta$ T cells, and B cells, as well as for innate immune cells such as neutrophils, eosinophils and $CD11b^+$ myeloid cells (Figure 10B). In Figure 10B is depicted the distribution of each cell subset in WT and *Ptpn22*$^{-/-}$ chimeric mice which were determined as a percentage of the total population of donor cells engrafted in each chimera. WT and Ptpn22$^{-/-}$ chimeras after adoptive transfer presented haematopoietic reconstitution with similar proportions of the analysed cell populations.

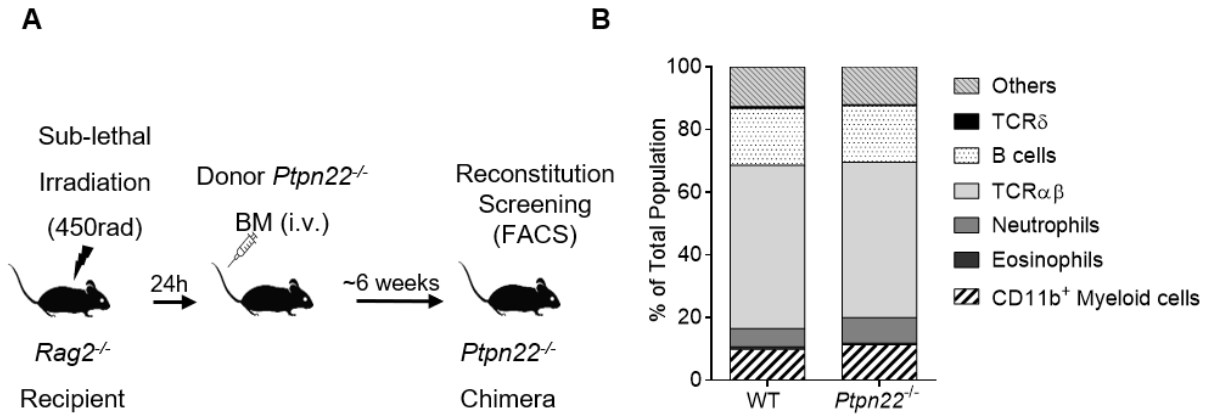

Figure 10 | Generation of Ptpn22-/- bone marrow chimeric mice. (A) Bone marrow chimera generation. Recipient *Rag2*$^{-/-}$ mice were sub-lethally irradiated, at 450rad, 24h hours before engraftment. Bone marrow cells were isolated from the hind legs of donor *Ptpn22*$^{-/-}$ *and* WT mice. Single-cells suspensions were prepared at a concentration of 2.5x10^{7} cells/mL, in PBS. Recipient Rag*2*$^{-/-}$ mice were intravenously (i.v.) injected with 200µL of either *Ptpn22*$^{-/-}$ *or* WT cells. **(B)** Reconstitution of immune populations in peripheral blood after bone marrow cell transplant into lymphopenic mice. Reconstitution of hematopoietic-derived cell repertoire was assessed by FACS analysis of peripheral blood of WT and *Ptpn22*$^{-/-}$ chimeras, approximately 6 to 9 weeks post adoptive cell transfer. Bone marrow chimeras were screened for the presence of TCRβ, and TCRδ T cells, B cells, neutrophils, eosinophils and CD11b^{+} myeloid cells, and their proportions were determined. Pooled data from two independent experiments (Ptpn22$^{-/-}$ BM chimeras, n=17; WT BM chimeras, n=15).

In order to understand what impact Ptpn22 has on IEL activation, we used an *in vivo* model of colitis. The DSS-induced colitis model chemically induces damage to the intestinal epithelium and leads to the activation and recruitment of leukocytes. It is commonly used as a model for colon inflammation but also leads to proliferation of CD8αα IEL in the small intestine (unpublished data). Figure 11A describes the experimental setup, with all experimental groups receiving 2.5% DSS in drinking water for 6 days and subsequently normal drinking water until they recover. Mice were monitored for body weight loss and disease severity, as evaluated by macroscopic observation of faeces consistency, haemorrhaging and overall wellbeing, throughout the experiment. The experimental groups included the WT and *Ptpn22*$^{-/-}$ BM chimeras, as well as *Rag2*$^{-/-}$ female and male mice serving as a control for symptoms and recovery in the same genetic background of the BM chimeras generated. As baseline controls for disease onset and severity, we included DSS-treated C57BL/6J mice.

C57BL/6 mice showed a classical response to DSS treatment with weight loss until day 9 and a gradual recovery until day 24 post-treatment onset (Figure 11B). Disease severity peaks at day 5/6 and quickly resolves after discontinuation of the DSS treatment (Figure 11C).

We observed that *Rag2*$^{-/-}$ mice are highly sensitive to DSS induced colitis and experience severe weight loss of more than 20% (Figure 11B). Additionally, *Rag2*$^{-/-}$ mice also presented the highest observed severity scores (Figure 11C), which required the euthanasia of all female and 3 out of 4 male mice, in compliance with animal welfare guidelines (Figure 11D).

In both experimental groups that received either WT or *Ptpn22*$^{-/-}$ BM cells, we observed a bodyweight loss of up to 10%. Interestingly, after stopping the DSS treatment, the mice that received WT cells quickly recovered their body weight and showed no signs of disease on day 11 post-treatment. In contrast, the *Ptpn22*$^{-/-}$ chimeras just recovered on day 20 after DSS treatment (Figure 11C), indicating that the absence of PTPN22 leads to a prolongation of disease and impaired recovery.

In order to understand if IEL from *Ptpn22*$^{-/-}$ mice are more activated and like this might contribute to the prolonged disease, we decided to analyse a group of mice on the peak of the disease at day 7 post DSS treatment. WT and *Ptpn22*$^{-/-}$ BM chimeras as well as C57BL/6 mice treated with DSS as positive and non-treated C57BL/6 as negative controls, were sacrificed and the IELs from the small intestine and the colon were isolated.

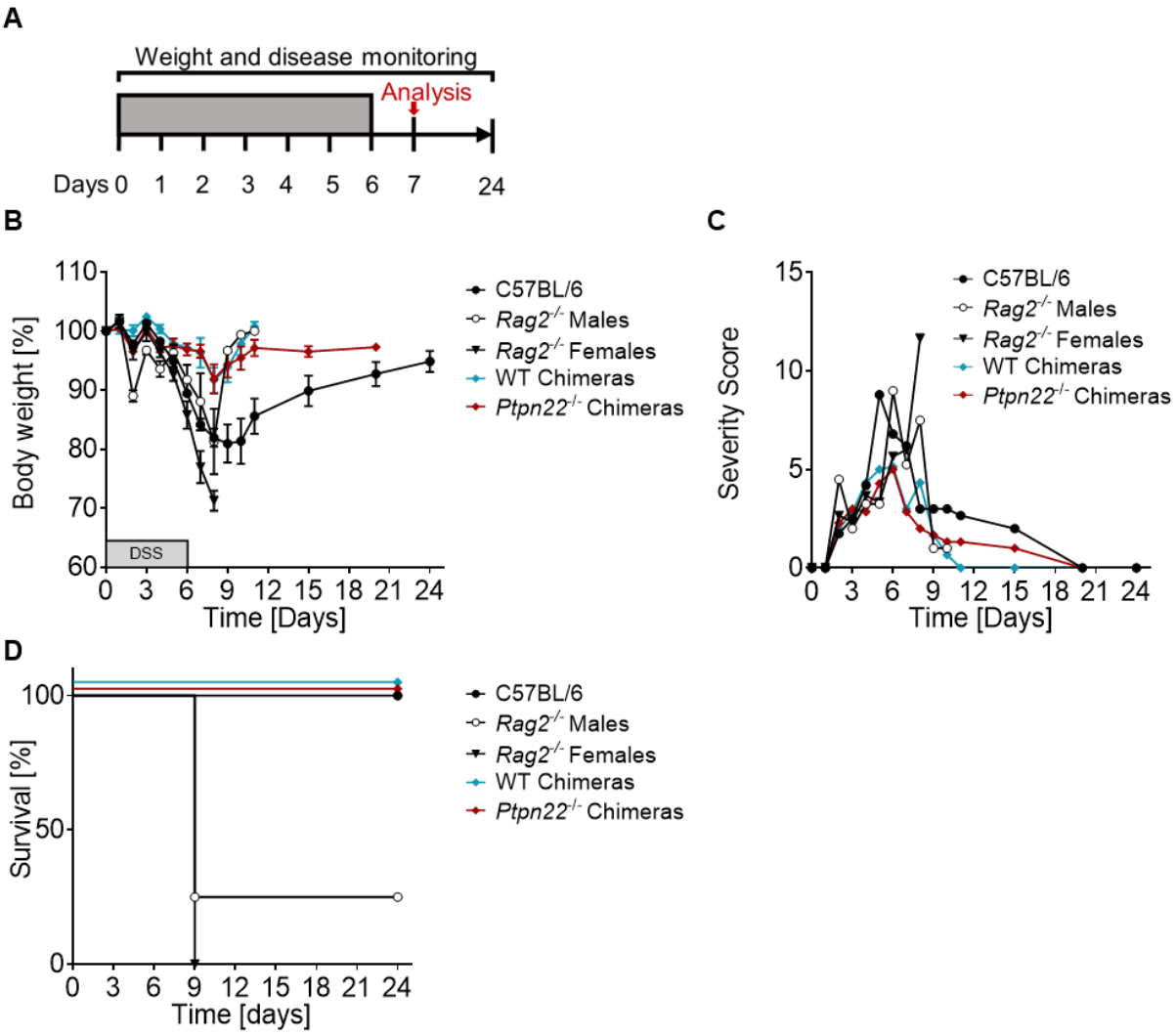

Figure 11 | Ptpn22 impact during DSS-induced experimental colitis. (A) Experimental DSS-induced colitis model in C57BL/6J, female *Rag2*$^{-/-}$ and male *Rag2*$^{-/-}$ mice, and in WT and *Ptpn22*$^{-/-}$ BM chimeras. Colitis was induced by administration of a 2.5% DSS solution, in the drinking water, for 6 days. At day 7, IELs were isolated from the small intestine and colon of non-treated C57BL/6J mice as well as DSS-treated C57BL/6J and WT and *Ptpn22*$^{-/-}$ BM chimeras. **(B)** Bodyweight change in DSS-treated mice expressed as a percentage of initial weight. **(C)** Disease severity scoring of DSS-treated mice, based on an evaluation of mice bodyweight decrease, stool consistency and haemorrhaging, described in detail in the Material and Methods section. Bodyweight and disease severity were monitored frequently only in DSS-treated experimental groups, until day 24 (C57BL/6J, n=3; male *Rag2*$^{-/-}$, n=4; female *Rag2*$^{-/-}$, n=3; WT BM Chimera, n=3; *Ptpn22*$^{-/-}$ BM chimera, n=3). **(D**) Survival curve of mice exposed to DSS from day 1 to 24. The same mice as in (A) and (B) are included.

We assessed IEL proliferation by measuring intracellular expression of Ki67, as a readout for IEL activation. Absolute cell counts and Ki67 expression values in small intestinal and colonic IELs, such as TCRβ^{+}CD4^{+}, TCRβ^{+}CD8αα^{+}, TCRβ^{+}CD8αβ^{+} and TCRδ^{+}CD8αα subsets, are shown in Figure 12 and Figure 13, respectively. In the small intestine, we observed that in all IEL subsets analysed, DSS-treated C57BL/6J mice presented a higher percentage of Ki67-

expressing IELs relative to non-treated C57BL/6J mice, indicating a higher proliferation of IELs during colitis (Figure 12). Specifically, in DSS-treated C57BL/6J mice small intestinal TCRβ $CD4^+$ (Figure 12A), TCRβ CD8αα (Figure 12B) and TCRδ CD8αα IELs (Figure 12D), expression of Ki67 was around 10 to 15% while in TCRβ CD8αβ cells (Figure 12C) Ki67 expression was slightly lower than 5%. Contrastingly, among the same experimental groups but in colonic IELs, Ki67 expression was significantly increased in TCRβ $CD4^+$ IELs where more than 20% of the population expressed the marker (Figure 13A), while in the other subsets the expression of Ki67 was slightly under 20% yet still higher than in the small intestine. The higher proliferation of colonic IELs is explained by the nature of the disease, which primarily targets the colon.

In the small intestine, when comparing *Ptpn22*$^{-/-}$ *and* WT BM chimera IEL populations, we observed similar expression of Ki67 between the experimental groups, indicating that PTPN22 deficiency does not lead to higher activation of IELs in this gut segment (Figure 12). In the colon, we observed a slightly increased proliferation in the natural IEL populations expressing CD8αα in the absence of PTPN22 when compared to the WT BM chimera (Figure 13 B and D). This increase was more pronounced in the TCRβ IEL population and reached a similar proliferation as in C57BL/6 mice. In terms of cell numbers, we observed no significant differences in both, colon (Figure 13 F to J) and small intestine (Figure 12 F to J), except a consistently increased number of IELs in DSS treated WT chimeras in the small intestine, compared to the other experimental groups.

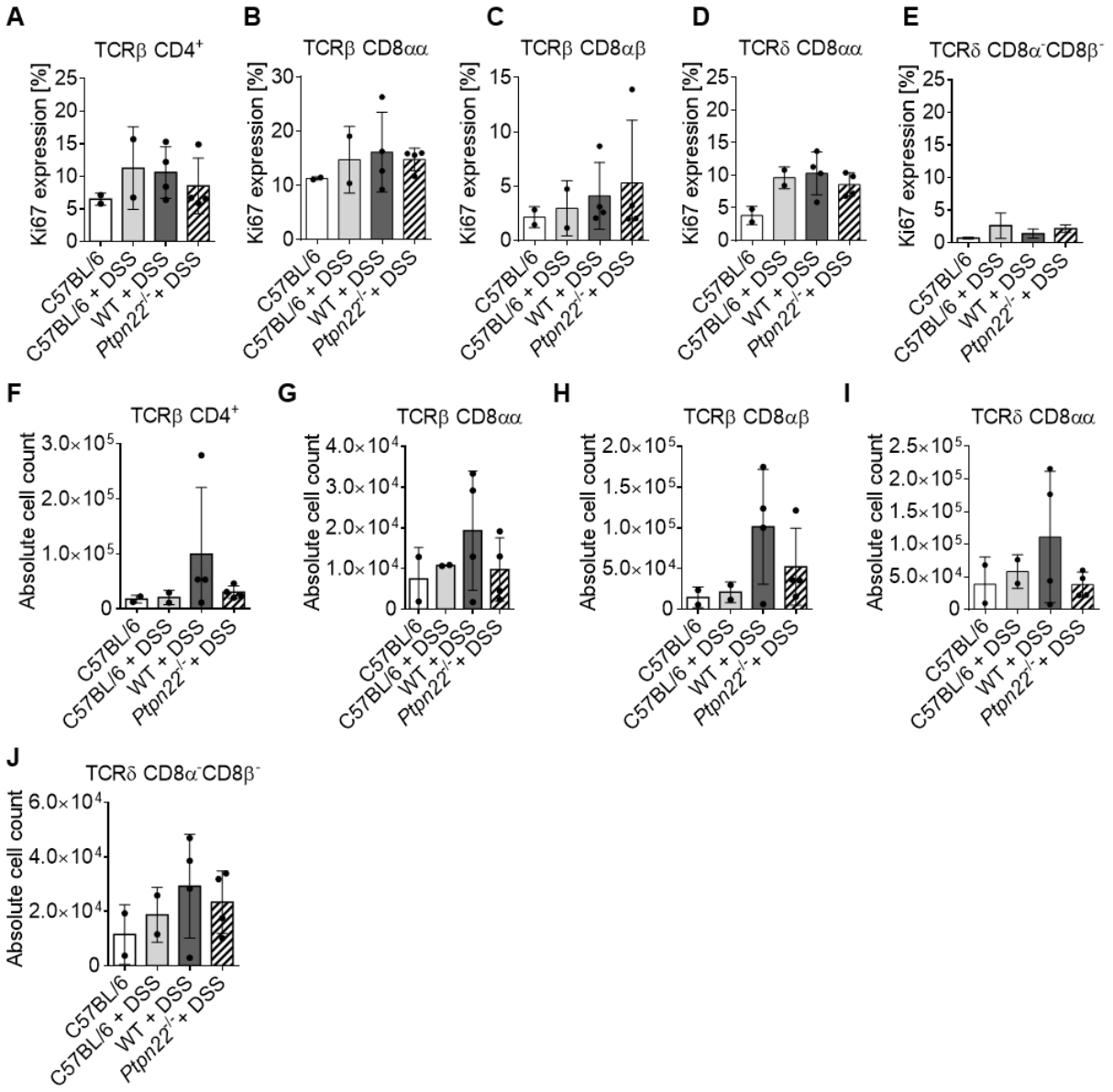

Figure 12 | Ptpn22 impact on IEL activation in the small intestine during DSS-induced experimental colitis. Graphs display Ki67 expression in **(A)** TCRβ$^+$CD4$^+$, **(B)** TCRβ$^+$CD8αα$^+$, **(C)** TCRβ$^+$CD8αβ$^+$, **(D)** TCRδ$^+$CD8αα and **(E)** TCRδ$^+$CD8α$^-$CD8β$^-$ IEL subsets during colitis. Graphs display absolute cell counts of **(F)** TCRβ$^+$CD4$^+$, **(G)** TCRβ$^+$CD8αα$^+$, **(H)** TCRβ$^+$CD8αβ$^+$, **(I)** TCRδ$^+$CD8αα and **(J)** TCRδ$^+$CD8α$^-$CD8β$^-$ IEL populations in the small intestine after DSS treatment for induced colitis. On day 7, mice were sacrificed (non-treated C57BL/6J n=2; DSS-treated C57BL/6J n=2; WT BM Chimera n=4; *Ptpn22*$^{-/-}$ BM chimera n=4) and IELs were isolated from the small intestine for flow-cytometric analysis. Cells were stained for Ki67, and expression of this marker was determined in each IEL subset analysed, shown in (A) through (E). Absolute cell counts of each IEL subset in the small intestine were determined, shown in (F) through (J). Each symbol represents an individual mouse. Error bars represent ± SD. Statistical significance was determined by one-way ANOVA and post-hoc Holm-Sidak's multi comparisons test (*P < 0.05, **P < 0.01).

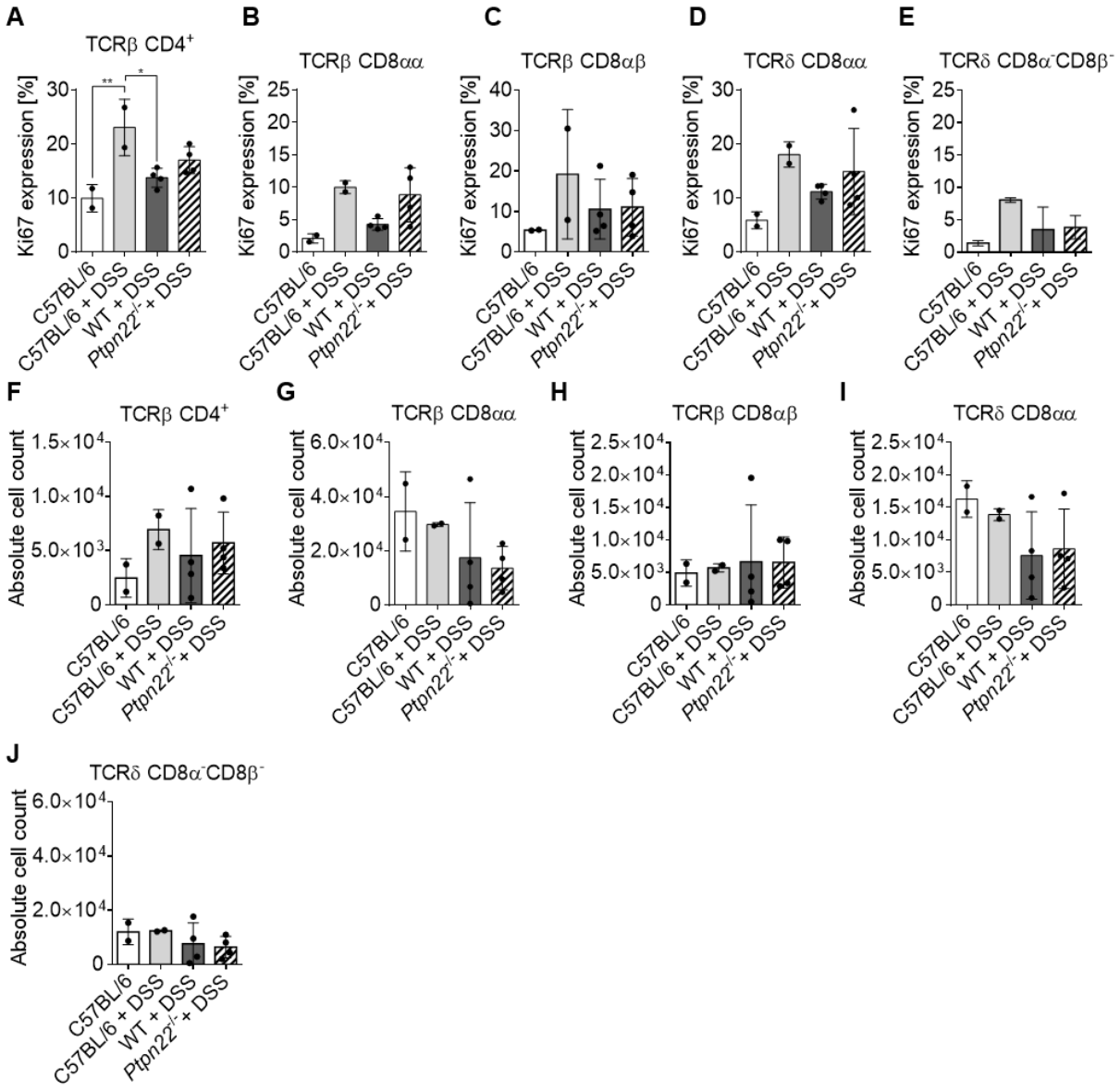

Figure 13 | Ptpn22 impact on IEL activation in the colon during DSS-induced experimental colitis. Graphs **(A)** through **(E)** display Ki67 expression in **(A)** TCRβ$^+$CD4$^+$, **(B)** TCRβ$^+$CD8αα$^+$, **(C)** TCRβ$^+$CD8αβ$^+$, **(D)** TCRδ$^+$CD8αα and **(E)** TCRδ$^+$CD8α$^-$CD8β$^-$ IEL subsets during colitis. Graphs **(F)** through **(J)** display absolute cell counts of colonic **(F)** TCRβ$^+$CD4$^+$, **(G)** TCRβ$^+$CD8αα$^+$, **(H)** TCRβ$^+$CD8αβ$^+$, **(I)** TCRδ$^+$CD8αα and **(J)** TCRδ$^+$CD8α$^-$CD8β$^-$ IEL populations after DSS treatment for induced colitis. On day 7, mice were sacrificed (non-treated C57BL/6J n=2; DSS-treated C57BL/6J n=2; WT BM Chimera n=4; *Ptpn22*$^{-/-}$ BM chimera n=4) and IELs were isolated from the colon for flow-cytometric analysis. Cells were stained for Ki67, and expression of this marker was determined in each IEL subset analysed, shown in (A) through (E). Absolute cell counts of each IEL subset in the colon were determined, shown in (F) through (J). Each symbol represents an individual mouse. Error bars represent ± SD. Statistical significance was determined by one-way ANOVA and post-hoc Holm-Sidak's multi comparisons test (*P < 0.05, **P < 0.01). 13

4.5. Impact of PTPN22 on TCR activation in vivo

Using the DSS model of colitis, we observed only mild differences in the disease severity of mice harbouring PTPN22 deficient cells and a slight increase in cell proliferation. To further understand the role of *Ptpn22* in the activation of IELs, we investigated how WT and *Ptpn22*-deficient IELs responded when stimulated directly through the TCR-CD3 complex. Here, we used an *in vivo* model for the initiation of TCR signalling by administrating stimulatory anti-CD3 to WT and *Ptpn22*$^{-/-}$ BM chimeras by intraperitoneal injection (Figure 14A). Cells were isolated 48 hours after α-CD3 stimulation and assessed by flow cytometry for proliferation and activation markers (Figure 14A). The different subsets of IELs and splenocytes were evaluated for expression of the intracellular molecules Ki67 (Figure 14) and GzmB (Figure 15) and the expression of the surface receptor PD-1 (Figure 16).

Ki67 expression, a marker strictly associated with cell proliferation, can provide insight on whether cells are in mitotic phase or actively proliferating faster. Hence, we analysed Ki67 expression in several IEL subsets present in the small intestine (Figure 14B to F) and in conventional T cells in the spleen (Figure 14H to J).

In both IEL and splenocyte subsets, we observed an upregulation of Ki67 following α-CD3 stimulation, indicating that these cells are proliferating upon stimulation. Specifically, in stimulated splenocytes, we observed a 5-fold increase in Ki67 expression by CD4^{+} cells (Figure 14H) and a 4-fold increase in TCRδ cells (Figure 14J), while in TCRβCD8αβ splenic cells Ki67 expression was around 9 times greater than basal levels (Figure 14I). Basal levels of Ki67 expression in non-stimulated WT and *Ptpn22*$^{-/-}$ chimeras were around 15% in CD8^{+} IELs and increased to about 60%-70% in TCRβ CD8αβ (Figure 14D), representing a 3 to 4-fold increase, and to around 40%-50% in natural TCRβ CD8αα and TCRδ CD8αα IELs, a 2-fold increase (Figure 14C and E). In non-stimulated CD4^{+} IELs, the basal level of Ki67 was higher, at around 20%, and when stimulated the expression of Ki67 rises to about 90%, representing a 3 to 4-fold increase (Figure 14B). When comparing Ki67 expression values in *PTPN22* sufficient and deficient IELs, we did not observe any significant differences, across all IEL populations analysed. Figure 14G portrays Ki67 expression in stimulated and non-stimulated CD4^{+} IELs, illustrating the similarity between the two conditions, which was found across all IEL subsets. The same pattern was also found in splenocytes in the same conditions, echoing what was verified for non-stimulated controls. Indeed, the maintenance of Ki67 expression levels among WT and PTPN22 deficient cells, in both unstimulated and stimulated IELs and splenocytes, indicates that proliferation may not be directly impacted by the lack of PTPN22 alone.

Hence, we were unable to find a direct correlation linking PTPN22 deficiency to IEL proliferation, at least by evaluating Ki67 expression. Therefore, we set out to further investigate the behaviour of IELs in the absence of PTPN22 and assess their functional response to activation.

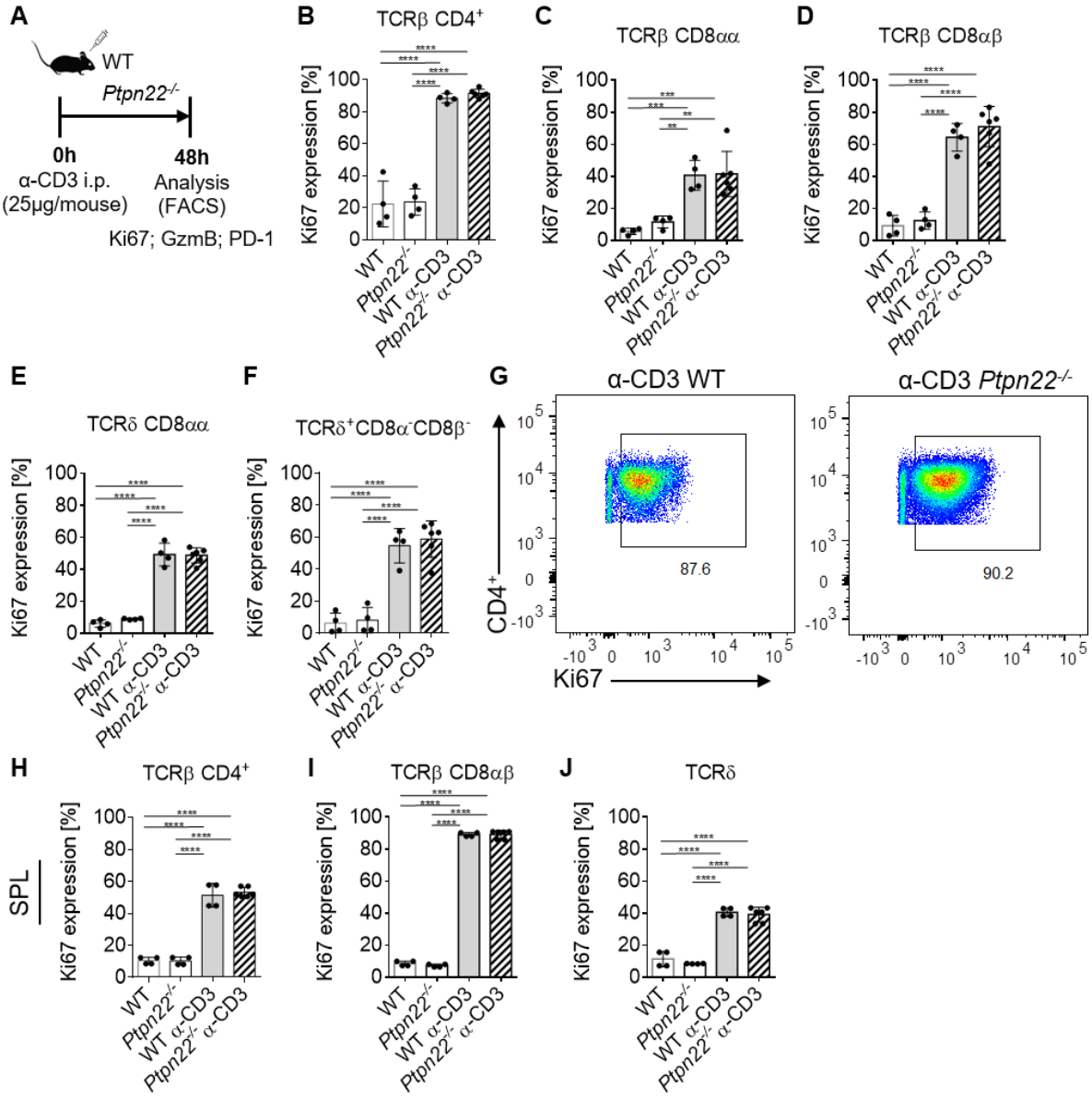

Figure 14 | Ptpn22 impact on IEL and splenocyte proliferation following in vivo α-CD3 stimulation. (A) Representation of the α-CD3 T cell activation model used. WT and *Ptpn22*$^{-/-}$ bone marrow chimeras were generated. T cell activation was induced by intraperitoneal administration of α-CD3 (25µg/mouse) to WT and *Ptpn22*$^{-/-}$ chimeras. IELs and splenocytes were isolated from the small intestine and spleen of α-CD3 stimulated and non-stimulated WT and *Ptpn22*$^{-/-}$ chimeras, 48h post-α-CD3 stimulation. Cells were analysed, by flow cytometry, for expression of Ki67, GzmB and PD-1. Expression of Ki67 is displayed in percentage for several IEL subsets including **(B)** TCRβCD4^{+}, **(C)** TCRβCD8αα, **(D)** TCRβCD8αβ and **(E)** TCRδCD8αα and **(F)** TCRδCD8α^{-}CD8β^{-}, in non-stimulated and α-CD3 stimulated *Ptpn22*$^{-/-}$ and WT BM chimeras. **(G)** Representative FACS dot plot of Ki67 staining in unstimulated and α-CD3 stimulated CD4^{+} IELs. Analysis of Ki67 expression in splenocyte populations including **(H)** TCRβCD4^{+}, **(I)** TCRβCD8αβ and **(J)** TCRδ is displayed in percentage, in non-stimulated and α-CD3 stimulated *Ptpn22*$^{-/-}$ and WT BM chimeras. Each symbol represents an individual mouse (non-treated *Ptpn22*$^{-/-}$, n=4; non-treated WT, n=4; α-CD3 *Ptpn22*$^{-/-}$, n=3; α-CD3 WT, n=4). Error bars represent ± SD. Data represent 2 biological repeats (n=2). Statistical significance was determined by one-way ANOVA and post-hoc Holm-Sidak's multi comparisons test (*P < 0.05, **P < 0.01, ***P < 0.001, ****P < 0.0001).

We then analysed GzmB expression as a functional readout for IEL activation, as increased levels of GzmB in IELs translate into an augmented cytolytic capacity and therefore a more robust cytotoxic response.

We analysed the percentage of cells positive for GzmB expression as well as their mean fluorescence intensity (MFI) and observed that, generally, GzmB was more expressed in IELs of α-CD3 stimulated *Ptpn22*$^{-/-}$ animals than in IELs of stimulated WT animals. In fact, upon stimulation, in PTPN22-deficient mice, we observed augmented GzmB expression levels and an increase in the proportion of cells expressing this granzyme, in several IEL populations such as CD4^{+} (Figure 15A and F), TCRβCD8αα (Figure 15B and G), TCRβCD8αβ (Figure 15C and H) and TCRδCD8α^{-}CD8β^{-} (Figure 15E and J) when compared to WT mice.

Conversely, the proportion of WT and *Ptpn22*$^{-/-}$ TCRδCD8αα IELs expressing GzmB was similar between stimulated IELs (Figure 15D), whereas the expression levels of GzmB were augmented in TCRδCD8αα *Ptpn22*$^{-/-}$ IELs (Figure 15I).

In *Ptpn22*$^{-/-}$ mice, upon stimulation, we observed a significant increase of GzmB expression in CD4^{+} (Figure 15 A, F and K) and TCRδCD8α^{-}CD8β^{-} IELs (Figure 15J). Specifically, we observed that basal levels of GzmB expression in steady-state CD4^{+} and TCRδCD8αα IELs are lower in *Ptpn22*$^{-/-}$ BM chimeric mice than in WT mice (Figure 15F). Despite presenting lower basal levels of GzmB, when stimulated with α-CD3, CD4^{+} IELs of *Ptpn22*$^{-/-}$ chimeras reach higher GzmB expression levels showing a 4.5-fold increase whereas WT chimeras only present an increase of 1.4-fold when stimulated (Figure 15F and K). Therefore, non-stimulated *Ptpn22*$^{-/-}$ CD4^{+} IELs show lower levels of GzmB expression, yet upon stimulation, the production of this granzyme increases robustly and reaches higher values than observed in WT IELs. Interestingly, this means that GzmB expression remains high in PTPN22-deficient IELs, suggesting that PTPN22 might have a role in hampering IEL effector functions and dampening GzmB expression. In contrast to WT CD4^{+} and TCRδCD8α^{-}CD8β^{-} IEL populations where at steady-state around 40% to 50% of the cells expressed GzmB, in other WT CD8^{+} IEL subsets in the intestine the proportion of IELs expressing GzmB at steady-state was higher around 80%. Interestingly, in WT TCRβCD8αβ (Figure 15C and H) and TCRδCD8α^{-}CD8β^{-} IELs (Figure 15E and J) the proportion of cells expressing GzmB does not seem to vary when stimulated with α-CD3 and expression levels are maintained.

However, across all IEL subsets analysed more *Ptpn22*$^{-/-}$ cells do express GzmB and at higher expression levels than WT individuals when stimulated with aCD3. These data indicate that PTPN22 might indeed act as a break for the induction of T cell effector functions and could be involved in dampening GzmB expression, explaining why in *Ptpn22*-deficient chimeras the

expression of this molecule is increased to higher expression levels, upon stimulation, than WT chimeras in the same condition.

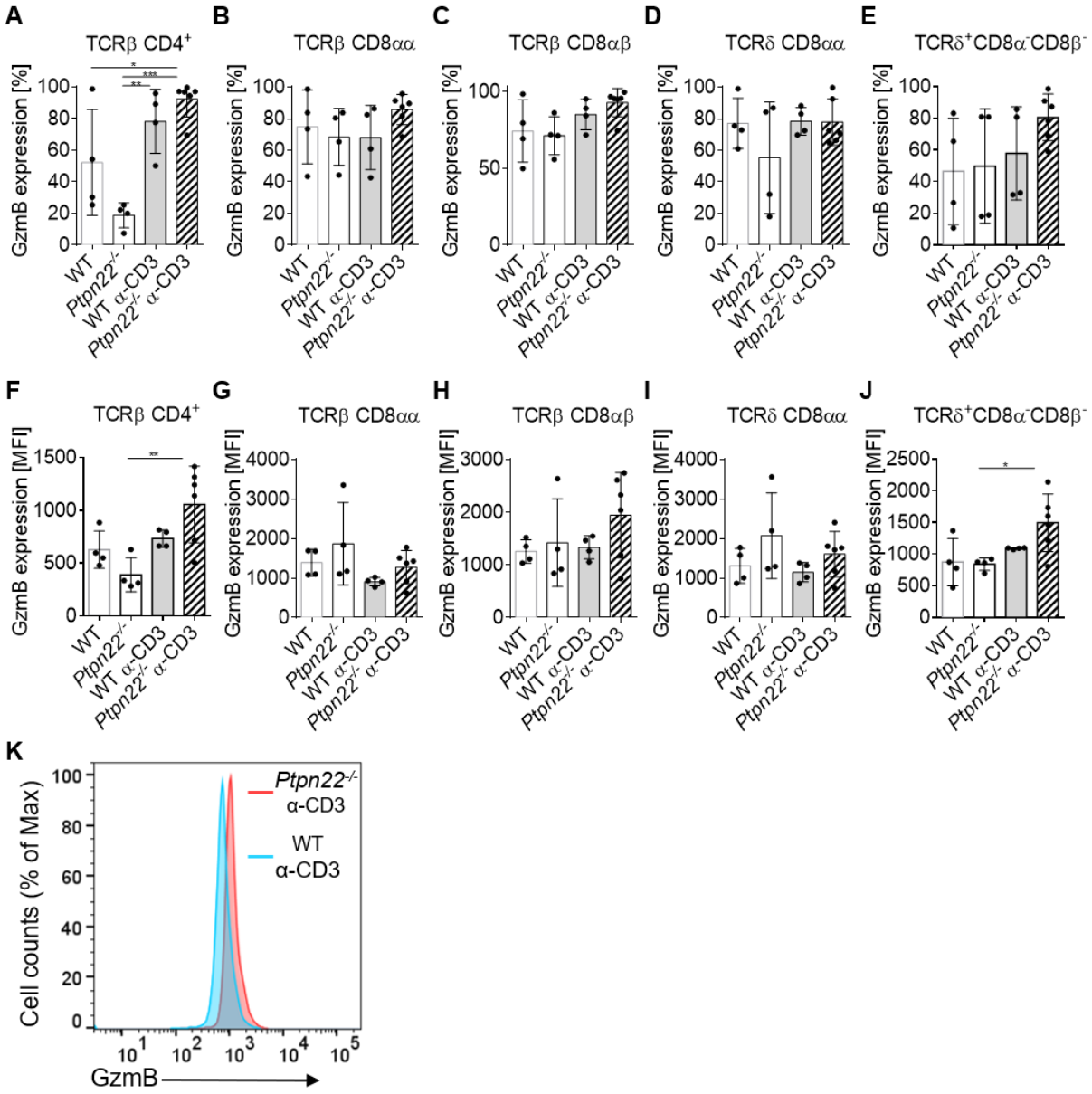

Figure 15 | Ptpn22 impact on IEL cytotoxic capacity following in vivo α-CD3 stimulation. Analysis of the proportion of GzmB expressing IELs is displayed in percentage for several IEL subsets including **(A)** TCRβCD4$^+$, **(B)** TCRβCD8αα, **(C)** TCRβCD8αβ and **(D)** TCRδCD8αα and **(E)** TCRδCD8α$^-$CD8β$^-$, in non-stimulated and α-CD3 stimulated *Ptpn22*$^{-/-}$ and WT BM chimeras. Analysis of GzmB expression levels in IELs is displayed in MFI for several IEL subsets including **(F)** TCRβCD4$^+$, **(G)** TCRβCD8αα, **(H)** TCRβCD8αβ and **(I)** TCRδCD8αα and **(J)** TCRδCD8α$^-$CD8β$^-$, in non-stimulated and α-CD3 stimulated *Ptpn22*$^{-/-}$ and WT BM chimeras. **(K)** Representative histogram of GzmB expression levels in TCRβCD4$^+$ IELs in α-CD3 stimulated *Ptpn22*$^{-/-}$ and WT BM chimeras. Each symbol represents an individual mouse. (non-treated *Ptpn22*$^{-/-}$, n=4; non-treated WT, n=4; α-CD3 *Ptpn22*$^{-/-}$, n=3; α-CD3 WT, n=4). Error bars represent ± SD. Data represent 2 biological repeats (n=2). Statistical significance was determined by one-way ANOVA and post-hoc Holm-Sidak's multi comparisons test (*P < 0.05, **P < 0.01, ***P < 0.001, ****P < 0.0001).

Additionally, we also evaluated IEL activation status by analysis of the expression of PD-1, a negative regulator of T cell activation, providing another readout for IEL activity. In $CD4^+$ IELs, we observed similar PD-1 expression in WT and *Ptpn22*$^{-/-}$ chimeric mice at steady-state, as approximately 50% of cells expressed this marker (Figure 16A). After stimulation with α-CD3, the percentage of PD-1 positive cells increased to about 90%. Around 5-10% of natural TCRβCD8αα IELs express PD-1 at steady-state (Figure 16B), which increased during α-CD3 stimulation to 40% with no difference between WT and *Ptpn22*$^{-/-}$ chimeras. A similar baseline expression of PD-1 was found in TCRβCD8αβ IELs that increased upon stimulation to around 70% in both experimental groups (Figure 16C). Moreover, in all $CD8^+$ IEL populations analysed, PD-1 expression is lower in *Ptpn22*$^{-/-}$ mice than in WT chimeric mice, both at steady-state and after stimulation (Figure 16B to E). Indeed, in TCRδCD8αα IELs of stimulated WT chimeras, expression of PD-1 was significantly higher than in *Ptpn22*$^{-/-}$ chimeras (Figure 16D and F). Our data suggest that PTPN22 deficiency can prevent the upregulation of PD-1, consequently weakening PD-1 role in the negative regulation of T cell function. Upon stimulation, as expected, peripheral $CD4^+$ and $CD8^+$ splenocytes behaved similarly to IELs, as they presented a significant increase in PD-1 expression in comparison to steady-state splenocytes. However, PD-1 expression values were similar between non-stimulated splenocytes as well as between their stimulated counterparts, in the $CD4^+$ (Figure 16G), TCRβCD8 (Figure 16H) and TCRδ (Figure 16I) IEL subsets.

Therefore, these findings indicate that upon stimulation, both IELs and splenocytes upregulated the PD-1 surface receptor, however, specifically in TCRδCD8αα IELs of *Ptpn22*$^{-/-}$ chimeras (Figure 16D), PD-1 expression was significantly decreased when compared to their WT counterparts. Notably, we have observed that the natural TCRβCD8αα (Figure 16B) and TCRδCD8αα (Figure 16D) IELs exhibited an overall lower expression of PD-1, across WT and *Ptpn22*$^{-/-}$ individuals, when compared to the other IEL subsets.

Altogether, the collected data indicate that at 48h post-stimulation, in all subsets of *Ptpn22*-deficient and WT IELs, we verified that proliferation was highly increased, and both registered similar values. Additionally, we observed that levels of GzmB expression were higher in *Ptpn22*$^{-/-}$ α-CD3 stimulated individuals when comparing to their WT counterparts, which might translate into a higher cytotoxic capacity of these cells, suggesting a potential role for *Ptpn22* in dampening IEL function. Furthermore, both IELs and splenocytes of the WT and *Ptpn22*$^{-/-}$ chimeras were shown to upregulate PD-1 expression upon activation. Moreover, we also verified that upon activation, *Ptpn22*$^{-/-}$ IELs present a lower proportion of PD-1 expressing IELs, suggesting a possible role for PTPN22 in allowing PD-1 upregulation and promoting its subsequent role in negatively regulating IEL function.

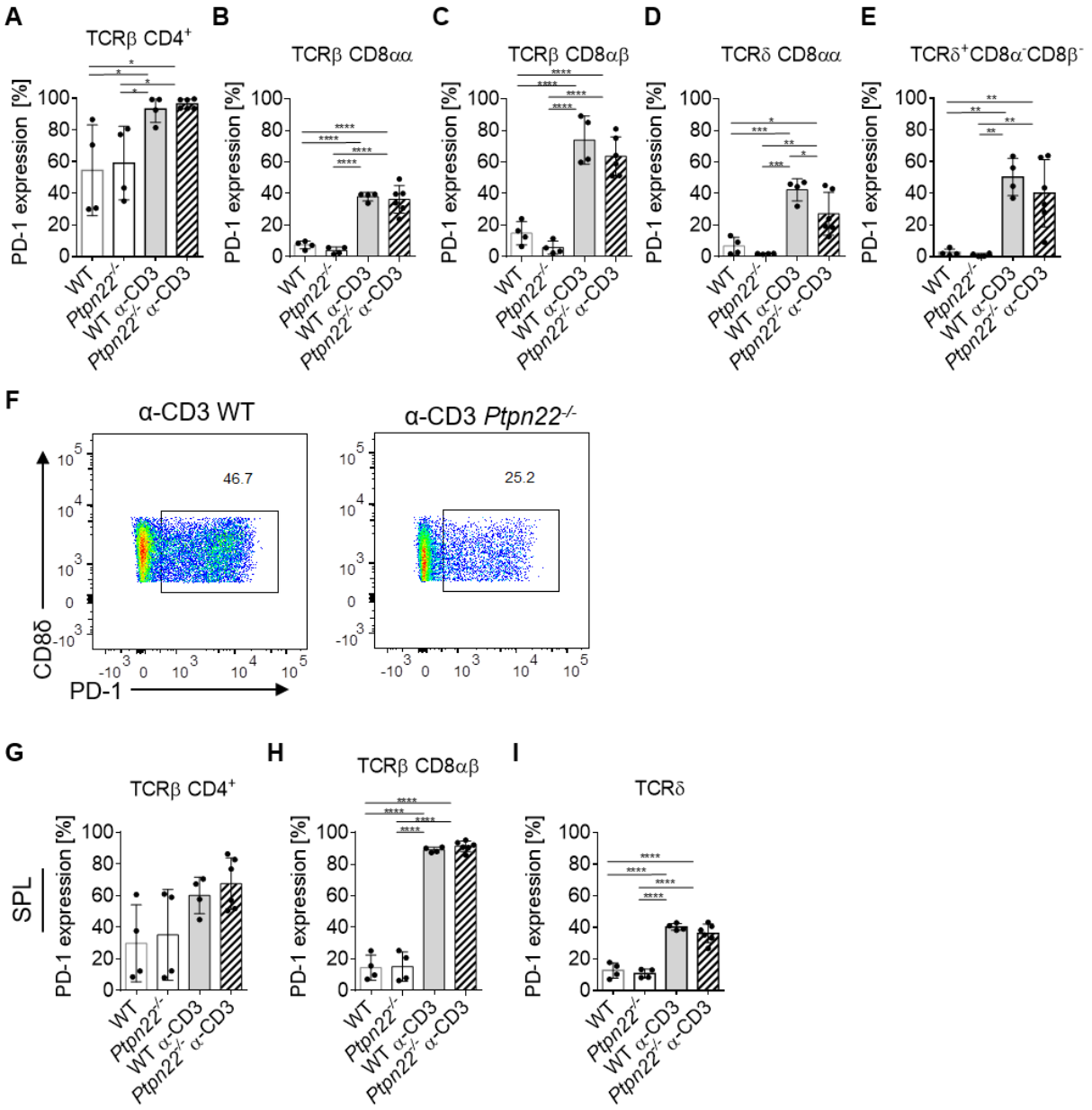

Figure 16 | Ptpn22 impact on IEL activity following in vivo α-CD3 stimulation. Analysis of PD-1 expression in IEL populations including **(A)** TCRβCD4+, **(B)** TCRβCD8αα, **(C)** TCRβCD8αβ and **(D)** TCRδCD8αα and **(E)** TCRδCD8α-CD8β-, in non-stimulated and α-CD3 stimulated *Ptpn22*-/- and WT BM chimeras. **(F)** Representative FACS dot plot of PD-1 expression in TCRδCD8αα IELs of α-CD3 stimulated *Ptpn22*-/- and WT BM chimeras. Analysis of Ki67 expression in splenocyte populations including **(G)** TCRβCD4+, **(H)** TCRβCD8αβ and **(I)** TCRδ is displayed in percentage, in non-stimulated and α-CD3 stimulated *Ptpn22*-/- and WT BM chimeras. Each symbol represents an individual mouse. (non-treated *Ptpn22*-/-, n=4; non-treated WT, n=4; α-CD3 *Ptpn22*-/-, n=3; α-CD3 WT, n=4). Error bars represent ± SD. Data represent 2 biological repeats (n=2). Statistical significance was determined by one-way ANOVA and post-hoc Holm-Sidak's multi comparisons test (*P < 0.05, **P < 0.01, ***P < 0.001, ****P < 0.0001).

4.6. Influence of broad PTP inhibition on TCR activation in vivo

Our previous observations indicated that PTPs are widely expressed in IELs and we report highly increased PTP activity in the CD8αα and CD8αβ subsets, especially in the former. Therefore, we then aimed to dissect PTPs impact in IELs' specific functional capacity during activation. We designed a model for PTP inhibition during *in vivo* IEL activation, by administrating SOV, a general inhibitor of PTPs, and inducing T cell activation by α-CD3 injection (Figure 17). As in the previous experiment, the analysed time points for T cell activation were 24h and 48h after administration of α-CD3 (Figure 17). In order to inhibit PTPs during stimulation, we treated C57BL/6J mice with SOV throughout the experiment at 18h and 1h prior to α-CD3 stimulation, as well as post-stimulation at 6h for the 24h time point and 6h and 30h for the 48h time point (Figure 17). Control mice did not receive SOV but were stimulated with α-CD3 and analysed simultaneously with the SOV-treated mice. For the flow cytometry analysis, we included a control group of C57BL/6J mice without any treatment, to assess the baseline expression of the activation markers analysed. Ki67, PD-1 and GzmB expression was analysed by flow cytometry in several IEL subsets including TCRβCD8αα, TCRβCD8αβ, TCRδCD8αα and TCRδCD8α$^-$CD8β$^-$, and also in splenocytes including TCRβCD4$^+$, TCRβCD8$^+$ and TCRδ.

Figure 18 displays the proportion of Ki67-expressing IELs (Figure 18A to E) and Ki67-expressing splenocytes (Figure 18F to H) in percentage. In addition, the levels of Ki67 expression were also determined by analysing the MFI for IELs (Figure 18I to M) and splenocytes (Figure 18N to P).

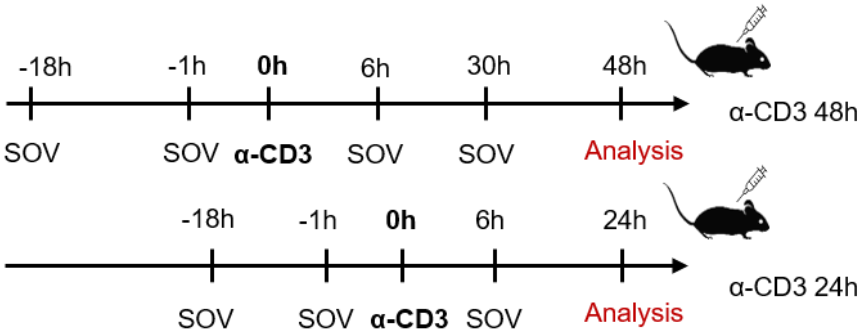

Figure 17 | The effect of PTP general inhibitor sodium orthovanadate in IEL activation in vivo. Scheme of IEL activation *in vivo* model during SOV-induced inhibition of PTPs. T cell activation was induced by intraperitoneal administration of α-CD3 (25µg/mouse) at the indicated 0h timepoint. Two distinct timepoints were set for analysis, 24h and 48h. For analysis at 24h, SOV (200µg/mouse) was administrated by intraperitoneal injection at 18h and 1h before stimulation and 6h post-stimulation. For analysis at 48h, SOV was administered at 18h and 1h before stimulation and after stimulation at 6h and 30h. Mice were sacrificed, and spleen and small intestine were collected. Tissues were processed, and splenocytes and IELs isolated and co-stained for Ki67, PD-1 and GzmB.

In both IELs and splenocytes, we registered a gradual increase in proliferation from the 24h to 48h, as the percentage of Ki67-expressing cells increased. In all the IEL subsets analysed, among control and SOV-treated mice no significant difference was found in the proportion of Ki67-expressing cells, which at 48h was around 40-60% (Figure 18A to E). Interestingly, we observed a higher Ki67 staining intensity across all SOV-treated IEL subsets at 48h, indicating that Ki67 expression levels were heightened (Figure 18I to M). Specifically, SOV-treated TCRβCD4^{+} (Figure 18I) and TCRβCD8αα (Figure 18J) IELs expressed significantly higher levels of Ki67 at 48h compared to WT control cells, indicating that SOV-treated cells proliferate more, whereas WT control IELs are already returning to homeostatic proliferation levels. Expression of Ki67 in splenocytes was considerably higher than in IELs, at 48h, and Ki67 levels were identical between controls and SOV-treated mice (Figure 18F to H). These findings suggest that upon stimulation IELs where PTP activity was inhibited by SOV treatment, seem to be highly proliferating. On the contrary, peripheral T cells show a similar proliferation rate in treated and untreated cells, indicating that PTP activity impairment does not influence the proliferation of these cells.

Additionally, we analysed PD-1 expression as a readout for IEL activation (Figure 19). Across all IEL (Figure 19A to E) and spleen (Figure 19 F to H) populations, we observed an increase in proliferation from 24h to 48h, as expected following T cell stimulation. Our data shows that the proportion of IELs expressing PD-1 was not significantly different between controls and SOV-treated mice in several IEL populations (Figure 19A to D). Conversely, less TCRδCD8β^{-} CD8α^{-} IELs are proliferating when treated with SOV, as a significant decrease in Ki67 expression was observed in this population (Figure 19E). However, at 48h post-stimulation in SOV-treated mice, PD-1 levels were augmented in every IEL subset (Figure 19I to M), especially in TCRβCD8αα (Figure 19K) and TCRδCDαα (Figure 19L) IELs where these levels were significantly higher than in non-treated mice. These findings indicate that upon α-CD3 stimulation and impairment of PTP function, IELs upregulate PD-1 increasing its expression levels, possibly in an attempt to suppress activation. This suggests a role for PTP in the shaping of IEL activation status.

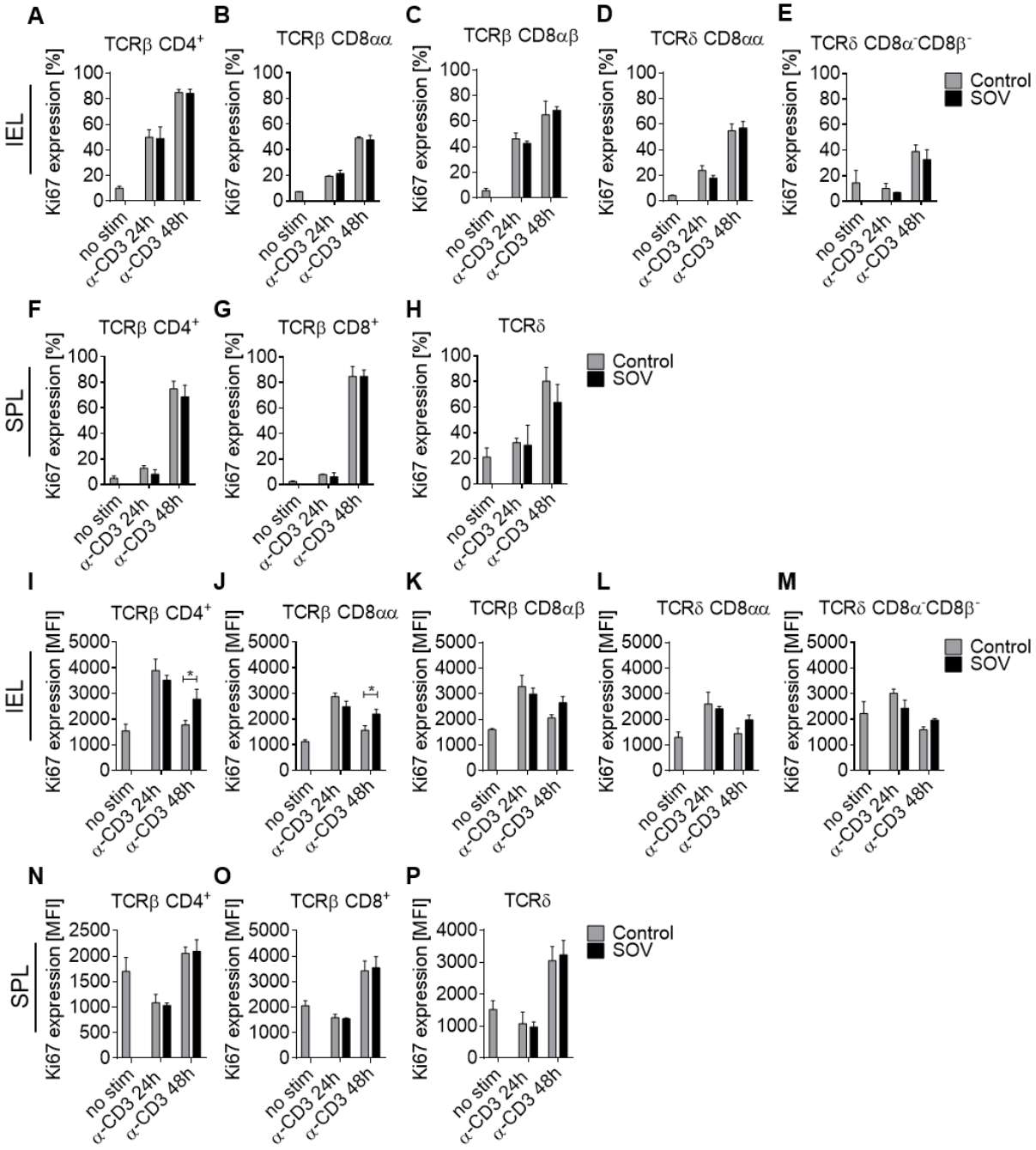

Figure 18 | The effect of PTP general inhibitor sodium orthovanadate in IEL proliferation in vivo. Mice treated with SOV and untreated control mice were sacrificed, and splenocytes and IELs were isolated and stained for Ki67. Ki67 expression is displayed in percentage and was analysed by flow cytometry in several IEL subsets including **(A)** TCRβCD4$^+$, **(B)**TCRβCD8αα, **(C)** TCRβCD8αβ, **(D)** TCRδCD8αα and **(E)** TCRδCD8α$^-$CD8β$^-$ and in splenocytes including **(F)** TCRβCD4$^+$, **(G)** TCRβCD8αβ and **(H)** TCRδ populations. Ki67 expression levels were also determined in **(I)** TCRβCD4$^+$, **(J)**TCRβCD8αα, **(K)** TCRβCD8αβ, **(L)** TCRδCD8αα and **(M)** TCRδCD8α$^-$CD8β$^-$ IELs and in splenocytes including **(N)** TCRβCD4$^+$, **(O)** TCRβCD8αβ and **(P)** TCRδ subsets and are expressed in MFI. Data represents 1 experiment (no α-CD3, n=2; control α-CD3 24h, n=2; control α-CD3 48h, n=2; SOV α-CD3 24h, n=3; SOV α-CD3 48h, n=3). Error bars represent ± SD. Statistical significance was determined by one-way ANOVA and post-hoc Holm-Sidak's multi comparisons test (*P < 0.05).

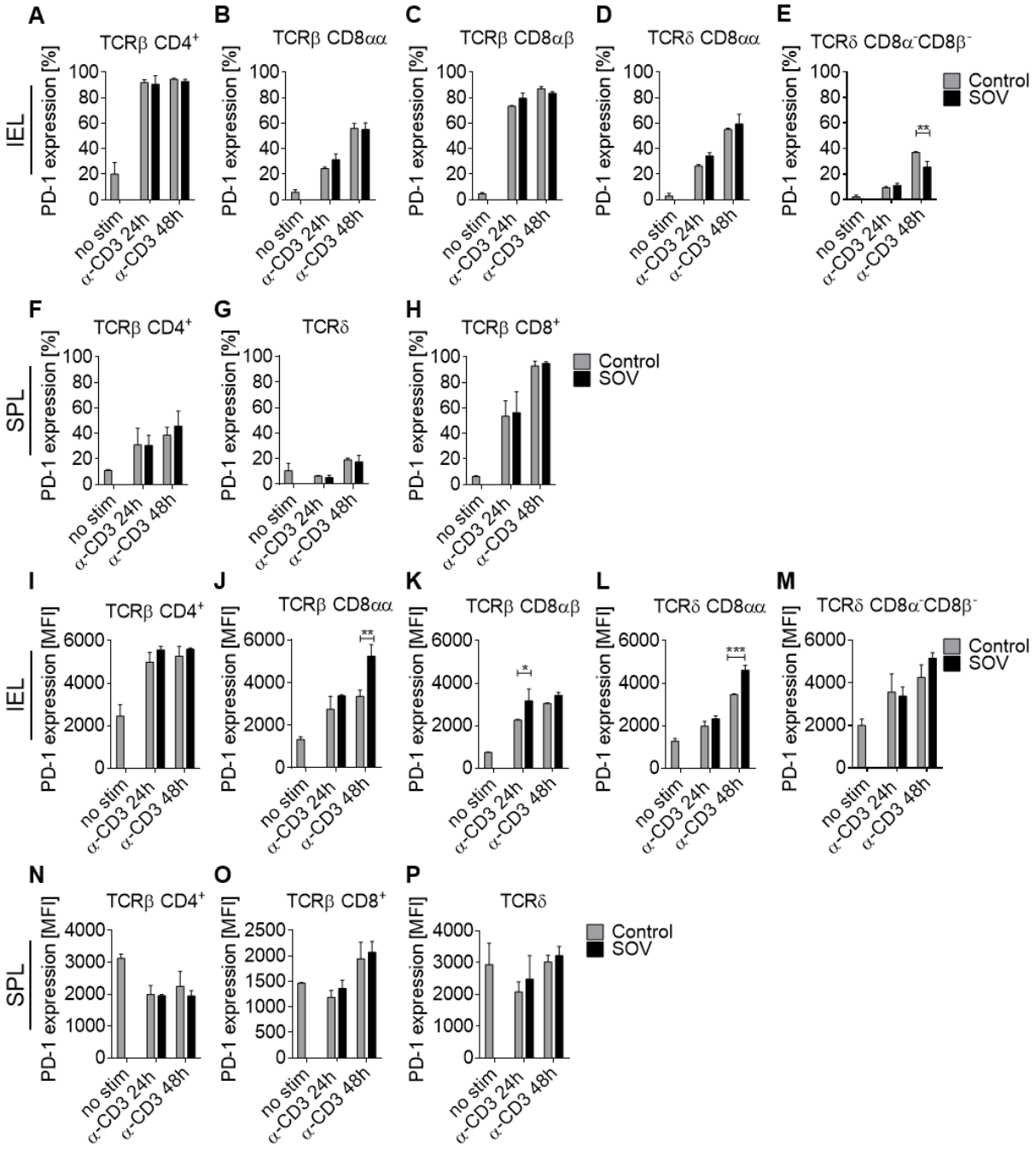

Figure 19 | The effect of PTP general inhibitor sodium orthovanadate in IEL activation in vivo. Mice treated with SOV and control untreated mice were sacrificed, and splenocytes and IELs were isolated and stained for PD-1. PD-1 expression is displayed in percentage and was analysed by flow cytometry in several IEL subsets including **(A)** TCRβCD4+, **(B)**TCRβCD8αα, **(C)** TCRβCD8αβ, **(D)** TCRδCD8αα and **(E)** TCRδCD8α-CD8β- and in splenocytes including **(F)** TCRβCD4+, **(G)** TCRβCD8αβ and **(H)** TCRδ populations. PD-1 expression levels were also determined in **(I)** TCRβCD4+, **(J)**TCRβCD8αα, **(K)** TCRβCD8αβ, **(L)** TCRδCD8αα and **(M)** TCRδCD8α-CD8β- IELs and in splenocytes including **(N)** TCRβCD4+, **(O)** TCRβCD8αβ and **(P)** TCRδ subsets and are expressed in MFI. Data represents 1 experiment (no α-CD3, n=2; control α-CD3 24h, n=2; control α-CD3 48h, n=2; SOV α-CD3 24h, n=3; SOV α-CD3 48h, n=3). Error bars represent ± SD. Statistical significance was determined by one-way ANOVA and post-hoc Holm-Sidak's multi comparisons test (*P < 0.05).

Aiming to study the effect of PTP inhibition on IEL effector functions such as cytotoxicity, we determined GzmB expression. We observed that, at 24h post-stimulation, a large percentage of both control and SOV-treated IELs expressed GzmB (Figure 20A to E). Similarly, GzmB expression levels were increased comparably in control and SOV-treated IELs (Figure 20I to M). Interestingly, all IEL populations at 48h post-stimulation showed a reduction in GzmB expression (Figure 20A to E) accompanied by a decrease in GzmB expression levels (Figure 20I to M) in control mice; however, in SOV-treated individuals, GzmB expression remained heightened. Indeed, the persistent high expression of GzmB in IELs with impaired PTP activity by contrast with non-treated IELs where GzmB expression reverted to lower and even to homeostatic levels in some cases, indicates that IELs may rely on PTPs to regulate their activation state and consequently their function. In splenocytes, GzmB expression is identical among control and treated mice (Figure 20N to P), which suggests that peripheral T cells are not affected by the inhibition of PTPs. These findings indicate that PTP inhibition shapes IEL activation status and cytotoxicity as these are sustained, and no cue for suppression of activation seems to be received, which hints at a role for PTPs in this process.

Our collected data indicates that IEL function is affected by an impairment of PTP activity. In fact, in the presence of a general PTP inhibitor, we observed an increase in PD-1 and GzmB expression in IELs, which potentiates their effector functions and sustained activity status. Contrastingly, conventional T cells behave differently and do not upregulate these molecules. Taken together, our data suggest a shaping role for PTP in the regulation of IEL function.

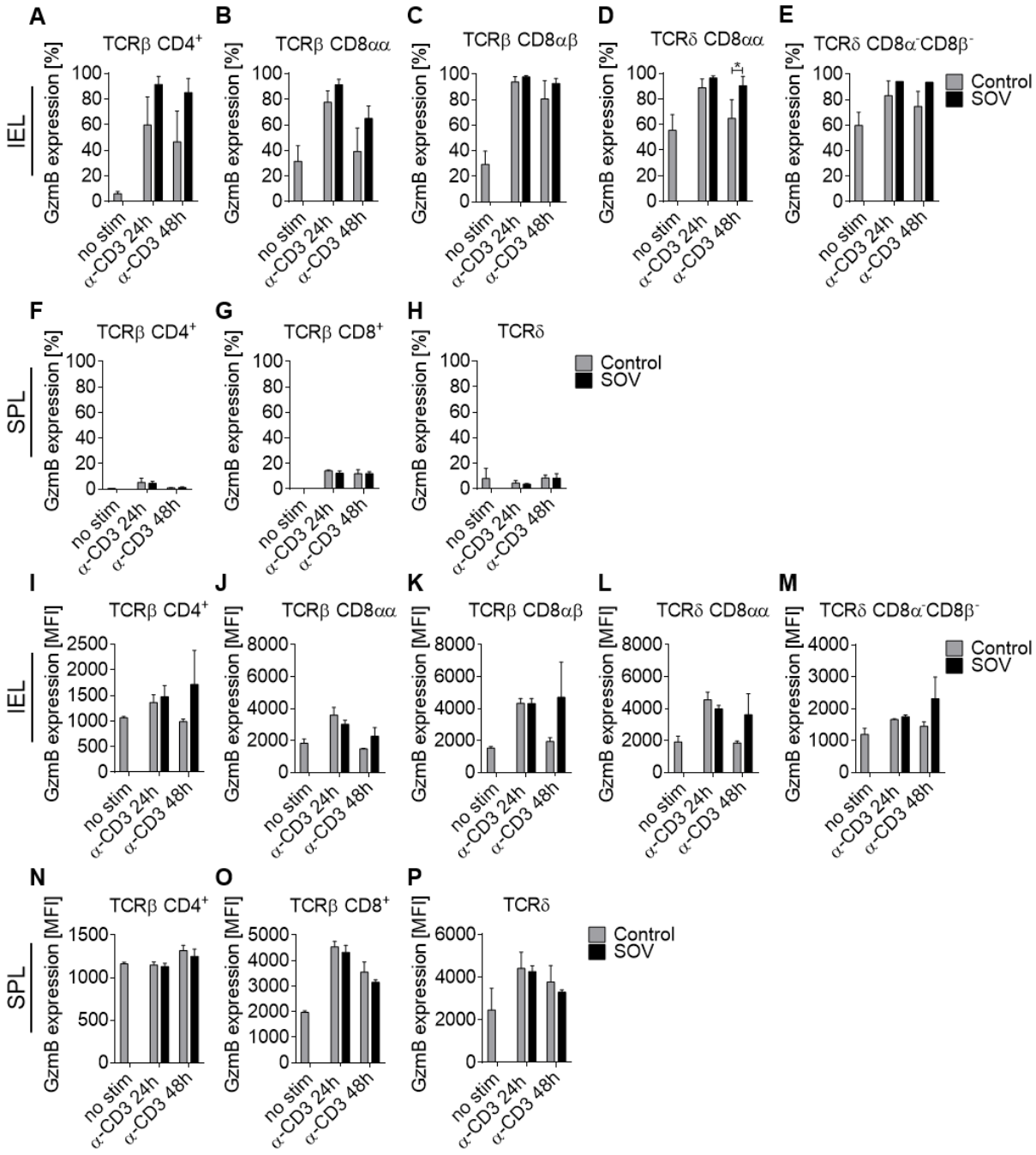

Figure 20 | The effect of PTP general inhibitor sodium orthovanadate in IEL cytotoxic capacity in vivo. Mice treated with SOV and control untreated mice were sacrificed and splenocytes and IELs were isolated and stained for GzmB. GzmB expression is displayed in percentage and was analysed by flow cytometry in several IEL subsets including **(A)** TCRβCD4$^+$, **(B)**TCRβCD8αα, **(C)** TCRβCD8αβ, **(D)** TCRδCD8αα and **(E)** TCRδCD8α$^-$CD8β$^-$ and in splenocytes including **(F)** TCRβCD4$^+$, **(G)** TCRβCD8αβ and **(H)** TCRδ populations. GzmB expression levels were also determined in **(I)** TCRβCD4$^+$, **(J)**TCRβCD8αα, **(K)** TCRβCD8αβ, **(L)** TCRδCD8αα and **(M)** TCRδCD8α$^-$CD8β$^-$ IELs and in splenocytes including **(N)** TCRβCD4$^+$, **(O)** TCRβCD8αβ and **(P)** TCRδ subsets and are expressed in MFI. Data represents 1 experiment (no α-CD3, n=2; control α-CD3 24h, n=2; control α-CD3 48h, n=2; SOV α-CD3 24h, n=3; SOV α-CD3 48h, n=3). Error bars represent ± SD. Statistical significance was determined by one-way ANOVA and post-hoc Holm-Sidak's multi comparisons test (*P < 0.05).

5. Discussion

Notably, IELs share features of memory and effector T cells, reflecting their heightened yet poised activation status. This suggests that IELs have received an activation signal yet are stalled from progressing to full effector status. The cues that maintain and release IEL effector function are still largely unknown, and whilst TCR signalling is essential to activate conventional T cells, the role for TCR in natural IEL activation and function remains unclear. TCR signalling and subsequent T cell activation is tightly regulated by the balance between PTKs and PTPs and the control they exert over the phosphorylation status of downstream signalling molecules. Several PTPs have been described to act as negative regulators of TCR signalling, inhibiting T cell activation [3]. Therefore, we hypothesize that PTPs, as major regulators of TCR signal transduction could be involved in hampering IEL activation.

Here we found that natural IELs, upon direct stimulation via the TCR signalling complex, do not show phosphorylation of TCR signalling molecules downstream of ZAP70, suggesting a proximal TCR signalling block. We show that IELs express higher mRNA levels of PTPs compared to their conventional T cell counterparts. Specifically, we found that PTPN expression is significantly higher in natural CD8αα IELs, than in conventional $CD8^+$ splenocytes, as we observed a substantial increase in the expression of *PTPN22*, *PTPN6*, *PTPN11*, *PTPN9* and *PTPN12* (Figure 7). In addition, we show that CD8αα IELs hold a considerably higher protein content of PTPN22 and SHP-2 than conventional $CD8^+$ T cells (Figure 8). Besides higher expression of PTPs, we also report a markedly higher PTP activity in natural IELs as opposed to conventional T cells (Figure 9). Furthermore, we found that *PTPN22* deficiency appears to affect TCR sensitivity in intestinal IELs and probably their activation threshold. During *in vivo* chemically induced colitis, PTPN22-deficient BM chimera manifested prolonged disease and impaired recovery, suggesting a protective role for PTPN22, which acts as a suppressor of inflammatory response. Moreover, we provide data that during induced T cell activation *in vivo*, by α-CD3 stimulation, PTPN22-deficient IELs exhibit a substantially increased cytotoxic potential, supporting the notion of a potential role for PTPN22 in arresting IEL effector functions. We also report that in mice treated with a general inhibitor of PTPs during α-CD3 induced IEL activation, IELs proliferated faster for a longer period, upregulated PD-1 probably in an attempt to suppress activation, and also sustained a highly increased GzmB expression.

It remains unclear how IELs sustain their heightened yet poised state of activation and whether TCR signalling plays a role in the regulation of this state.

Activation of ZAP70 leads to the phosphorylation and activation of multiple downstream signalling molecules and effectors such as PLCγ and ERK. Indeed, γδ IELs treatment with proximal TCR kinases ZAP70/Syk inhibitors or with blocking antibodies did not prevent infection-induced changes in migration or defence in response to pathogen invasion [70]. Although the TCR is essential to activate and induce functional responses in conventional T cells, TCR stimulation does not appear to induce signalling in natural IELs of both γδ and αβ TCRs [96], thus, we hypothesise there are mechanisms in place hampering TCR function and signalling. Consistent with this hypothesis, our data showed that PTP activity is in fact highly increased in CD8αα IELs. Thus, high expression of PTPNs seems to correlate with a higher activity of phosphatases and given their predominantly TCR inhibitory role, it is likely that they could be suppressing TCR signalling in natural IELs, hampering their activation status.

Previous studies have identified the expression patterns of PTPs commonly expressed in several immune cells, including in T cells, providing insight for further functional studies [97, 98].

Notably, the thoroughly studied phosphatase *PTPN22* plays a specific a role in the early suppression of TCR signal transduction by dephosphorylating activating Tyr residues of LCK and ZAP70, therefore restraining or completely inhibiting TCR response [77]. Previous studies have confirmed a specific role for *PTPN22* in the dampening of T cell activation and the safeguarding of T cell homeostasis, showing that in *Ptpn22*$^{-/-}$ mice, at steady-state, the numbers of effector and memory T cell populations are largely increased in comparison with their wild-type counterparts [78]. Furthermore, other studies have also confirmed that *PTPN22* allows T cells to be activated by cognate antigens, whereas in the presence of self-antigens or weak ligands PTPN22 restrains TCR signalling in order to avoid exacerbated immune responses [81]. Hence, given *PTPN22* role in TCR signalling suppression and considering our reports of augmented expression of *PTPN22* in natural IELs versus conventional T cells, we hypothesized that PTPN22 could be involved in dampening TCR signalling in these cells and therefore explain their poised state of activation. In this work, the generation of *Ptpn22*$^{-/-}$ bone marrow chimeras allowed us to assess the response of *Ptpn22*$^{-/-}$ IELs to different activating stimuli. To evaluate *PTPN22* contribution to IEL activation we used a model of chemically induced colitis, which causes injury to the gut epithelium and subsequently leads to leukocyte infiltration. Our data revealed that in the absence of *PTPN22* the disease is prolonged, and recovery is impaired, indicating that these individuals are more susceptible to colitis. Indeed, this finding supports previous studies showing that *Ptpn22*$^{-/-}$ mice are more susceptible to colitis and develop a severe form of the disease, which is mainly driven by an innate proinflammatory response [99, 100]. However, our data show that profoundly lymphopenic mice are highly sensitive to colitis exhibiting very severe symptoms therefore indicating that T

cells probably play a protective role in this context. In addition, we show that wildtype mice present higher proliferation of IELs during colitis comparing to non-treated mice possibly suggesting that these cells are being recruited for repairing functions. Yet, we have also found that *Ptpn22*$^{-/-}$ and WT IELs seem to proliferate in a similar fashion therefore suggesting that PTPN22 deficiency does not induce higher IEL activation in the small intestine in response to colitis.

Ptpn22$^{-/-}$ and WT IELs proliferate at similar levels, and therefore we did not find a specific correlation between *PTPN22* deficiency and IEL proliferation levels. Previous studies have shown that effector CD8^{+} T cell populations derived from naïve *Ptpn22*$^{-/-}$ T cells displayed increased proliferation and cytokine production upon TCR stimulation [78]. This comes to show that the role of PTPN22 in TCR signalling and subsequent T cell activation, could in fact be different between conventional T cells and IELs. Nonetheless, we focused on the same mechanism by also analysing IEL function in the presence and absence of *PTPN22,* hence, allowing us to further compare the different performances of IELs and conventional T cells, in response to stimulation. Previous studies have already reported that effector *Ptpn22*$^{-/-}$ CD8^{+} T cells have enhanced cytolytic capacity and cytokine production in response to low affinity antigens, specifically weak tumour-associated antigens [101]. The elevated production of GzmB we found in *Ptpn22*$^{-/-}$ IELs compared to their WT counterparts further supports the idea that *PTPN22* deficiency allows for an enhanced IEL activity and maybe cytolytic function.

The enhanced PD-1 expression in stimulated cells was expected given the similar behaviour of CD8^{+} splenocytes in response to TCR stimulation and is also consistent with previous studies in CD8^{+} T cells. We also report that PD-1 expression is consistently reduced in *Ptpn22*$^{-/-}$ CD8^{+} IELs, in comparison with their WT counterparts, which is especially noticeable in natural TCRδ IELs. PD-1 is an activation marker, expressed in transiently activated T cells, and studies have shown PD-1 upregulation in CD8 T cells at the early stages of T cell activation during the transition into functional effector T cells [102]. PD-1 negatively regulates T cell function through the recruitment of SHP-2 which dephosphorylates early TCR stimulatory signalling molecules and therefore inhibits TCR signalling, promoting peripheral tolerance [103]. Our data suggests that *Ptpn22*$^{-/-}$ IELs are not upregulating PD-1 to the same extent as WT IELs, which might reduce PD-1 mediated recruitment of SHP-2 and therefore dampen negative regulation of IEL function. This may promote a higher and longer activation of IELs, by evading these established shutdown mechanisms. Additionally, the fact that in *PTPN22*-deficient natural TCRδ IELs this reduction is more noticeable and significant may relate to the protective role of these cells in the mucosal environment.

Together with the already well-known role of *PTPN22* in switching off the TCR, this increased function and activation observed in *Ptpn22*$^{-/-}$ IELs leads us to believe that in WT cells this PTP may be seizing the complete activation of IELs upon stimulation, and therefore dampening IEL cytolytic functions. In line with this work, it would be interesting to investigate the impact of *PTPN22* deficiency at a later stage by extending the analysis endpoint and investigating whether the absence of *PTPN22* interferes with IEL proliferation and/or activation at later timepoints. Indeed, *PTPN22* deficiency could have repercussions not only in the immediate response of IELs to stimulation, but also in the proper shutdown mechanisms of IELs after stimulation, which could be affected by PTPs absence. Therefore, when compared to an already well characterized CD8^{+} T cell response to TCR stimulation, an extended analysis of *Ptpn22*$^{-/-}$ IEL response to activation allow for a better characterization of cell behaviour and function.

In this work we also evaluated IEL response to stimulation in the absence of functional PTPs, by generally inhibiting PTPs via SOV treatment. In the presence of this inhibitor, TCR signalling should be increased and therefore promoting T cell activation. We assessed IEL proliferation and functional capacity after α-CD3 stimulation, in both the presence and absence of SOV and observed an increase in IEL proliferation from 24h to 48h as expected. Interestingly, we show that at the 48h timepoint IELs exposed to SOV are proliferating at higher levels than their WT counterparts which seem to be returning to homeostatic proliferation levels. Indeed, IELs with impaired PTP activity maintain higher levels of proliferation for a longer period, whereas in conventional T cells the proliferation rate does not vary between SOV-treated and untreated cells. An explanation would be that IELs are more reliant on PTPs for the regulation of their activation status, especially for the resolution and contraction phase after activation, a dependence that is intrinsically not manifested in conventional T cells. Furthermore, our data also revealed that 48h after stimulation, PD-1 levels were highly increased in IELs treated with SOV, especially in natural IEL subsets, comparing to non-treated controls. As previously mentioned, the upregulation of PD-1 is implicated in the suppression of TCR signal transduction, through the recruitment of SHP-2 and consequent dephosphorylation of positive regulators of TCR signalling. In this work, we observe an upregulation of PD-1 in stimulated IELs where PTPs activity has been impaired. Hence, in the absence of PTPs, whose function enables the arrest of T cell activation status, an alternative arises as PD-1 seems to be upregulated for recruitment of SHP-2 in an attempt to effectively restrain T cell activation. Contrastingly, in stimulated *Ptpn22*$^{-/-}$ IELs we registered low PD-1 levels indicating that despite having an impaired negative regulation of TCR activation due to the absence of PTPN22, these cells are able to recruit other phosphatases

and restrain IEL activation. Once more, our data indicate that PTPs have a key role in the regulation of IEL activation.

Moreover, our data show that GzmB expression is similarly increased in IELs of both SOV-treated and control mice at the 24h timepoint, resulting in a high cytolytic function. Interestingly, at the 48h timepoint GzmB expression remains heightened in IELs of SOV-treated mice whereas we observed a considerable reduction in control mice, which leads us to the conclusion that due to the impairment of PTP function, IEL activation cannot be terminated or reduced as observed in the WT controls. This suggests that IELs with no functional PTPs may take longer to shutdown activation, and therefore it could be useful to assess IEL function at later timepoints and perhaps prolong SOV treatment, to determine if that is the case. Notably, in the spleen, conventional T cells in both conditions show very similar expression levels of GzmB indicating that PTPs inhibition highly impacts IEL activation status but not peripheral T cells. Therefore, it appears that IEL activation state and cytotoxic function are sustained when PTP function is impaired. Conceivably, in WT IELs, PTPs could potentially be restraining IEL activation status therefore contributing to their semi-activated state, or perhaps maintaining their activation threshold high. In this regard, it would be useful to experiment with different frequencies of administration of SOV and α-CD3 concentrations for stimulation. This would help to determine if the activation threshold is being modulated by PTPs and if it can be decreased with the administration of SOV. From an IBD perspective it could be beneficial to use additional murine models of spontaneous colitis and perhaps also models of PTP deficiency, possibly genetic, as it remains unclear if PTP inhibitors would be valuable in inflammatory diseases such as UC and CD. Collectively, these data show that PTPs are key regulators of IEL activation status and function and we can gather that they are essential to dampen or completely terminate TCR signalling in IELs.

IELs exert both cytolytic and regulatory functions in order to protect the intestinal epithelium, which encompass avoiding unnecessary or aberrant immune responses as well as preventing pathogen invasion. Whereas TCRαβ IELs are particularly involved in the elimination of infected IECs, TCRδ IELs are engaged in the onset of inflammation resolution and return to homeostasis. Given the different immunological roles of distinct IEL populations, it is of extraordinary importance to understand the weight of PTP regulation in their regulation and function.

Due to their constant exposure to the intestinal microenvironment, which harbours several commensal and pathogenic microorganisms, IELs must be capable to balance immune tolerance and immune responses to threats. Indeed, to achieve this balance IELs require a

tight control over their function and especially over their poised state of activation. In this work we highlight PTPNs fundamental role in regulating IELs activation status and function. Conversely, if the control over IEL mediated immune responses is disrupted, IELs could prompt exacerbated immune responses and contribute to worsen autoimmune diseases or IBDs such as CD or coeliac disease [23, 49, 50, 104, 105]. Therefore, it is of extreme importance to understand the cues that enable IEL full activation and the mechanisms through which IELs are sustained in a poised state of activation.

6. Conclusion and future perspectives

This research sought to determine the impact of PTPs on the activation of IELs and characterize PTP contribution to their poised state of activation, so distinct from conventional T cells.

Given that most PTPs are thought to have a negative regulatory role on TCR signalling, we can presume that the correlation found between a higher expression of PTPNs and heightened phosphatase activity is indicative of a possible role for PTPNs in shaping TCR signalling in IELs. Collectively, the higher expression and activity of PTPs in IELs joined by the fact that PTP-deficient IELs present enhanced effector functions also support our hypothesis that PTPs might be dampening IEL activation state and function. Accordingly, these results interpreted in the light of PTP negative role on TCR signalling through the dephosphorylation of TCR positive regulators, may clarify how they can actively contribute to IEL poised activation status. The current work may therefore help to decipher the cues that drive the rather unconventional activation state of IELs.

The role of IELs in the preservation of the integrity of the intestinal barrier, ensuring tissue homeostasis and repair, validates the importance of their immunological function and of their contribute for health and pathology in the intestine. The contribution of PTPs towards the regulation of the signalling networks that preserve lymphocyte homeostasis and activation is vital and, according to our work, may be associated with the semi-activated status of IELs.

Indeed, the present knowledge of murine IELs will need to be validated in humans, as IBD therapeutic strategies are scarce thus remaining an exciting and puzzling field for future research and clinical progress.

7. References

1. McDermott, A.J. and G.B. Huffnagle, *The microbiome and regulation of mucosal immunity.* Immunology, 2014. **142**(1): p. 24-31.
2. Cheroutre, H., F. Lambolez, and D. Mucida, *The light and dark sides of intestinal intraepithelial lymphocytes.* Nat Rev Immunol, 2011. **11**(7): p. 445-56.
3. Stanford, S.M., N. Rapini, and N. Bottini, *Regulation of TCR signalling by tyrosine phosphatases: from immune homeostasis to autoimmunity.* Immunology, 2012. **137**(1): p. 1-19.
4. Moens, E. and M. Veldhoen, *Epithelial barrier biology: good fences make good neighbours.* Immunology, 2012. **135**(1): p. 1-8.
5. Russell, M.W., et al., *Overview:The Mucosal Immune System*, in *Mucosal Immunology*. 2015, Elsevier. p. 3-8.
6. Belkaid, Y. and O.J. Harrison, *Homeostatic Immunity and the Microbiota.* Immunity, 2017. **46**(4): p. 562-576.
7. Olivares-Villagomez, D. and L. Van Kaer, *Intestinal Intraepithelial Lymphocytes: Sentinels of the Mucosal Barrier.* Trends Immunol, 2018. **39**(4): p. 264-275.
8. Mowat, A.M. and W.W. Agace, *Regional specialization within the intestinal immune system.* Nat Rev Immunol, 2014. **14**(10): p. 667-85.
9. Agace, W.W. and K.D. McCoy, *Regionalized Development and Maintenance of the Intestinal Adaptive Immune Landscape.* Immunity, 2017. **46**(4): p. 532-548.
10. Neish, A.S., *Mucosal immunity and the microbiome.* Ann Am Thorac Soc, 2014. **11 Suppl 1**: p. S28-32.
11. Brandtzaeg, P., *Function of mucosa-associated lymphoid tissue in antibody formation.* Immunol Invest, 2010. **39**(4-5): p. 303-55.
12. Esterhazy, D., et al., *Compartmentalized gut lymph node drainage dictates adaptive immune responses.* Nature, 2019. **569**(7754): p. 126-130.
13. Brandtzaeg, P. and R. Pabst, *Let's go mucosal: communication on slippery ground.* Trends Immunol, 2004. **25**(11): p. 570-7.
14. Tanoue, T., K. Atarashi, and K. Honda, *Development and maintenance of intestinal regulatory T cells.* Nat Rev Immunol, 2016. **16**(5): p. 295-309.
15. Paul, W.E., *Fundamental immunology*. 7th ed. 2013, Philadelphia: Wolters Kluwer Health/Lippincott Williams & Wilkins. 1 online resource (xviii, 1283 pages).
16. Ivanov, I.I., et al., *The Orphan Nuclear Receptor RORγt Directs the Differentiation Program of Proinflammatory IL-17+ T Helper Cells.* Cell, 2006. **126**(6): p. 1121-1133.
17. Veldhoen, M., et al., *TGFbeta in the context of an inflammatory cytokine milieu supports de novo differentiation of IL-17-producing T cells.* Immunity, 2006. **24**(2): p. 179-89.
18. Romagnani, S., *T-cell subsets (Th1 versus Th2).* Annals of Allergy, Asthma & Immunology, 2000. **85**(1): p. 9-21.
19. Del Prete, G., *The concept of type-1 and type-2 helper T cells and their cytokines in humans.* Int Rev Immunol, 1998. **16**(3-4): p. 427-55.
20. Ferguson, A., *Intraepithelial lymphocytes of the small intestine.* Gut, 1977. **18**(11): p. 921-37.
21. Veldhoen, M., et al., *Metabolic wiring of murine T cell and intraepithelial lymphocyte maintenance and activation.* Eur J Immunol, 2018. **48**(9): p. 1430-1440.
22. Meresse, B., G. Malamut, and N. Cerf-Bensussan, *Celiac disease: an immunological jigsaw.* Immunity, 2012. **36**(6): p. 907-19.
23. Abadie, V., V. Discepolo, and B. Jabri, *Intraepithelial lymphocytes in celiac disease immunopathology.* Semin Immunopathol, 2012. **34**(4): p. 551-66.

24. Kaser, A., S. Zeissig, and R.S. Blumberg, *Inflammatory bowel disease.* Annu Rev Immunol, 2010. **28**: p. 573-621.
25. Roda, G., et al., *Crohn's disease.* Nat Rev Dis Primers, 2020. **6**(1): p. 22.
26. Torres, J., et al., *Crohn's disease.* The Lancet, 2017. **389**(10080): p. 1741-1755.
27. Ungaro, R., et al., *Ulcerative colitis.* The Lancet, 2017. **389**(10080): p. 1756-1770.
28. Chassaing, B., et al., *Dextran sulfate sodium (DSS)-induced colitis in mice.* Curr Protoc Immunol, 2014. **104**: p. 15.25.1-15.25.14.
29. Cheroutre, H., *IELs: enforcing law and order in the court of the intestinal epithelium.* Immunol Rev, 2005. **206**: p. 114-31.
30. Hayday, A., et al., *Intraepithelial lymphocytes: exploring the Third Way in immunology.* Nat Immunol, 2001. **2**(11): p. 997-1003.
31. Sheridan, B.S. and L. Lefrancois, *Intraepithelial lymphocytes: to serve and protect.* Curr Gastroenterol Rep, 2010. **12**(6): p. 513-21.
32. Mayassi, T. and B. Jabri, *Human intraepithelial lymphocytes.* Mucosal Immunol, 2018. **11**(5): p. 1281-1289.
33. Ma, H., Y. Qiu, and H. Yang, *Intestinal intraepithelial lymphocytes: Maintainers of intestinal immune tolerance and regulators of intestinal immunity.* J Leukoc Biol, 2020.
34. Van Kaer, L. and D. Olivares-Villagómez, *Development, Homeostasis, and Functions of Intestinal Intraepithelial Lymphocytes.* J Immunol, 2018. **200**(7): p. 2235-2244.
35. Vandereyken, M., O.J. James, and M. Swamy, *Mechanisms of activation of innate-like intraepithelial T lymphocytes.* Mucosal Immunol, 2020. **13**(5): p. 721-731.
36. Di Marco Barros, R., et al., *Epithelia Use Butyrophilin-like Molecules to Shape Organ-Specific γδ T Cell Compartments.* Cell, 2016. **167**(1): p. 203-218.e17.
37. Staton, T.L., et al., *CD8+ recent thymic emigrants home to and efficiently repopulate the small intestine epithelium.* Nat Immunol, 2006. **7**(5): p. 482-8.
38. Gangadharan, D., et al., *Identification of Pre- and Postselection TCRαβ+ Intraepithelial Lymphocyte Precursors in the Thymus.* Immunity, 2006. **25**(4): p. 631-641.
39. Qiu, Y., et al., *TLR2-Dependent Signaling for IL-15 Production Is Essential for the Homeostasis of Intestinal Intraepithelial Lymphocytes.* Mediators Inflamm, 2016. **2016**: p. 4281865.
40. Yu, Q., et al., *MyD88-dependent signaling for IL-15 production plays an important role in maintenance of CD8 alpha alpha TCR alpha beta and TCR gamma delta intestinal intraepithelial lymphocytes.* J Immunol, 2006. **176**(10): p. 6180-5.
41. Jiang, W., et al., *Recognition of gut microbiota by NOD2 is essential for the homeostasis of intestinal intraepithelial lymphocytes.* J Exp Med, 2013. **210**(11): p. 2465-76.
42. Konjar, S., et al., *Intestinal Barrier Interactions with Specialized CD8 T Cells.* Front Immunol, 2017. **8**: p. 1281.
43. Veldhoen, M., et al., *The aryl hydrocarbon receptor links TH17-cell-mediated autoimmunity to environmental toxins.* Nature, 2008. **453**(7191): p. 106-9.
44. Konjar, S., et al., *Mitochondria maintain controlled activation state of epithelial-resident T lymphocytes.* Sci Immunol, 2018. **3**(24).
45. Veldhoen, M., *Interleukin 17 is a chief orchestrator of immunity.* Nat Immunol, 2017. **18**(6): p. 612-621.
46. Peluso, I., F. Pallone, and G. Monteleone, *Interleukin-12 and Th1 immune response in Crohn's disease: pathogenetic relevance and therapeutic implication.* World J Gastroenterol, 2006. **12**(35): p. 5606-10.
47. Hüe, S., et al., *A Direct Role for NKG2D/MICA Interaction in Villous Atrophy during Celiac Disease.* Immunity, 2004. **21**(3): p. 367-377.
48. Ismail, A.S., et al., *Gammadelta intraepithelial lymphocytes are essential mediators of host-microbial homeostasis at the intestinal mucosal surface.* Proc Natl Acad Sci U S A, 2011. **108**(21): p. 8743-8.
49. Nüssler, N.C., et al., *Enhanced cytolytic activity of intestinal intraepithelial lymphocytes in patients with Crohn's disease.* Langenbecks Arch Surg, 2000. **385**(3): p. 218-24.

50. Kawaguchi-Miyashita, M., et al., *An accessory role of TCRgammadelta (+) cells in the exacerbation of inflammatory bowel disease in TCRalpha mutant mice.* Eur J Immunol, 2001. **31**(4): p. 980-8.
51. Sujino, T., et al., *Tissue adaptation of regulatory and intraepithelial CD4⁺ T cells controls gut inflammation.* Science, 2016. **352**(6293): p. 1581.
52. Birnbaum, Michael E., et al., *Deconstructing the Peptide-MHC Specificity of T Cell Recognition.* Cell, 2014. **157**(5): p. 1073-1087.
53. Gaud, G., R. Lesourne, and P.E. Love, *Regulatory mechanisms in T cell receptor signalling.* Nat Rev Immunol, 2018. **18**(8): p. 485-497.
54. Hořejší, V., W. Zhang, and B. Schraven, *Transmembrane adaptor proteins: organizers of immunoreceptor signalling.* Nature Reviews Immunology, 2004. **4**(8): p. 603-616.
55. Brownlie, R.J. and R. Zamoyska, *T cell receptor signalling networks: branched, diversified and bounded.* Nat Rev Immunol, 2013. **13**(4): p. 257-69.
56. Rhee, I. and A. Veillette, *Protein tyrosine phosphatases in lymphocyte activation and autoimmunity.* Nat Immunol, 2012. **13**(5): p. 439-47.
57. Levine, A.G., et al., *Continuous requirement for the TCR in regulatory T cell function.* Nat Immunol, 2014. **15**(11): p. 1070-8.
58. Polic, B., et al., *How alpha beta T cells deal with induced TCR alpha ablation.* Proc Natl Acad Sci U S A, 2001. **98**(15): p. 8744-9.
59. Vahl, J.C., et al., *Continuous T Cell Receptor Signals Maintain a Functional Regulatory T Cell Pool.* Immunity, 2014. **41**(5): p. 722-736.
60. Klein, J.R., *T-cell activation in the curious world of the intestinal intraepithelial lymphocyte.* Immunol Res, 2004. **30**(3): p. 327-37.
61. Montufar-Solis, D., T. Garza, and J.R. Klein, *T-cell activation in the intestinal mucosa.* Immunol Rev, 2007. **215**: p. 189-201.
62. Kim, S.K., et al., *Activation and migration of CD8 T cells in the intestinal mucosa.* The Journal of Immunology, 1997. **159**(9): p. 4295-4306.
63. Pietschmann, K., et al., *Toll-Like Receptor Expression and Function in Subsets of Human γδ T Lymphocytes.* Scandinavian Journal of Immunology, 2009. **70**(3): p. 245-255.
64. Li, Y., et al., *Exogenous stimuli maintain intraepithelial lymphocytes via aryl hydrocarbon receptor activation.* Cell, 2011. **147**(3): p. 629-40.
65. Martin, B., et al., *Interleukin-17-Producing γδ T Cells Selectively Expand in Response to Pathogen Products and Environmental Signals.* Immunity, 2009. **31**(2): p. 321-330.
66. Jandke, A., et al., *Butyrophilin-like proteins display combinatorial diversity in selecting and maintaining signature intraepithelial gammadelta T cell compartments.* Nat Commun, 2020. **11**(1): p. 3769.
67. Wang, H.C., et al., *Most murine CD8+ intestinal intraepithelial lymphocytes are partially but not fully activated T cells.* J Immunol, 2002. **169**(9): p. 4717-22.
68. Swamy, M., et al., *Intestinal intraepithelial lymphocyte activation promotes innate antiviral resistance.* Nat Commun, 2015. **6**: p. 7090.
69. Ferran, C., et al., *Cytokine-related syndrome following injection of anti-CD3 monoclonal antibody: further evidence for transient in vivo T cell activation.* Eur J Immunol, 1990. **20**(3): p. 509-15.
70. Hoytema van Konijnenburg, D.P., et al., *Intestinal Epithelial and Intraepithelial T Cell Crosstalk Mediates a Dynamic Response to Infection.* Cell, 2017. **171**(4): p. 783-794 e13.
71. Malinarich, F.H., et al., *Constant TCR triggering suggests that the TCR expressed on intestinal intraepithelial gammadelta T cells is functional in vivo.* Eur J Immunol, 2010. **40**(12): p. 3378-88.
72. Wencker, M., et al., *Innate-like T cells straddle innate and adaptive immunity by altering antigen-receptor responsiveness.* Nat Immunol, 2014. **15**(1): p. 80-7.

73. Hermiston, M.L., J. Zikherman, and J.W. Zhu, *CD45, CD148, and Lyp/Pep: critical phosphatases regulating Src family kinase signaling networks in immune cells.* Immunol Rev, 2009. **228**(1): p. 288-311.
74. Cloutier, J.F. and A. Veillette, *Cooperative inhibition of T-cell antigen receptor signaling by a complex between a kinase and a phosphatase.* J Exp Med, 1999. **189**(1): p. 111-21.
75. Cloutier, J.F. and A. Veillette, *Association of inhibitory tyrosine protein kinase p50csk with protein tyrosine phosphatase PEP in T cells and other hemopoietic cells.* The EMBO Journal, 1996. **15**(18): p. 4909-4918.
76. Gjörloff-Wingren, A., et al., *Characterization of TCR-induced receptor-proximal signaling events negatively regulated by the protein tyrosine phosphatase PEP.* European Journal of Immunology, 1999. **29**(12): p. 3845-3854.
77. Wu, J., et al., *Identification of substrates of human protein-tyrosine phosphatase PTPN22.* J Biol Chem, 2006. **281**(16): p. 11002-10.
78. Hasegawa, K., et al., *PEST domain-enriched tyrosine phosphatase (PEP) regulation of effector/memory T cells.* Science, 2004. **303**(5658): p. 685-9.
79. Bottini, N. and E.J. Peterson, *Tyrosine phosphatase PTPN22: multifunctional regulator of immune signaling, development, and disease.* Annu Rev Immunol, 2014. **32**: p. 83-119.
80. Brownlie, R.J., R. Zamoyska, and R.J. Salmond, *Regulation of autoimmune and anti-tumour T-cell responses by PTPN22.* Immunology, 2018. **154**(3): p. 377-382.
81. Salmond, R.J., et al., *The tyrosine phosphatase PTPN22 discriminates weak self peptides from strong agonist TCR signals.* Nat Immunol, 2014. **15**(9): p. 875-883.
82. Pao, L.I., et al., *Nonreceptor protein-tyrosine phosphatases in immune cell signaling.* Annu Rev Immunol, 2007. **25**: p. 473-523.
83. Johnson, K.G., et al., *TCR signaling thresholds regulating T cell development and activation are dependent upon SHP-1.* J Immunol, 1999. **162**(7): p. 3802-13.
84. Zhang, J., A.-K. Somani, and K.A. Siminovitch, *Roles of the SHP-1 tyrosine phosphatase in the negative regulation of cell signalling.* Seminars in Immunology, 2000. **12**(4): p. 361-378.
85. Stefanová, I., et al., *TCR ligand discrimination is enforced by competing ERK positive and SHP-1 negative feedback pathways.* Nat Immunol, 2003. **4**(3): p. 248-54.
86. Fowler, C.C., et al., *SHP-1 in T cells limits the production of CD8 effector cells without impacting the formation of long-lived central memory cells.* J Immunol, 2010. **185**(6): p. 3256-67.
87. Davidson, D. and A. Veillette, *PTP-PEST, a scaffold protein tyrosine phosphatase, negatively regulates lymphocyte activation by targeting a unique set of substrates.* EMBO J, 2001. **20**(13): p. 3414-26.
88. Davidson, D., et al., *The phosphatase PTP-PEST promotes secondary T cell responses by dephosphorylating the protein tyrosine kinase Pyk2.* Immunity, 2010. **33**(2): p. 167-80.
89. Cho, Y.C., B.R. Kim, and S. Cho, *Protein tyrosine phosphatase PTPN21 acts as a negative regulator of ICAM-1 by dephosphorylating IKKbeta in TNF-alpha-stimulated human keratinocytes.* BMB Rep, 2017. **50**(11): p. 584-589.
90. Stanford, S.M., et al., *High-throughput screen using a single-cell tyrosine phosphatase assay reveals biologically active inhibitors of tyrosine phosphatase CD45.* Proc Natl Acad Sci U S A, 2012. **109**(35): p. 13972-7.
91. Secrist, J.P., et al., *Stimulatory effects of the protein tyrosine phosphatase inhibitor, pervanadate, on T-cell activation events.* J Biol Chem, 1993. **268**(8): p. 5886-93.
92. Liu, W., et al., *T lymphocyte SHP2-deficiency triggers anti-tumor immunity to inhibit colitis-associated cancer in mice.* Oncotarget, 2017. **8**(5): p. 7586-7597.
93. Zheng, J., et al., *Meta-analysis reveals an association of PTPN22 C1858T with autoimmune diseases, which depends on the localization of the affected tissue.* Genes Immun, 2012. **13**(8): p. 641-52.

94. Diaz-Gallo, L.-M., et al., *Differential association of two PTPN22 coding variants with Crohn's disease and ulcerative colitis.* Inflammatory Bowel Diseases, 2011. **17**(11): p. 2287-2294.
95. Brownlie, R.J., et al., *Lack of the phosphatase PTPN22 increases adhesion of murine regulatory T cells to improve their immunosuppressive function.* Sci Signal, 2012. **5**(252): p. ra87.
96. Mosley, R.L., M. Whetsell, and J.R. Klein, *Proliferative properties of murine intestinal intraepithelial lymphocytes (IEL): IEL expressing TCRαβ or TCRτδ are largely unresponsive to proliferative signals mediated via conventional stimulation of the CD3-TCR complex.* International Immunology, 1991. **3**(6): p. 563-569.
97. Arimura, Y. and J. Yagi, *Comprehensive expression profiles of genes for protein tyrosine phosphatases in immune cells.* Sci Signal, 2010. **3**(137): p. rs1.
98. Mustelin, T., T. Vang, and N. Bottini, *Protein tyrosine phosphatases and the immune response.* Nat Rev Immunol, 2005. **5**(1): p. 43-57.
99. Chang, H.H., et al., *PTPN22 modulates macrophage polarization and susceptibility to dextran sulfate sodium-induced colitis.* J Immunol, 2013. **191**(5): p. 2134-43.
100. Wang, Y., et al., *The autoimmunity-associated gene PTPN22 potentiates toll-like receptor-driven, type 1 interferon-dependent immunity.* Immunity, 2013. **39**(1): p. 111-22.
101. Brownlie, R.J., et al., *Deletion of PTPN22 improves effector and memory CD8+ T cell responses to tumors.* JCI Insight, 2019. **5**.
102. Ahn, E., et al., *Role of PD-1 during effector CD8 T cell differentiation.* Proc Natl Acad Sci U S A, 2018. **115**(18): p. 4749-4754.
103. Chemnitz, J.M., et al., *SHP-1 and SHP-2 Associate with Immunoreceptor Tyrosine-Based Switch Motif of Programmed Death 1 upon Primary Human T Cell Stimulation, but Only Receptor Ligation Prevents T Cell Activation.* The Journal of Immunology, 2004. **173**(2): p. 945.
104. Park, S.G., et al., *T regulatory cells maintain intestinal homeostasis by suppressing γδ T cells.* Immunity, 2010. **33**(5): p. 791-803.
105. Catalan-Serra, I., et al., *Gammadelta T Cells in Crohn's Disease: A New Player in the Disease Pathogenesis?* J Crohns Colitis, 2017. **11**(9): p. 1135-1145.